Università degli Studi di Ferrara

DOCTORAL COURSE IN
SCIENZE DELL'INGEGNERIA

CICLO XXXIII

COORDINATOR Prof. Stefano Trillo

Optimal Control on Electrical Substation for Enhanced Stability Transient Considering Frequency and Voltage

Scientific/Disciplinary Sector (SDS) ING-INF/04

Supervisor
Prof. Inga Esteban

Supervisor
Prof. Simani Silvio

Candidate
Dott. Pavon Wilson

Anni 2017/2021

Contents

List of Figures

List of Tables

Abstract

Smart grid is a fast-growing technology, and this growth implies an enormous demand for better modelling and control. Non-linear behaviour and uncertainties represent for control a challenging task to overcome. These considerations drive the lack of advanced modelling and further development of optimal control strategies, with the primary aim of maximising the energy efficiency.
The research proposes an optimal approach for network layout and control for a smart grid electrical substation with photo-voltaic generation. The optimisation method relies on heuristics and hierarchical control, minimising the network length and the steady state error. Smart power substation is the name for the planned scheme.
The network layout is multi-layered and bases on heuristic algorithms. The first and second layer routes underground geo-reference electrical networks, which minimises network length. Maximising the power quality, the network reliability and reducing the implementation cost. The third layer optimally allocates the photo-voltaic rooftop panels with a geo-reference criterion.
Hierarchical control appears from the primary controller, which controls the current and the voltage outputs. The secondary control regulates the references for voltage amplitude and frequency, which based on the expected active and reactive power. Finally, the tertiary control deals with energy management and dispatching, which implements a communication coordination among the individual controllers.
The cost functions determine the optimal coefficients values for each individual controller to reduce the steady state error. For this purpose, the investigation tests several performance indices to notice which reach the less error, like as integral square error indices methods. The system steady state is over-damped, and it has not over-shoot. However, it has a 5% of oscillations around the desired voltage level, which keep a constant pattern. The response time is fast, considering the non-linear elements behaviour and the multiple system interactions. Hence, the establishing time is less than 0.4 seconds where, despite the increase in load, the system output satisfies the system's requirements in terms of power and voltage.

Chapter 1

Introduction

The main research objective is to find the optimal routing and control in Electrical Distribution System (EDS) for MG using heuristic methods and Hierarchical Control System (HCS) minimising length for electrical path connection and absolute error for the controllable parameters.
The optimal routing for an EDS minimises implementation cost, environmental impact and accomplish the best technical, regulatory advantages for an electrical network (Aghaei et al., 2014). Since technical perspective a SG, which is a integration EDS and DG is only possible when the system has an optimal planning, and it is considered the allocation for generation units (Theo et al., 2017). Thus, an efficient MG is implemented upon a minimal extension EDS.
The optimal control is focused in minimising the error for loop control but maintaining an acceptable operational cost. The SG is controlled by a SPSS implementing an optimal HCS, which minimises the absolute error, and improves power quality, taking on consideration frequency and voltage parameters (Hirsch et al., 2018).
SPSS is implemented in SG to reach a best performance in the general systems, for instance, voltage and frequency regulation, load sharing, Renewable Energy Resources (RES) coordination, synchronisation with the main grid, power control and optimising the operating cost (Irfan et al., 2017).
The model is validated comparing with similar techniques, under parameters such as, the computational cost, transient response, and others. Including a complete analysis in the system performance against abrupt change, dynamic behaviour and some types of faults, incipient or instantaneous and the % of Total Harmonic Distortion Total Harmonics Distortion (THD).
The review explores several methodologies for optimal planning and control for SG, taking on account flexibility, reliability, sustainable, security and two way power and communication sharing (Colak et al., 2015). The research explores some optimisation techniques to find the optimal control, the objective function can minimise the response time, the energy consumption, and maximise the reliability by means the improving the controller to be more robust (Twaha and Ramli, 2018).
The traditional EDS has the similar structure around the world, and its power is unreliable, susceptible to blackouts, has poor power quality, high losses, thus, it is not possible to integrate DER. Therefore, a well controlled SG is a solution for improve the

electricity power in transmission and distribution level Majeed Butt et al. (2021). SPSS controls a SG, which implements advanced, integrated and reliable equipment to reach measurement, monitoring, control and intelligent function, like as, analysis, fault detection and a smart operation (Li and Wang, 2011). The SPSS controller is in charge of controlling, dispatching and scheduling in an EDS. Event though, the SPSS meet different weaknesses, such as heterogeneous environments, bandwidth limitation, privacy burdens, among others (Feng et al., 2021).
The research has a worldwide impact due to the SG are one of the most promising technology in the fighting against the climate change; additionally, there are project in the region, which are planning to install SG system (Lidula and Rajapakse, 2011). However, there is a huge gap in Ecuador comparing with other countries, and the researchers are worried to boost the technological advances in this field.
Figure 1.1 presents the main features in the research, including the motivation for the research, the applied methodology and the major discussion topics.

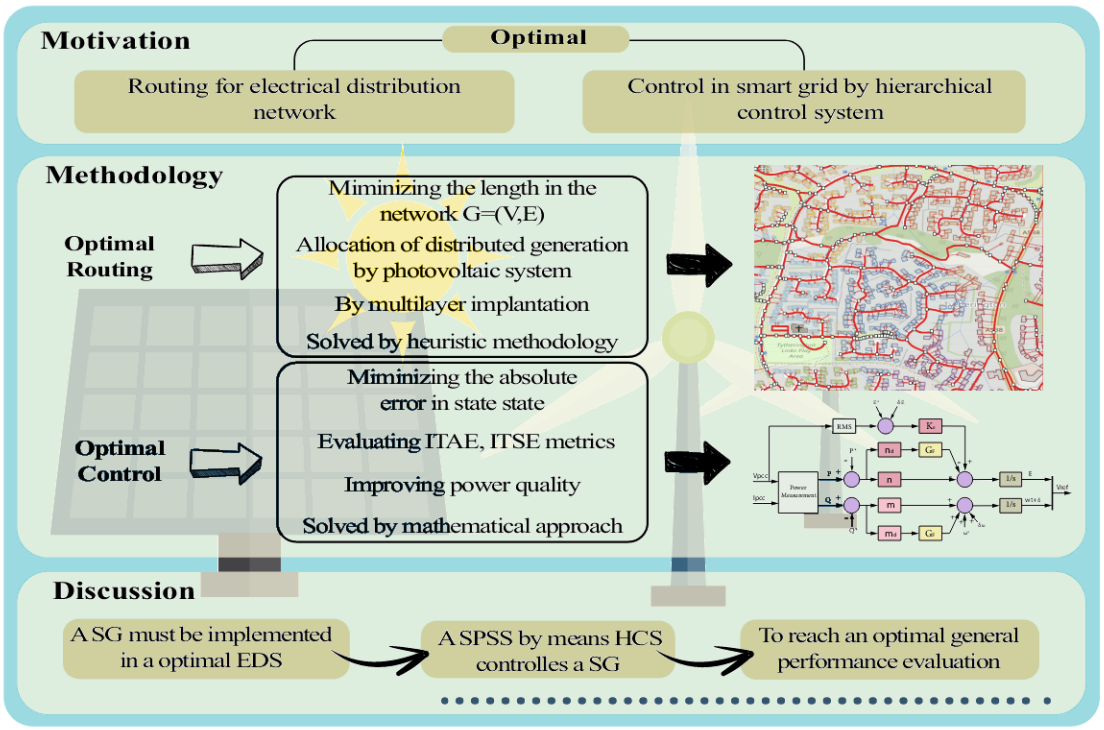

Figure 1.1: Conceptual research map, including motivation, methodology and discussion.

The section below presents the hypothesis, which are proposed before the verification. At final, based on the discussion can be concluded whether the hypothesis was accomplish.

- There might be a soft computer or heuristic method, which allows to design the electrical network in underground implementation, in other words, that it can follow the street path.

- There might be a soft computer or heuristic method, which allows to determine an optimal allocation for distributed generation. It can be based for SG implementation.

- There might be the appropriate, identifiable, encapsulated in a mathematical model for the system under study, where it could represents all the dynamic and transient for several electrical characteristics.

- It is considered that the system is non-linear, thus it could not be represented by a identification techniques of classic control theory; for instance, state space. It is necessary to appeal to more complex control structures, including identification tools, like soft computing models to find an accurate model. The model quality depends on their ability to modelling the transient and stable state behaviour, including the time variant and dynamics changes of the system.

- There might be control structures, which can be implemented by a SPSS, in order to improve its transition stability against different disturbance. Additionally, it is assume that the control can be optimise through algorithms to tackle the control problem and minimising the absolute error in steady state.

- It is supposed that there are mechanisms to determine "how good" are the algorithms, which is applied to the optimised controller. Even if, it could not be the optimal solution; perhaps, it can be found an local optimal using heuristic approaches.

It is also supposed that the implemented methodology would not reached an optimal performance due to the following reasons: a) The optimal multi-layer routing strategy is complicated and take more time than mathematical approaches a) Adequate identification process has not been developed, which allow obtain the total representation in a mathematical model including the dynamic system behaviour, and b) comparison between optimisation techniques in the controllers has not been reach a clear results, showing clearly the best methodology. To this end, a quasi or totally optimal controller will be defined to take into account energy management or another parameter.

1.1 Nomenclature

The main definitions were taken from (Isermann and Balle, 1997) and (IEEE, 1970) listed in the following section, regarding to electrical power, control system, modelling, and system properties.

- **Electrical Power**:
  - **Power System**: A group of one or more generating sources and/or connecting transmission lines operated under common management or supervision to supply load.
  - **Control Area**: A power system, a part of a system, to which a common generation control scheme is applied.
  - **Net Interchange**: The algebraic sum of the power of Power and/or Energy on the area tie lines of a control area.
  - **System Frequency**: The actual frequency of the power system alternating voltage.
  - **Unit Control Error**: The unit generation minus the assigned unit generation.
  - **Master Controller**: device that generates a corrective action, in response to the area control error.
- **Control System**:
  - **Error**: a deviation between a measured or computed value of an output variable and its true or theoretically correct one.
  - **Proportional Control Action**: Action in which there is a linear relation between the output and the input of the controller.
  - **Integral Control Action**: Action in which the output of the controller is proportional to the time integral of the input.
  - **Derivative Control Action**: Action in which the output of the controller is proportional to the first time derivative of the input.
  - **Closed-Loop Control System**: A control system in which the controlled quantity is measured and compared with the desired performance.
  - **Final Controlling Element**: The controlling element which directly changes the value of the manipulated variable.
  - **Disturbance**: an unknown and uncontrolled input acting on a system.
- **Models**:
  - **Quantitative model**: use of static and dynamic relations among system variables and parameters in order to describe the system behaviour in quantitative mathematical terms.
  - **Qualitative model**: use of static and dynamic relations among system variables in order to describe the system behaviour in qualitative terms, such as causalities.
  - **Analytical model**: the mathematical relations among the system variables are based on physical laws deriving by the knowledge of the system behaviour.

  - **Data-driven model**: the mathematical relations among the system variables are inferred on the basis of a data set acquired from the system itself.

- **System properties**:

  - **Reliability**: ability of a system to perform a required function under stated conditions, within a given scope, during a given period of time.
  - **Safety**: ability of a system not to cause danger to persons or equipment or the environment.
  - **Availability**: probability that a system or equipment will operate satisfactorily and effectively at any point of time.

1.2 Outline of the Thesis

The contents of the thesis are briefly summarized in the following, in order to provide an overview of the PhD thesis.

- **Chapter 2**: it presents a discussion about projects and researches papers that have been published in some relevant journals in the scientific content to contribute to solve the proposed problem. Then, a comparison between centralised and distributed system generation is described based on bibliographic reference. Next, the methodology for controlling a SG is listed in chronological order, including identification, controller, optimisation and verification.

- **Chapter 3**: Here is presented the optimal routing, which is based on heuristic algorithms. It is used to solve the routing underground electrical networks problem in a georeferenced area. The model proposed is a multi-layered algorithm.

- **Chapter 4**: In this chapter is presented the optimal control methodology for the smart substation; the SPSS, which controls the SG. The SPSS is based on Hierarchical Control HCS to operate the entire network. The control system is divided in layers, from the primary, secondary and tertiary controller.

- **Chapter 5**: this chapter addresses the performances achieved by developed SPSS control, implemented on SG. It reports the result obtained in comparison with other schemes proposed in literature, and briefly described. Then, the validation is also performed by means of a performance indices.

- **Chapter 6**: the conclusions and the future work are presented in the section.

Chapter 2

State of the Art

In the present section is presented a discussion about projects and researches papers that have been published in some relevant journals in the scientific content to contribute to solve the proposed problem. The SotA is divided into relevance and impact in the world and regionally. However, there is a lack of research evidence about a proper developing in the region. Therefore, the most of the research considered are from another places around the world.
SotA includes models developed by other researches, which have proposed to solve the problem, as well as, several methodologies around the field and different models used for solving optimisation.
The most important review article in the field are listed below:

- The paper (Ustun et al., 2011) reviews the MG concept, including the current literature, and the recent research projects, and the relevant standards.
- In (Planas et al., 2013, 2015) presents a description of MG, including the main features and the control systems.
- In (Hossain et al., 2014) compares the implemented MG in various regions, defining the features of them. Including the existing MG test-beds.
- (Olivares et al., 2014) reviews the major issues and challenges in MG control. The author classified the control into three levels, primary, secondary and tertiary.
- (Tareen et al., 2017) explains the current techniques and limitations for developing and inverted devices for RES, specially PV and Wind Energy Conversion Systems (WECS).
- In (Nutkani et al., 2015) proposed an autonomous droop scheme for energy management for inter-tied MG in Grid-Connected Mode (GCM) or stand-alone mode.
- In (Eghtedarpour and Farjah, 2014) designed a power management system for power interchange for hybrid ac/dc MG.

The work (Dineva et al., 2019) explores a review of soft computing models for controlling electrical applications, which includes fuzzy systems, Neural Network (NN), evolutionary composition, probabilistic applications and rough methods.
There are several heuristic approaches, among them, Adaptive Neuro-Fuzzy Inference System (ANFIS) method, which is an special NN structure, which improved the basic algorithm and can include new patterns through learning. This model is used in (Fatih et al., 2017) for controlling a WECS inverter to reduce the disturbance and reducing the % of THD.
Some authors proposed software based solutions for general optimisation problems, whose are mostly implemented in MATLAB/Simulink. In (Andersson et al., 2019) is considered a software framework for nonlinear optimisation and OCP, which solves constrained problems by differential equations. For instance, a software called "CasADi", which is proposed in (Leek, 2016) to solve problems related to OCP, the program mainly improves the solution performance including time variations discretization problem.
In (Zhang et al., 2017) a strategy is proposed to evaluate novel coordination methods in smart substation using Field Programmable Gate Array (FPGA); moreover, it proposes an experimental implementation using hardware in loop, which can help to demonstrate the real performance of any experimental application.
In MG research area, there are some innovative techniques to improve their performance. The work (Hajiakbari Fini and Hamedani Golshan, 2018) determines the optimal virtual inertia and the frequency control parameters to preserve the stability in the case of islanded MG. In (Heymann et al., 2018) it is addressed the procedure to implement the OCP in MG through rolling horizon formulation; moreover, it describes the problem as Mixed Integer Linear Programming (MILP), where the final operation cost is the objective function and the constraints are the physical battery conditions and its charge and discharge process.
Figure 2.1 shows a SG with all its constituent elements. Among them, there is implemented a MG with different resources, for instance PV generation, Hydraulic Power Generation (HG), WECS, Combined Heat and Power (CHP) and Electric Vehicles (EV). Each of those generation types has different characteristics and control techniques.
The work (Olivares et al., 2014) presented MG trends and the control problems that challenging this novel and spreading system type. The proposed problem is the system outputs must track their reference signals, and the control must ensure that the system oscillations are properly damped in the case of transition between operation modes. Additionally, the article divides the control types, including primary and secondary control; in particular, the first is the charge of maintaining the electrical parameters in acceptable limits, while the second is the responsible for the economical and reliable grid operation. Finally, the paper discusses about the system nature and its features.
Figure 2.2 shows the centralised control enables the implementation of online optimisation routines, while the decentralised control coordinates the action of a grid connected system with a MG.

The work (Hossain and Ali, 2015) compares the performances of three different soft computing models, like fuzzy logic controller, static non-linear controller and ANFIS.

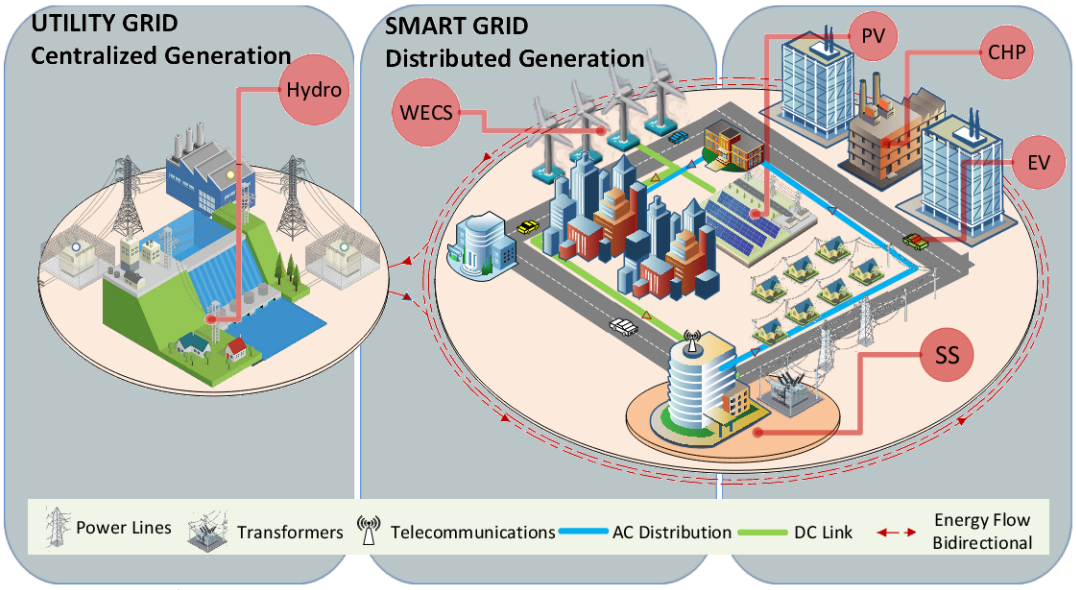

Figure 2.1: Schematic research, showing the SG components.

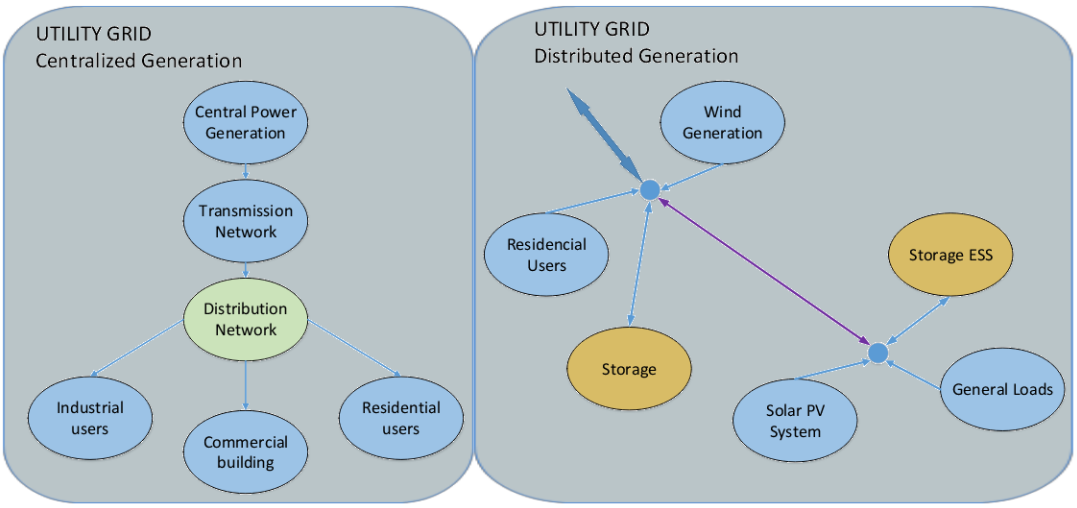

Figure 2.2: Comparison between a system with centralised and distributed generation.

These methods are applied to control of Variable Resistance for Fault Current Limiter (VR-FCL). The VR-FCL limits the maximum current in a smart grid with different source of renewable energy, such as PV, WECS and synchronous generation.
The paper (Huang et al., 2017) demonstrated that the implementation of distribution automation in SG around the world has been successfully exploited to improve the reliability and therefore improve the costumers energy. The SG normally presents peaks that depend of the loads and the intermittent and distributed energy resources. The optimisation of the model can research load shedding or shifting and optimise

the integration of distributed energy resources (Tulabing et al., 2016), (Duque et al., 2017).
(Gajić et al., 2008) is one of the most referenced book in the field of OCP. In particular, this reference analyses the weakly coupled systems, whose small parameters cause weak connections. The problem is solved through two methodologies, i.e. the recursive and the Hamilton approach, obtaining great performance in controlling the analysed systems.
The work (Dong et al., 2018) proposed a coordination strategy in the different substation transformers in a SG; the problem is defined as a multi-objective optimisation. Its objective function is minimising the bus voltage deviation and the total power loss; on the other hand, the control is implemented in a Static Var Compesator (SVR), which is solved with a genetic algorithm with Pareto frontier.
The paper (Wang et al., 2018a,b) proposed a load optimal control algorithm, which improve the model of game theory because it cannot accurately optimise the load control of a SG; on the other hand, it is planned a load distribution using clustering to improve the load change rate. It is investigated the coordination problem to improve the reliability in the network and to reduce the cost of energy of the imported power from the commercial grid. Moreover, a complete network with the calculation procedure is shown in (Khalid et al., 2018).
There are several MG implemented in the literature, for instance in (Ortiz et al., 2019). It is proposed a MG, which consists of hybrid Direct Current (DC) and Alternating Current (AC) buses with different types of loads and distributed generation at two voltage levels. The model was simulated using the MATLAB/Simulink environmental simulation platform.
The solution for the most optimisation problems can be solved by linear programming. However, due to its complexity, it can be used a hard mixed programming level, which is a problem computationally expensive. In the literature there are some authors, among them (Inga et al., 2016), who presented an optimisation model based on minimum spanning tree required to deploy Phase Measurement Unit (PMU) throughout the SG.
The work (Simani et al., 2018) presented a self-tuning control technique for wind turbine and HG plant. These systems have special interest due to their nonlinear dynamic nature; moreover, they have stochastic inputs, and the systems normally present excitation and disturbances. Therefore, the paper presents an analysis of the exploited benchmark in the control objectives, and the development of the control solutions improving reliability and robustness.
The methodology to control a SPSS is explained in chronological order, Figure 2.3. First, the SPSS model is determined, which is used to describe the plant model through soft computing identification techniques. In control engineering is important to define the plant to be controlled, and it is usual to implement several soft computing techniques; for example, NN or fuzzy logic and heuristic applied to system identification. The identification process can include complex variables of the power system, and it must include the static and dynamic static system behaviour.

Secondly, SPSS controller must be designed under criteria of improving the tran-

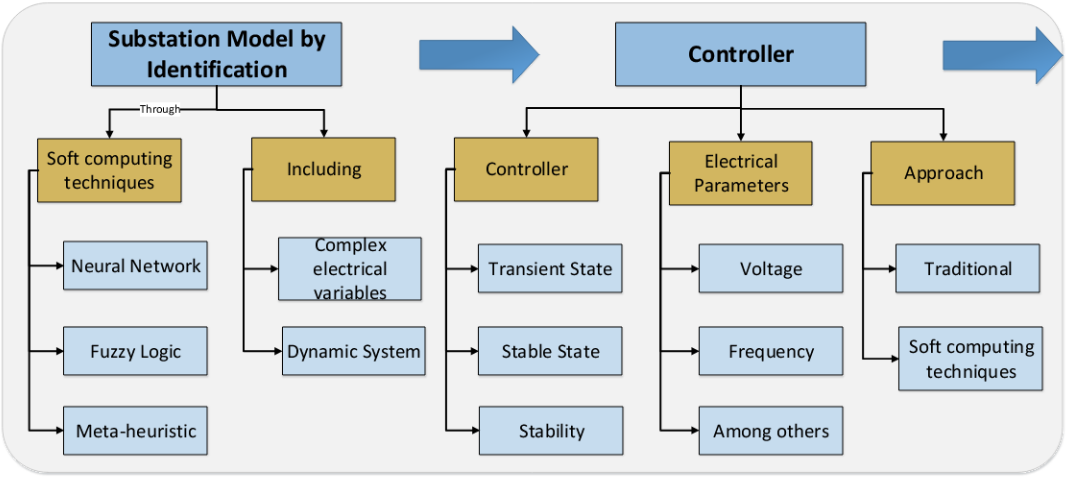

Figure 2.3: Methodologies used for controlling a SPSS listed in chronological order.

sient and stable behaviour of the electrical parameters, e.g. voltage or frequency. SPSS is part of EDS that will be transformed into an automated energy system; in particular, it is located in the first level of SG (Iqbal et al., 2014).
Next, the determination of an optimal model for the control leads to minimise the energy consumption but maintains the controllable parameters, see Figure 2.4. To this end, the research might explore some optimisation techniques to find the OCP; the objective function can minimise the response time, the energy consumption, or maximise the reliability by improving the controller to be more robust. The OCP can be defined to minimise the energy consumption, while maintaining the controllable parameters. To this aim, the research can explores some optimisation techniques to find the optimal control; in this case, the objective function should minimise the response time, the energy consumption, and maximise the reliability by the improving the controller to be more robust (Pauwels et al., 2014).
And finally, the model should be compared with similar techniques, analysing the computational cost of the proposed approach. A complete analysis should include in the system performance against abrupt change, dynamic behaviour and some types of faults, incipient or instantaneous and the % of Total Harmonic Distortion THD. Additionally, the comparison might follow an analytical strategy applied to the obtained results, by means of modelling the on obtained results modelling and engineering simulation, additionally using modern tools.

Evolving SG systems compromise the development of modern methods of storing and producing electrical energy, for instance, Battery Energy Storage System Battery Energy Storage System (BESS), fuel cells, PV and RES, as well as EV considered as smart appliances plug-in.
In consequence, EDS through SG has become more elaborated (Giustina et al., 2015) and should transform from a passive, local/limited automation, monitoring and controlled system to an active, self-monitoring, global/integrated, semi-automated

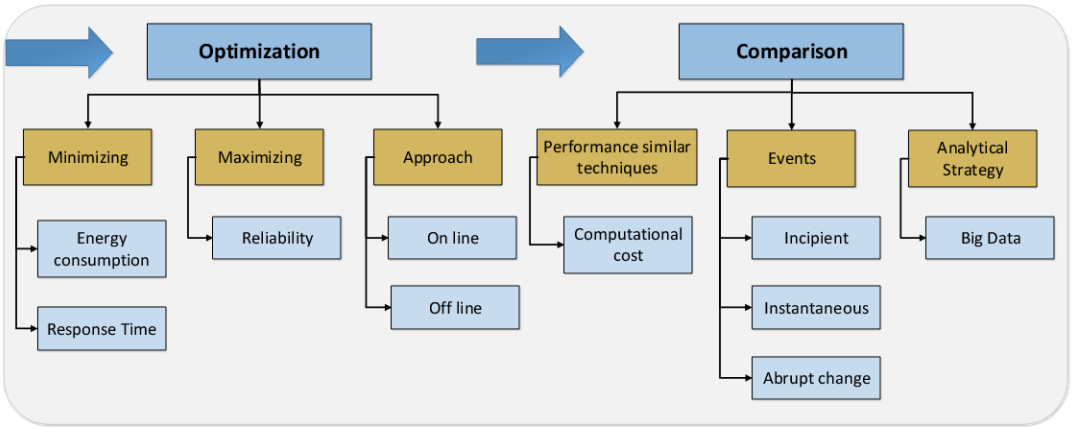

Figure 2.4: Methodologies used for controlling a SPSS listed in chronological order, second part.

system (Zheng et al., 2018).
The SG is now an active system that automatically responds to the dynamic behaviour of the electric grids. Thus, the SG urges new methodologies to control and monitoring the systems, resulting in better efficiency and load management, while the outages should be reduced (McDonald et al., 2013), (Wei et al., 2017).
There are three well defined SG as follow 1.0, 2.0 and the future 3.0. The first is in charge of the distribution energy automation, Supervision and Control Data Acquisition (SCADA), Advanced Metering Infrastructure (AMI) networks and demand response. The second is known as an Advance SG, which is in charge of DER with renewable generation. Finally, the SG of the future with energy trading and roaming (Dkhili et al., 2020).
Substations are a part of every electrical generation, transmission, distribution systems and SG. Into the system, the electrical energy flows through substations between the generation plant and the final costumer, changing the voltage level in each step (McDonald et al., 2013). The development of SG profoundly affects the design, construction and operation of substation (Huang et al., 2017).
The conventional substation does not satisfy the requirements of modern power grid (Huang et al., 2017). In the design process of distribution substation is necessary to take into account multiple factors, including reliability and quality of the power supply. Additionally, the designer must consider parameters like safety, economics, maintainability, operation simplicity, and functionality. Moreover, the substations require a distributed control, protection system, and communication infrastructures (Sun et al., 2018).
The international standard for substation automation is IEC61850, which contains the general international recommendations for automation implementation in substations, and that guide the development and trend the substation technology (Marzal et al., 2018; Cintuglu et al., 2015).
In order to achieve the substation transformation, it is necessary to implement the centralised substation, Protection and Control Centralized Substation Protection and

Control (CPC), which is composed by a high-performance computing platform. The CPC provide monitoring, protection, control and communication functions through collecting the data using time synchronised measurements, and high-speed transfer in the substation (Brahma, 2016). The CPC implement the protection and control actions within the substation. The protection of the power system against abnormal operation is responsibility of the protection system (Brahma, 2016). This control system is supporting the operation of the devices with specific program installed in Intelligent Electric Device (IED) and protection relay (Giustina et al., 2015).
The optimisation problem would include the grid components and characteristics related for achieving the required technical constraints with the minimum investment cost (Khodr et al., 2009). An optimal substation model can consider all the cost associated, which will provide the optimal selection and scheduling of multistage transformer installations in the substation, taking into account the constraints in the substation system (Humayun et al., 2016). All those detailed topics are relevant for the novel research fields and they have not been fully explored.
SPSS includes the practical implementation of CPC in a SG or MG, depending on the implement location. SPSS implements an algorithm to solve the problem of designing a robust control to enhance the best transient performance of a substation, taking into account the electrical variables, in order to obtain the optimal energy management. The algorithm should be designed with distributed and extensible approach, declaring its limitation and future opportunities. A dynamic control of the system should consider different fault types, even though problems such as fault identification and isolation (Simani et al., 2011).
SPSS is shown in Figure 2.5 where the model is identified and exploited for the optimal control of the system, including a comparative analysis of the conditions under which the system enhance the transient performance of the electrical variables.

The MG mathematical modelling can be implemented as block diagram, where is represented the behaviour of each individual generator and their relationship using lines, feed-backs, feed-forwards loops, and addition points.
The entire system can be represented by state space model, in order to highlight the inputs and outputs and their association. Moreover, it is possible to define state variables and characterise their performance. There are several types of MG and they are different depending of their applications; regarding this issue, the technical literature pretend to find a agreement between the model accuracy and simplicity of the representation (Sen and Kumar, 2018).
In (Lee and Wang, 2008) it is presented a hybrid MG, which is presented in Figure 2.6, in the system, there are different DG, for instance,WECS, PV, electrolyte generator and Fuel Cell (FC) and a diesel generator to maintain the frequency. There are two elements for Energy Storage System (ESS), a flywheel and a BESS. The sources are connected to the MG using appropriate Power Energy Converter(PEC).
Figure 2.7 shows how the MG can be represented as block diagram, and the relationships between the block represent the interchange of power. It is shown that the storage energy devices have a bidirectional power behaviour. Meanwhile, each block can be represented by a transfer function depending of the accuracy of the DG model,

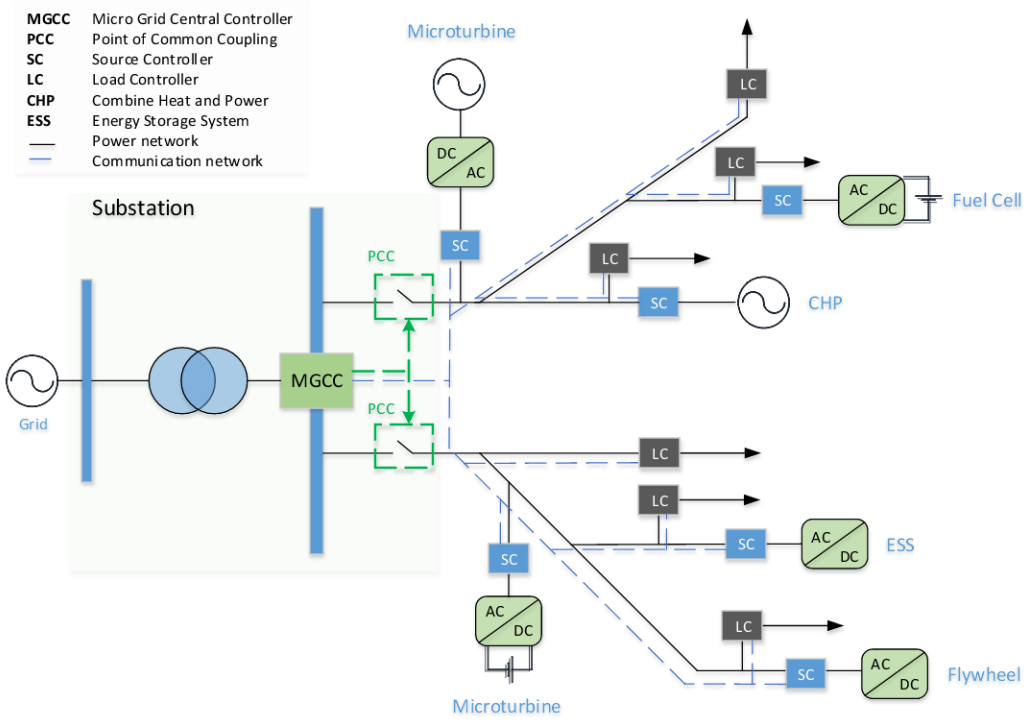

Figure 2.5: OCP strategy in a SPSS.

which is required depending on the importance of the source in the system.

A MG has two operation modes. On one hand GCM, where the grid feeds energy to all the devices in it; in this mode, the control has to manage active and reactive power coordination. On the other hand, stand alone or isolated mode, where the challenge is improving the voltage and frequency quality, ensuring acceptable parameters that allow MG accomplish the power demand (Ahmed et al., 2015).
The PEC operates in two different approaches depending on the MG mode. In the GCM, PEC tracks the grid voltage, operating as Current Sources Inverter (CSI). And, when the MG is isolated, the PEC handles as a Voltage Source Inverter Voltage Source Inverter (VSI) (Jadeja et al., 2020).
PEC operates as VSI in stand alone mode, because one or more PEC have the responsibility to regulate the MG voltage. There are different approaches to handle it. The first is the master-slave scheme, where one DER in the system works as VSI, establishing the reference voltage. On the other hand, the others VSI tracks the signal. However, in the case of the master failure, the entire MG can collapse. As second option, a multi-master scheme coordinates several VSI in the MG (Miret et al., 2017).
There are three methods for controlling a MG. The master-slave control is applied to small MG and it depends on the communication among the PEC. In this structure,

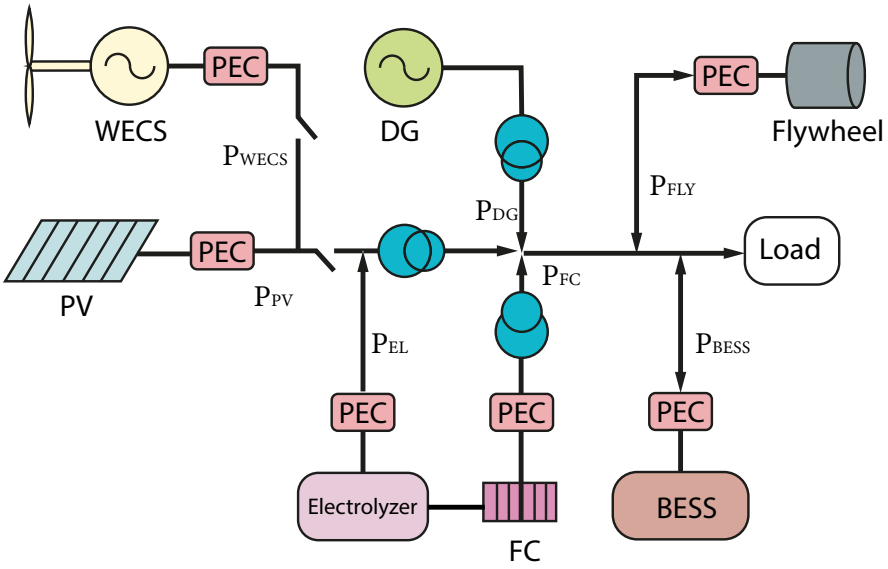

Figure 2.6: Hybrid MG with different DG.

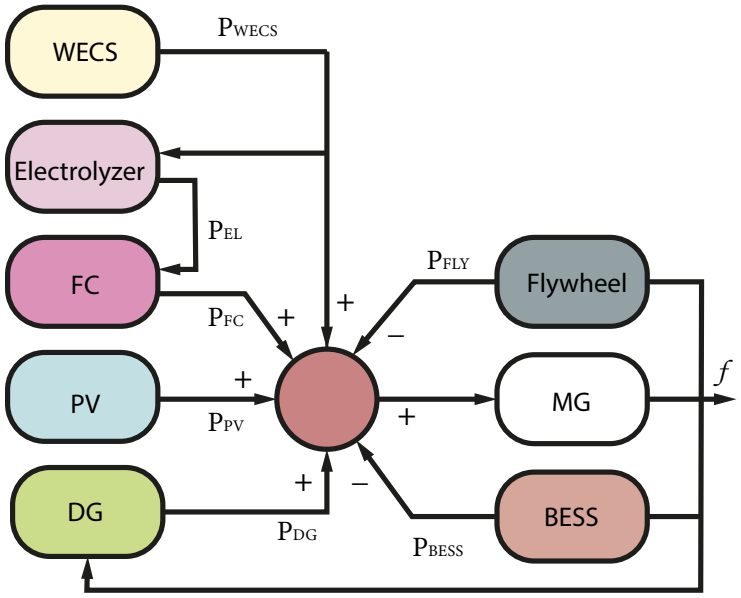

Figure 2.7: DG representation in a MG by block diagrams and transfer function.

the master controls the bus DC voltage and sends the reference signals to the others PEC. Hence, it requires a flexible communication network, which can improve the reliability and the system capability (Chethan Raj and Gaonkar, 2016).
The second one is known as peer control, where there are not masters or slaves, because all the DER take part on the active and reactive power regulation for maintaining the voltage and frequency stability. The droop control belongs to this category, and it does not need PEC intercommunication to develop its operation. The proportional load sharing is guaranteed by means droop control. The third controller is a mixed ver-

sion between master-slave and peer control; it implies a higher degree of complexity but gathers the advantages and disadvantages of the two controllers (Guerrero et al., 2011).
Hierarchical control coordinates the actions of each controller in a MG, starting in the lower level control to reach the higher level in a central controller (Wang et al., 2020). A hierarchical control normally reduces the power variations outside the MG and links the action of the external loops (Li et al., 2020).
The SotA is shown in the Table 2.1, which describes the considered topics. Moreover, the planed problem includes the objective function, meaning that problem can be solve by means of a optimisation model, and it can exploit a minimisation or maximisation procedure.
The third column of Table 2.1 describes the constraint that the papers has considered, here include their physical constraints. And finally, the implemented methodology used to solve the proposed problem.

Table 2.1: Summary of the related research in the SotA.

Paper	Thematic				Problem				Constraints				Approach			
Author	Control Structures	Solve Optimisation	Energy Management	Optimal Control	Droop Control	Optimal Operation	Optimal Control	Operational Cost	Voltage Stability	Security and Reliable	Non-Linear Constraints	Physical Constraints	Non-Linear Systems	Dynamic Optimisation	Energy Storage	Other Methods
Andersson (Andersson et al., 2019)		✠		✠			✠				✠		✠	✠		
Leek (Leek, 2016)		✠		✠			✠				✠					✠
Hajiakbari (Hajiakbari Fini and Hamedani Golshan, 2018)		✠					✠					✠			✠	
Gangl (Gangl et al., 2015)		✠									✠	✠	✠			✠
Olivares (Olivares et al., 2014)	✠	✠	✠	✠	✠	✠	✠			✠		✠			✠	✠
Heymann (Heymann et al., 2018)	✠	✠	✠	✠		✠	✠					✠				✠
Rocabert (Rocabert et al., 2012)	✠	✠			✠	✠	✠		✠			✠	✠	✠		✠
Hajimiragha (Hajimiragha and Zadeh, 2011)	✠	✠	✠			✠		✠				✠				✠
Bahrani (Bahrani et al., 2013)	✠	✠		✠		✠		✠	✠							✠
Kleftakis (Kleftakis and Hatziargyriou, 2019)		✠	✠	✠			✠	✠	✠						✠	
Dong (Dong et al., 2018)		✠		✠			✠		✠			✠				✠
Mirakhorli (Mirakhorli and Dong, 2018)		✠		✠	✠	✠	✠		✠	✠					✠	✠
Liu (Liu et al., 2019)	✠		✠		✠			✠	✠	✠					✠	✠
Mhankale (Mhankale and Thorat, 2018)	✠		✠	✠	✠	✠			✠	✠					✠	✠
BaoNguyen (Bao Nguyen et al., 2017)		✠	✠	✠		✠	✠			✠		✠		✠		
Wei (Wei et al., 2017)		✠	✠	✠			✠	✠				✠		✠	✠	✠
Wu (Wu and Wang, 2018)	✠	✠	✠	✠			✠	✠				✠	✠	✠		✠
Rahmani (Rahmani-Andebili, 2017)		✠	✠	✠		✠		✠		✠		✠		✠	✠	
Dissanayake (Dissanayake and Ekneligoda, 2018)	✠	✠	✠	✠		✠	✠		✠	✠				✠	✠	✠
Colak (Colak et al., 2015)			✠	✠		✠	✠		✠	✠				✠		✠

Figure 2.8 shows a summary of the topics which has been considered in 2.1. It can be seen that the researches have solved the problem using different methodologies. One of the most used approaches is optimal control, after that, physical constraints, followed by solving optimisation and optimal operation. The radial graphic of Figure 2.8 is a tool to decide the path that a research can follow to find the right implementation of SPSS.

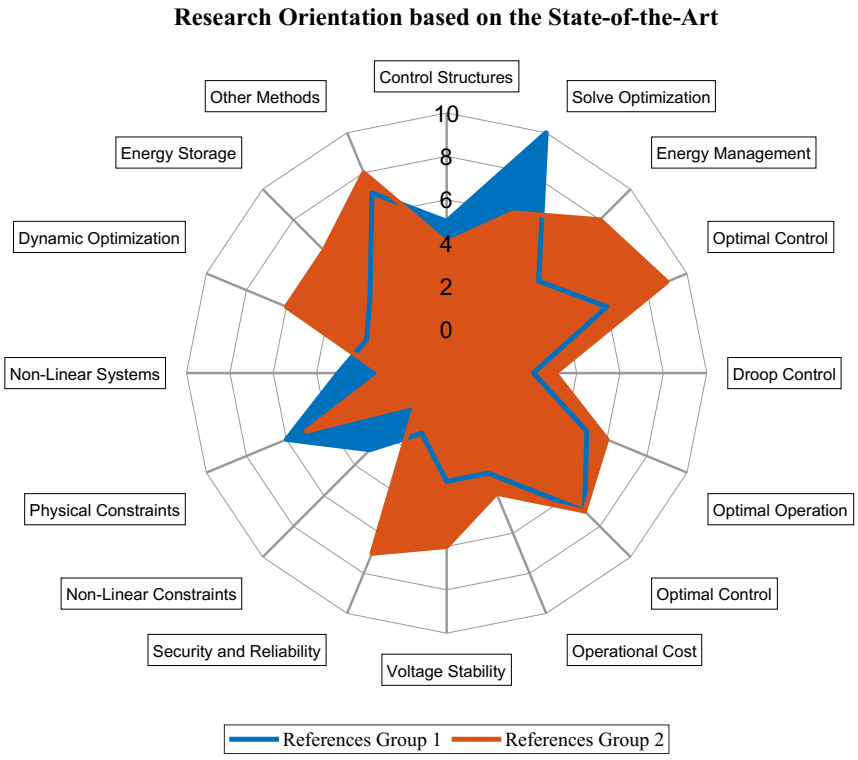

Figure 2.8: Research orientation based on the SotA.

Chapter 3

Optimal Distribution Network Planning

The objective of a electrical system planning should the achievement of total users connectivity, connecting all the points in the system, either as generator or consumer (Theo et al., 2017). In a centralised EDS, the network shapes a radial topology using the minimum expansion tree to achieve the maximum connectivity. By this methodology, the power balance in the network is achieved automatically, as well as the scalability requirement is guaranteed, whenever further residential or industrial loads are required to be connected to the system (Bhowmik et al., 2017).
In a georeferenced scenario, all the elements of the network are represented as nodes. Aside from the map information like streets, roads, and natural features of the selected region, this representation includes homes, transformers, generators and substations locations (Zhang et al., 2020).
In Figure 3.1 is shown an EDS, which is composed by PV and combined heat and power CHP generators. The EDS distributes the energy in DC & AC, depending on the source loads. The generators are connected to the distribution links though converters, which transform the energy level or nature depending of the amount of voltage and whether the distribution is DC or AC.
The EDS is also composed by electrical components like power lines, transformer and converters. The EDS must be designed to follow a path with the shortest length, as this represents a reduction of the implementation cost (Pavón et al., 2019).

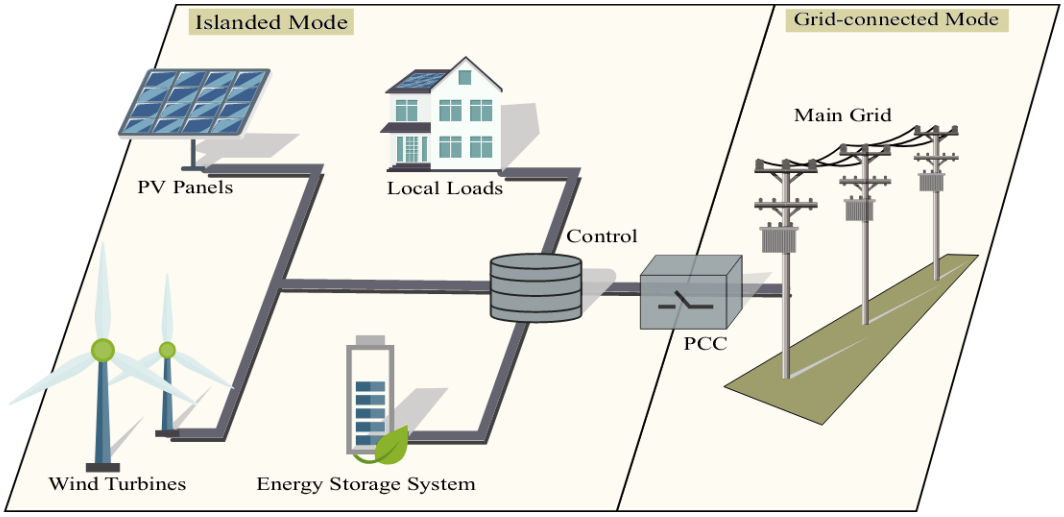

Figure 3.1: SG with DER, showing the importance of the bidirectional inverters.

The problem for its nature is NP-Complete and lacks a globally optimal solution (Mostafaie et al., 2020). As a result, the problem is solved using a heuristic approach finding a suboptimal solution, which minimises the objective function and accomplish the problem constraints ().
An optimisation model is constituted by an objective function and the problem constraints. The objective function can be proposed to optimise the reliability, safety, regulations of the system, thus it can have a large number of variables. Also, this objective function can be expressed as a single or multi-objective expression (Ehsan and Yang, 2019).

3.1 Optimal Routing Methodology

The optimal EDS planning is directly related to the connection route minimisation between the nodes, and this route should accomplish specific commitments. The first is the objective function and the second are the constraints of the mathematical model (Zubo et al., 2017).
The EDS planner design the system operation from different perspectives, as it depends of the aims of the system. For instance, the system can be configured to improve the load balance, the voltage profile, reduce the losses, among others (Ghadi et al., 2019).
Planning hybrid electrical systems with EDS integration implies several variables. The EDS reconfiguration is performed through opening or closing switches that connect the branches in the system. In a real EDS system, the number of switches is considerable and therefore it is impossible for the operator to determine the optimal configuration to solve the optimisation objective (Li et al., 2016).
Table 3.1 presents the variables used in the model to design the distribution network,

taking on account the parameters for the geographic elements location.

Table 3.1: Parameters and variables for optimal routing.

Nomenclature	Description
Cap	Capacity constraint for transformers
Cost	Total distance
dist	distance matrix
$dist_{\mathrm{N}}$	Distance customer, transformer
G	connectivity matrix
ij	geographic variables
N	Number of residential customers
M	Number of LV transformers
S	Number of substations
Path	Network connectivity route
PVs	PV amount in the network
PVC	PV rooftop location
PVP	PV power assignation
R	Distance constraint for all LV paths
SH	End user location
X	Latitude coordinate
Y	Longitude coordinate
$\mathrm{X}_s, \mathrm{Y}_s$	Customer location
$\mathrm{X}_{np}, \mathrm{Y}_{np}$	Street nearest customer
$\mathrm{X}_{se}, \mathrm{Y}_{se}$	Substation location
$\mathrm{X}_{be}, \mathrm{Y}_{be}$	Streets intersection
$\mathrm{X}_{tr}, \mathrm{Y}_{tr}$	Transformer location
$\mathrm{XL}_{st}, \mathrm{YL}_{st}$	Coordinates of L street

The objective function, in equation 3.1, minimises the length of expansion tree. Eqs 3.2 and 3.3 are the constraints for accomplish the radial nature for EDS. Moreover, the Eq. 3.4 represents the connection state, where the state 0 represents a disconnection, while the state 1 represents that the system is connected. To solve this problem it is used a heuristic model. The model is presented with *Algorithm 1* (Pavón et al., 2020).

$$\text{Minimise} \sum_{ij \in \mathrm{E}} \mathrm{C}_{ij} \mathrm{X}_{ij} \tag{3.1}$$

$$\text{Subject to} \sum_{ij \in \mathrm{E}} \mathrm{X}_{ij} = n - 1 \tag{3.2}$$

$$\sum_{ij \in \mathrm{E}: i \in \mathrm{S}, j \in \mathrm{S}} \mathrm{X}_{ij} \leq |\mathrm{S}| - 1 \quad \forall \mathrm{S} \subseteq \mathrm{V} \tag{3.3}$$

$$\mathrm{X}_{ij} \in \{0,1\} \quad \forall ij \in \mathrm{E} \tag{3.4}$$

Algorithm 1 Optimal planning of a EDS.

procedure
  Step: 1 Variables definition
  P, $dist$, X, Y, Cap, R
  Step: 2 Optimal transformer location
  $used \leftarrow Prim(\mathrm{X}, \mathrm{Y})$;
  $Ind \leftarrow find(sum(used) == 1)$;
  $\mathrm{X}_{tr} \leftarrow \mathrm{X}_{be}(Ind)$;
  $\mathrm{Y}_{tr} \leftarrow \mathrm{Y}_{be}(Ind)$;
  Step: 3 Street to customer minimum path
  L$oc1 \leftarrow [\mathrm{X}_s \mathrm{Y}_s]$;
  L$oc2 \leftarrow [\mathrm{XL}_{st} \mathrm{YL}_{st}]$;
  $dist_{i,j} \leftarrow$ *haversine*(L$oc1$, L$oc2$);
  $z \leftarrow find(dist_{i,j} == min(min(dist_{i,j})))$;
  E$ndFor$
  $\mathrm{X}_{np} \leftarrow$ L$oc2(z, 1)$;
  $\mathrm{Y}_{np} \leftarrow$ L$oc2(z, 2)$;
  Step: 4 Optimal Routing
  $\mathrm{X} \leftarrow [\mathrm{X}_{np} \mathrm{X}_{tr} \mathrm{X}_{se}]$;
  $\mathrm{Y} \leftarrow [\mathrm{Y}_{np} \mathrm{Y}_{tr} \mathrm{Y}_{se}]$;
  $dist_{i,j} =$ *haversine*(X, Y);
  G$(dist_{i,j} <= \mathrm{R}) \leftarrow 1$;
  $path \leftarrow Prim_{mst}(sparse(\mathrm{G}))$;
  Step: 5 Determining Cost
  $cost$MV $\leftarrow cost$MV $+ dist_{i,j}(path)$;
  Step: 6 Allocation of DER PV generator
  PV$s \leftarrow floor(length(\mathrm{SH}) * 0.1)$;
  PVC $\leftarrow kmedoids(\mathrm{SH}, \mathrm{PV}s)$;
  PVP $\leftarrow$ 10KW;
  End procedure

Algorithm 1 solves the mathematical problem using 6 consecutive steps. In the first place, the variables are declared, including the constraint constants, as distance and the maximum number of customer for each transformer. Open street map is the source of the geographic information, including the longitude and latitude of customers, streets, corners represented by coordinated points.

The second step uses Prim[1] algorithm, (Prim, 1957), for optimal transformer selection based on the street corner coordinates, as they are the candidate locations for the transformers. The third step finds the closed street point to each end-user using *Haversine*[2] distance function (Eppstein, 1994).
The step four finds the optimal path for distribution network, which implements a combination of *Haversine* and *Prim* functions. The connectivity matrix is calculated with the distance between the system nodes, and the matrix is modified based on the problem restrictions. After that, the *Prim* algorithm minimises the path, trying several possibilities in an exhausting search. The minimum cost represented by the total distance among the elements in the EDS is calculated in the step five.
Finally, the algorithm assigns the rooftop PV in the customer location, the location is designated by the centre of mass using *k-medoids*[3] (Jain et al., 1999) algorithm, and the criteria of assignation is the 10 % of the final users, who installs the PV generation (Vargas and Pavón, 2020).

3.2 Optimal Routing Results

the real implementation was developed in the geographic area of Foz do Iguaçu in Medianeira, Brazil. The limits in longitude are -54.595 to -54.589, and the latitude from -25.527 to -25.5235, the total area is 0.49 Km^2. In the scenario, there are 367 loads with a total planning power of 2.4 MW of consumption.
The presented model allows to plan the EDS network, the model designs an efficient and reliable deployment, with the minimum investment cost. The results can handle the network planning expansion using the initial configuration and expanding the EDS taking on account short and medium horizon period of time. This case has been implemented in *Matlab*, but it can be developed in any other programming language. Table 3.2 presents the parameters and the results of the simulation. The density in the studied area is the 700 customers per Km^2. The assigned constraint is a maximum distance of 40 meters from a customer to distribution transformer, and the coverage must be 100 %.

The system reaches the designed constraints like the under grounded path implementation with radial configuration. The expansion tree starts in the substation: as a result the main feeder is unique. Whilst, the voltage levels in the secondary coil substation is 11[Kv], and the LV network voltage is 400[V]. Finally, this procedure ensures that the final installed load is balanced.
Figure 3.2 is shown the studied scenario in the geographic area. It is divided into clus-

[1]Prim, R. C. (1957). Shortest connection networks and some generalisations. The Bell System Technical Journal, 36(6), 1389–1401. https://doi.org/10.1002/j.1538-7305.1957.tb01515.x

[2]Eppstein, D. (1994). Finding the k shortest paths. Proceedings 35th Annual Symposium on Foundations of Computer Science, 154–165. https://doi.org/10.1109/SFCS.1994.365697

[3]Jain, A. K., Murty, M. N., Flynn, P. J. (1999). Data clustering: a review. ACM Computing Surveys (CSUR), 31(3), 264–323.

Table 3.2: Simulation Parameters.

Item	Parameter	Value
End user information	Density	700 per Km^2
	Amount in study	367 in all study
	Location	Geo-reference
Deployment	Max transformer distance	40 meters
	MV Network transformer coverage	100 %
	LV Network end users coverage	100 %
MV network parameters	Installation type	Under-grounded
	Network configuration	Radial
	Number of primary feeders number	1
	Voltage level	11 [KV]
	Total power demand	5.4 [MVA]
LV network parameters	Installation type	Under-grounded
	Network configuration	Radial
	Voltage level	400 [V]
	Concentrated load	balanced

ters using *k-medoids* algorithm to assign the power consumption and the allocation of the PV panels. The end user the power consumption is assigned randomly, depending on the membership cluster. The substation location is aleatory is randomly selected. Further studies will improve this assumption.
In the same figure is shown the universe of possibilities of transformer location. This geographic coordinates correspond to the corners in the streets, which technically allows to construct an underground transformer.
These coordinate points are used in the step four in algorithm 1, adding the maximum distance between transformers, while the step four output is the number and location for the selected transformers. The step four also concerns the constraint of maximum distance between the customer and their feeder transformer.

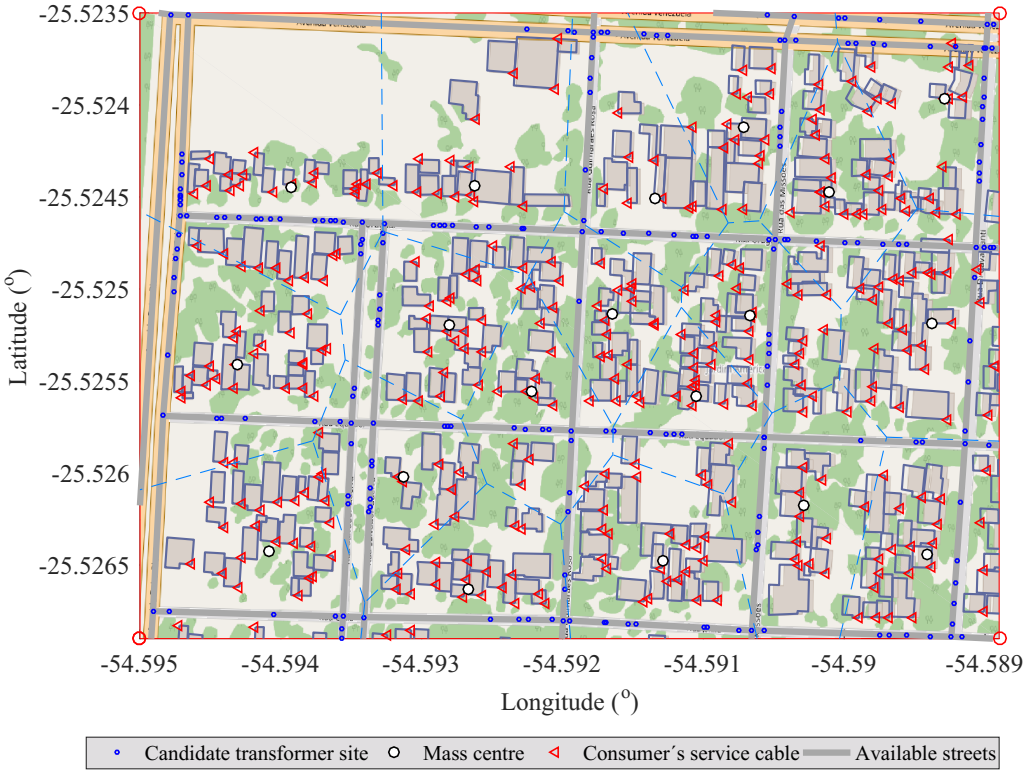

Figure 3.2: Studied scenario showing the transformer candidate location, in every corner in the map.

The connectivity matrix superimposes the distance matrix, which is depicted in Figure 3.3. It is a symmetrical square coloured matrix representation, where the number of rows and columns is the same and is the number of nodes in the system.
The same figure represents the distance between the nodes in the scenario, thus there are possible connections whether the colour is darker, whilst the connection is almost impossible if the colour is light. With this scenario, it can be noted that the distance can be between 0 to 800 meters.
The connectivity matrix initially imposes physical limitation; the first is the connection that cannot be with the same element. Moreover, it constraints the maximum distance as requirements in this problem. This restrictions are represented by the white dots. While, the number *nz* represents the number of total possible connections in the entire scenario.
The number *nz* is 3674, which allows to have an idea of how is difficult to meet the total connectivity condition. If the *nz* is low, the route is almost impossible or difficult, but when number is higher then is effortless to have an efficient and confident result.

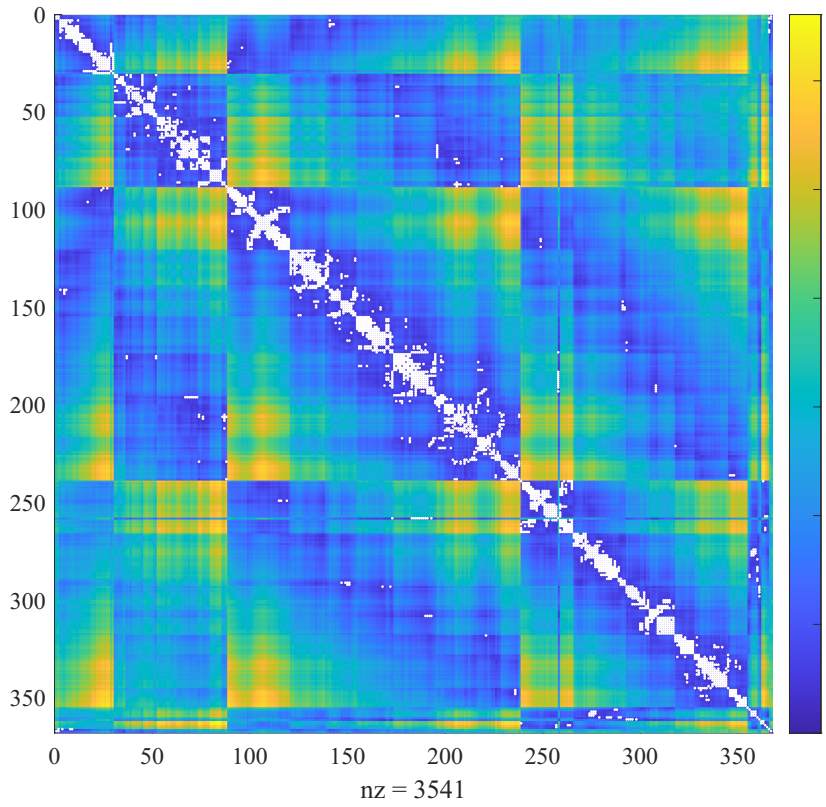

Figure 3.3: Distance and connectivity matrix represents in the same graphic the possibility to achieve a successful experiment.

Figure 3.4 shows the result of the designed methodology of algorithm 1, where a path that connects the elements in medium voltage and routs along the street to accomplish the underground implementation. The constraints applied to the Medium Voltage (MV) network was a maximum distance of 40$[m]$ and guaranteed a 100% of connectivity.

The resulting network must to be radial and must follow the streets path. Therefore, it can be deployed as an underground network. Moreover, the medium voltage network can connect all the transformers through *Minimal Steiner Tree* [4], for its radial nature (Imase and Waxman, 1991).

The medium voltage network starts in the substation and through one feeder supplies the power to the entire network of transformers. Moreover, the transformers allocation is shown in Figure 3.4 that is limited by the distance and connectivity constraints.

In Figure 3.5 it is shown the implementation of the low voltage network, which represents the result of the application of *Algorithm 1*.

The Lower Voltage(LV) network connects the end users to the nearest point in the path and then links it to the connection to the nearest transformer. The resulting connectivity is 100 %. The total distance in this network accomplishes the distance

[4]Imase, M., Waxman, B. M. (1991). Dynamic Steiner Tree Problem. SIAM Journal on Discrete Mathematics, 4(3), 369–384. https://doi.org/10.1137/0404033

constraint from the house to the transformer.
Figure 3.6 shows the studied scenario in the geographic area. It is divided into clusters using *k-medoids* algorithm to assign the power consumption and the allocation of the PV panels. Depending on end user cluster, the end user the power consumption is *10 [KW]* of power.

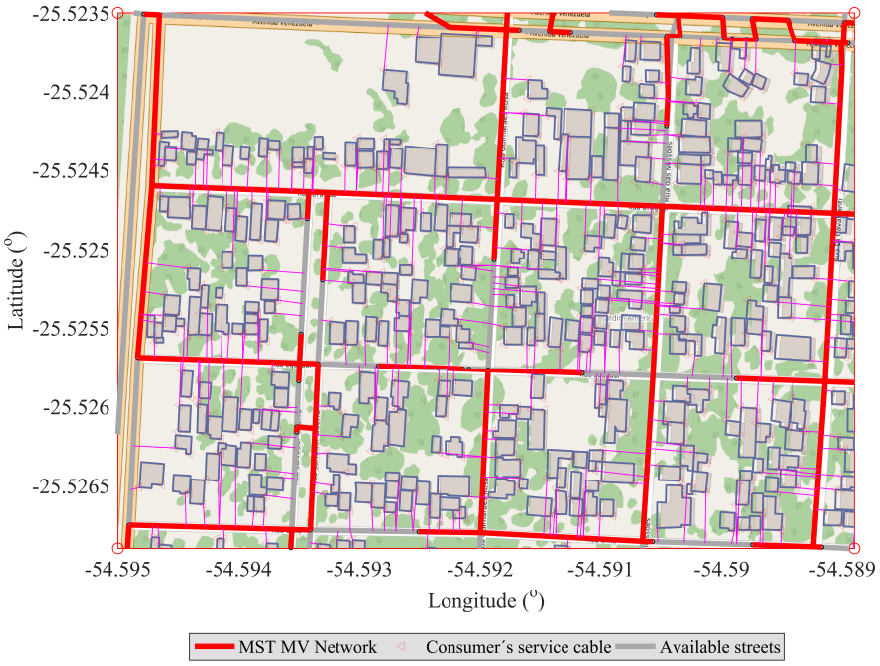

Figure 3.4: Optimal medium voltage network, that connect the substation with the transformers in Brazil.

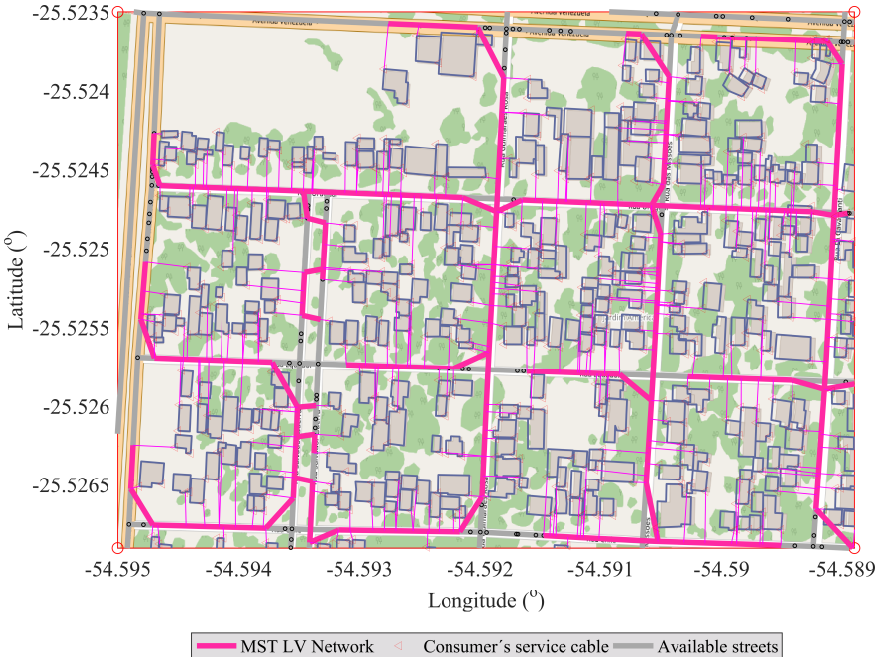

Figure 3.5: Optimal low voltage network connecting the transformers with customers, accomplishing the problems constraints.

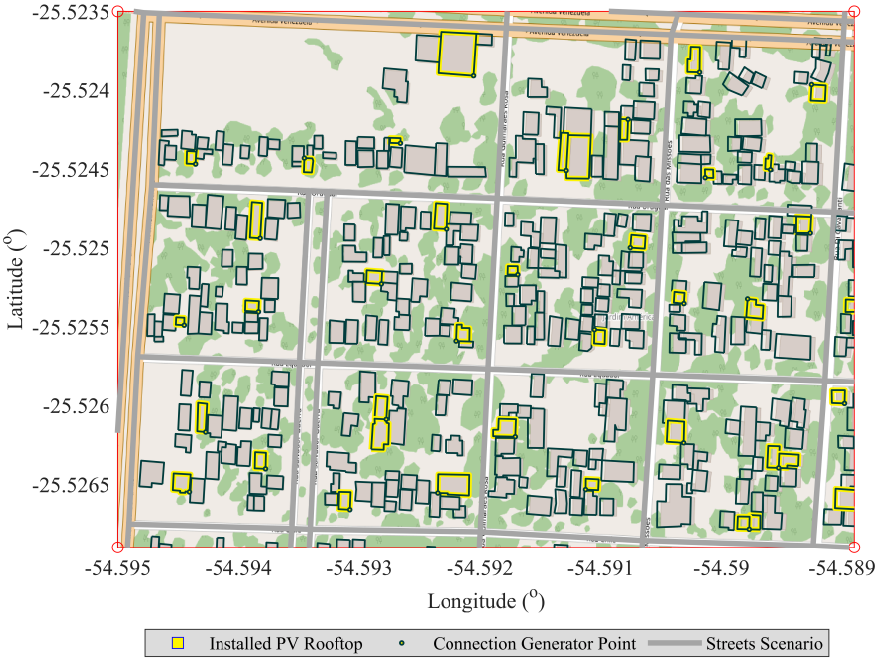

Figure 3.6: Optimal Medium Voltage Network, that connect the substation with the transformers in Brazil.

The second case study is part of the EDS of the area of *Tytherington* in the north of *Macclesfield* in *Cheshire*, England. The limits in longitude in the present study are -2.1360 to -2.1270, meanwhile, the latitude starts from 53.2730 to 53.2810, the total

area is 1.15 Km^2.
In the scenario, there are 813 loads with a total power of *5.4 [MW]*. The presented model deploys the EDS, including the network planning expansion. Therefore, the model designs an efficient and reliable EDS, with the lowest investment cost. The network planning expansion allows us to use the initial configuration and expand the EDS with a short and medium time period. The model was developed with the algorithm presented in the last section, which was implemented in *Matlab*.
In the Table 3.3 are presented the simulation parameters used in the implementation. The selected area has a density of 700 end users per Km^2, which is considered lower in comparison with the average density in the cities in Europe. The deployment requires a maximum distance of 100[m] from an end user to transformer, with a coverage of 100% in the entire network.
The installation type in both networks is under grounded and the configuration is radial in order to accomplish with the EDS requirements. The number of main feeders from the substation is one. Whilst, the voltage in the MV installation, between the substation and the transformers, is 11[KV], and the LV network voltage is 400[V]. Finally, the concentrated load is balanced in all the experimental procedure.

Table 3.3: Parameter of Model Simulation Model.

Item	Parameter	Value
End user information	Density	700 per Km^2
	Amount in study	813 in all study
	Location	Geo-reference
Deployment	Max transformer distance	100 m
	MV Network transformer coverage	100%
	LV Network end users coverage	100%
MV network parameters	Installation type	Under-grounded
	Network configuration	Radial
	Number of primary feeders number	1
	Voltage level	11 [KV]
	Total power demand	5.4 [MVA]
LV network parameters	Installation type	Under-grounded
	Network configuration	Radial
	Voltage level	400 V
	Concentrated load	balanced

Figure 3.7, which was generated with distance and connectivity constraints of 100[m] and 100%, correspondingly. In the present scenario, there are 55 transformers

located in the candidate sites, accomplishing the desired constraints. The planned routing is radial, following the routes of the streets, consequently, the MV network can be implemented as an underground network. The MV network length is 12.15[Km^2], connected by one conductor all the transformers through Minimal Spanning Tree (MST). In this scenario, there are 21 transformers and 2[Km] of conductor less than the initial simulation. However, those savings affects the LV distribution network design because the reduction in the transformers amount represents the overloading of them. Moreover, the transformers power capacity must be raised by reason that the corresponding demand will the higher.

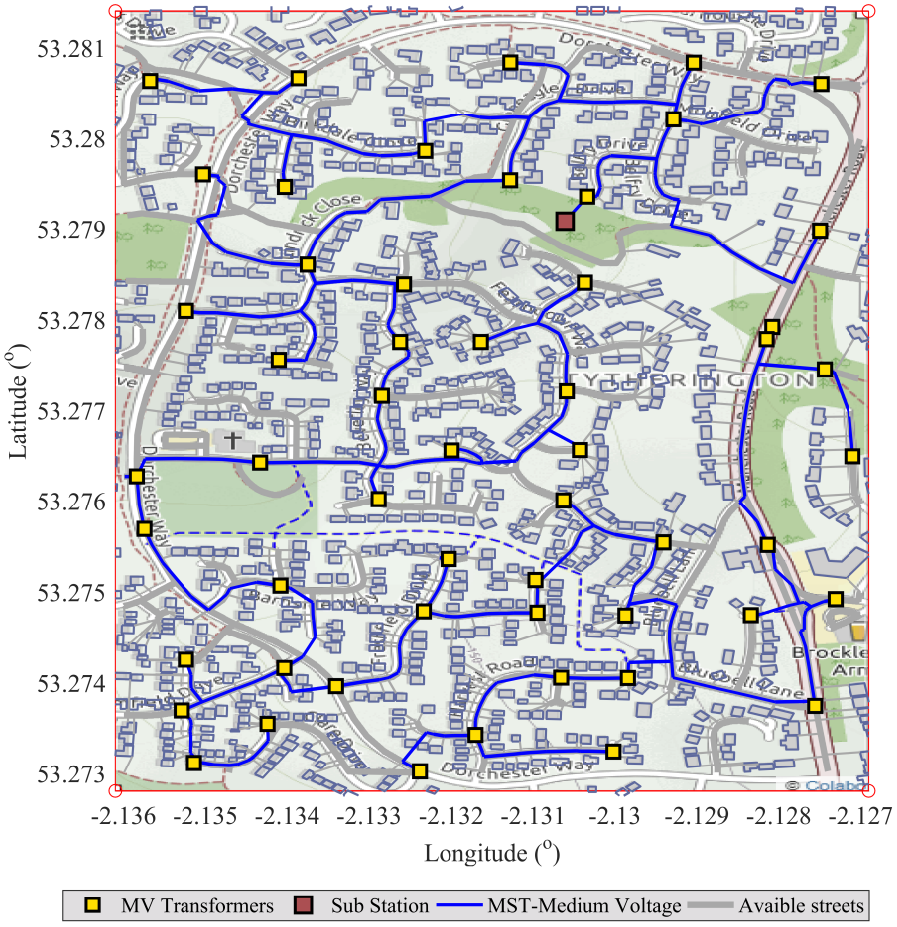

Figure 3.7: Optimal medium voltage network, that connect the substation with the transformers in UK.

The LV network was designed through Algorithm 1, explained in the sections above. The obtained result is presented in Figure 3.8, there is shown the georeferenced scenario withLV network implementation and irregular polygons sketched in the graph, delimiting the transformers area of service. The end users with 100% connectivity are connected to the LV network through the operator service cable. Those cables connect the home nearest point to the corresponding nearest street point; this calculation is included in the model. The distance in the LV network includes the length from house

to the street and from that point down the street to the transformer. The model for the LV network design is subject to the application of distance restriction.
Figure 3.9 shows the allocation of PV rooftop. All the PV panels have a power of 10[KVA]. The percentage of houses with PV panels are 10% of all the scenario, in total 79 houses, with a total power of 790[KV]. As a result, the rooftop PV panels contribute to 14.5% to the total power demand. Notice that the distribution of the rooftop PV are in all the maps, showing the practical allocation of the PV panels. The PV will reduce the power consumption of the power delivered from the substation in approximately 10%. The MV transformer should be bidirectional for the implementation. The design should include the protection and network control.
The results are shown in table 3.4, where the distance constraint in the scenario, between end user to the corresponding transformer are 100[m]. The coverage is 100% and the % of drop voltage is less than 2%. The number of activated transformers for the scenario a is 55 transformers with a MV grid length of 12.15[Km], and the distance of the transformer to the end user is 40[m].

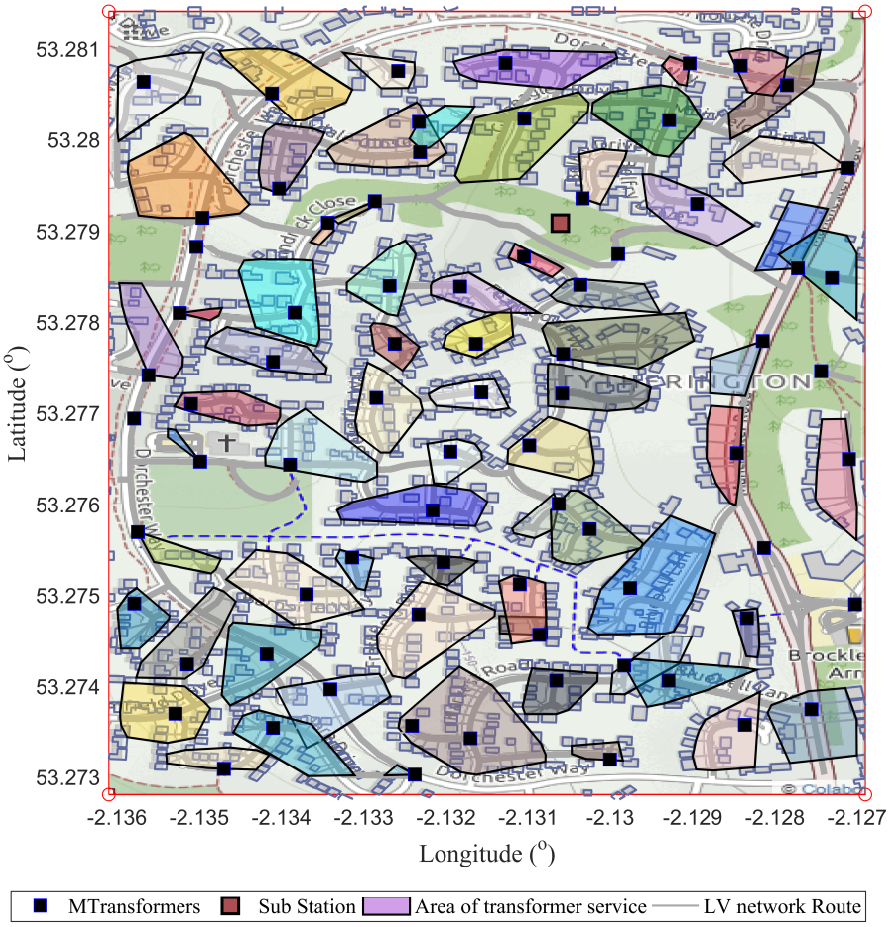

Figure 3.8: Optimal low voltage network connecting the transformers with customers, accomplishing the problems constraints.

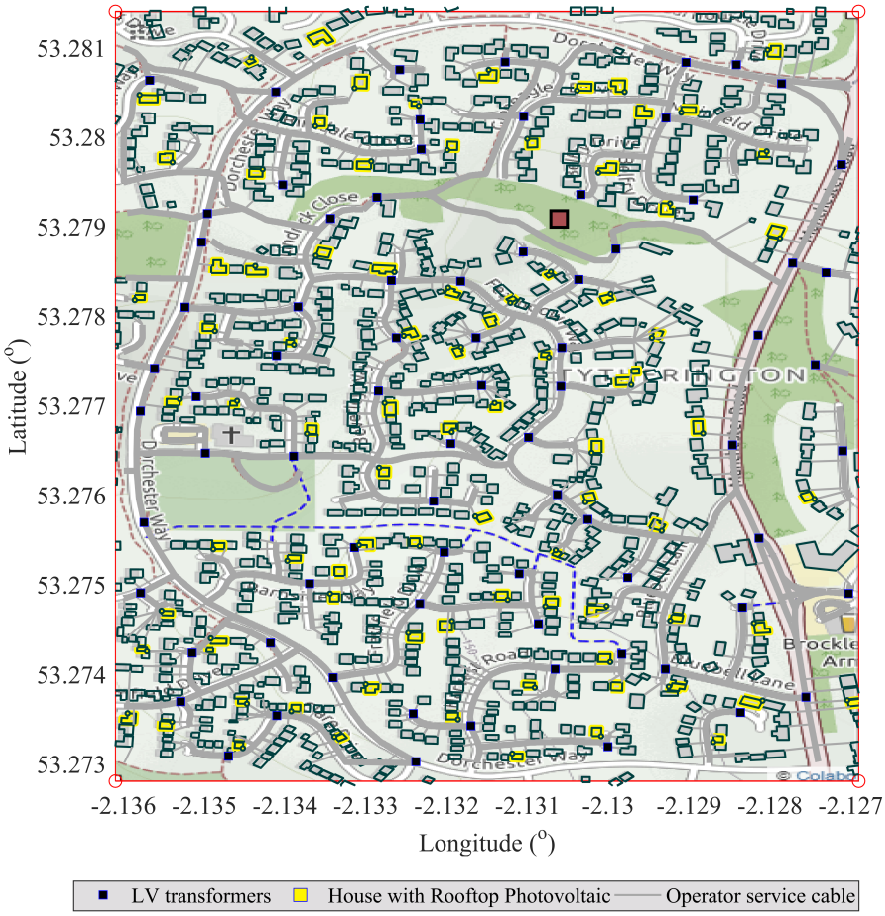

Figure 3.9: Location of PV generator using *K-medoids* algorithm in the 10 % of users.

Table 3.4: Implemented Results.

Specification	Scenario B
Max distance model constraint [m]	100
MV and LV Coverage [%]	100
Distribution transformers [number]	55
MV grid length [Km]	12.15
Voltage drop in [%]	Max. 2%
LV Transformer to end user average distance [m]	40m

Chapter 4

Control System Methodology

4.1 Microgrid Reference Model

The distribution system mostly operates in AC, but there are several DG, ESS and loads, which operates in direct current. Thus, an hybrid AC/DC MG combines DC and AC devices, joining the best characteristics of both types.
The hybrid MG challenges future research topics, for instance control strategies for power flow regulation, efficiency and reliability improvement.
The scalability of hybrid MG is going to easily integrates new RES technology in the future, and the cost for those changes might be minimum.
Several MG configurations have different features, each one presenting advantages and drawbacks, depending of the application. Among the hybrid MG, there exists the completely isolated type. On the one hand, it is low cost and maintenance, but it also has low scalability capacity. One example of EDS is on Figure 4.1. On the other hand, it has high dimensions, high reliability, also has medium capacity for controllability and fault management. All the characteristics should be compared with partially isolated (Unamuno and Barrena, 2015a).

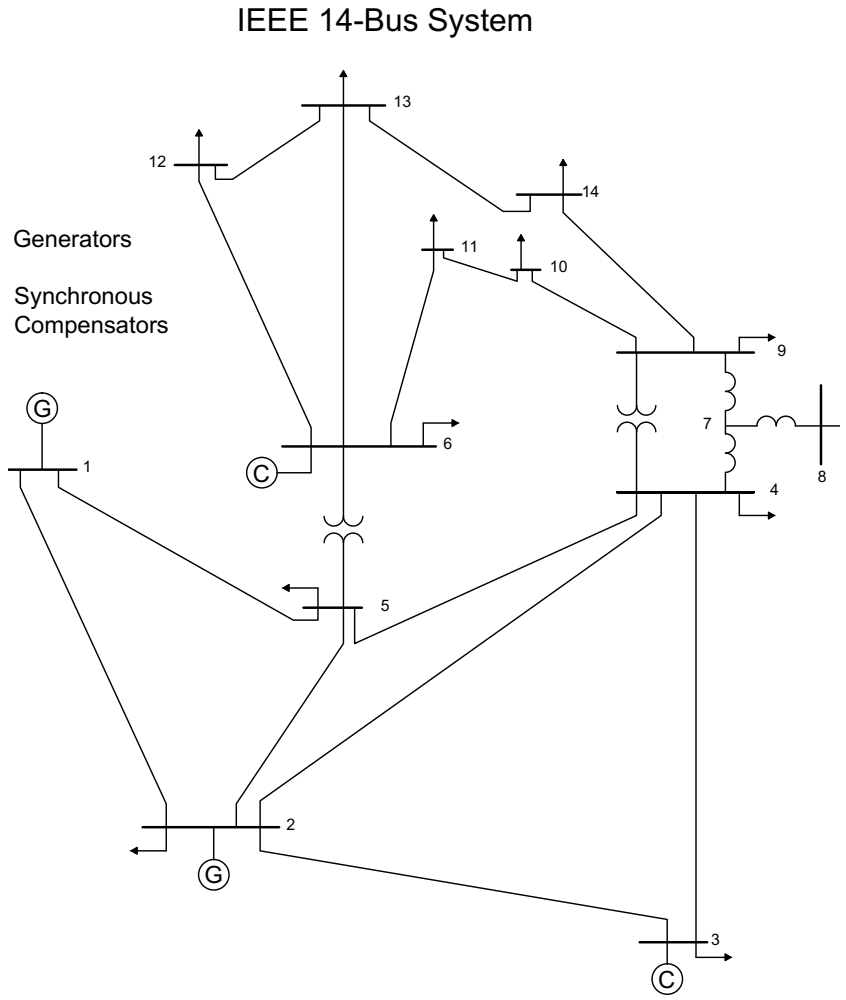

Figure 4.1: Reference model system from IEEE with 14 bus bar.

4.2 Plant Modelling

The identification is based on the correlation approach that uses the input and the outputs from the system. The data are acquired form an experimental procedure in a fixed time. For example, the input *u(k)* produces a output *y(k)* for k time. This information defines the mathematical model for the analysis of the static and dynamic behaviour of the system.
It is fundamental to define the input or excitation signal for the system, which must

have several components in frequency and amplitude (Valverde Gil and Gachet Páez, 2007). The use of strategies to reduce the system order results in lack of resolution in the representation of real system, however the model is convenient to design methodologies with effortless approaches.
The research has considered for the PV mathematical model, shown in Figure 4.2, based on a single-diode model with sufficient accuracy and a moderate complexity, as shown by Eqs. 4.1-4.7. The nomenclature is reported in Table 4.1 (Piliougine et al., 2021; Vallejos, 2017).
The model includes a R_S, as in Eq. 4.6, that represents the series resistance and the resistance in the cell. The R_S accurately shapes the Point of Maximum Power (MPPT) and the V_{OC}, according to Eq. 4.6. The diode includes a quality factor n to match accurately the PV curve.
The current-Voltage (I-V) relation follows Eq. 4.1, which is the difference between the photo-current I_L and the product of the reverse saturation current I_0 and an exponential component due to voltage and temperature.
The current source generates I_{ph} which is proportional to the sun light hitting the panel. In the night or shading conditions, the solar cell acts as p-n junction diode. The diode gives the I-V characteristics to the PV cells. Eq. 4.2 represents the temperature function of the cell.

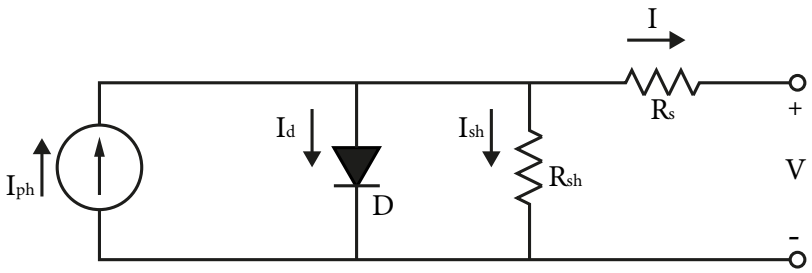

Figure 4.2: Equivalent circuit for the solar cell.

Table 4.1: Parameters and variables PV modelling.

Nomenclature	Description
I	Output current
I_d	Diode or dark current
I_0	Reverse saturation current
I_{ph}	Photo current
R_s	Cell series resistance
V_{OC}	Open circuit voltage
I_{SC}	Short circuit current
R_{sh}	Cell shunt resistance
n	Diode quality factor
S	Ambient irradiation
S_{nom}	Nominal irradiation
K_0	Temperature coefficient of I_{SC}

$$\mathrm{I} = \mathrm{I}_{ph} - \mathrm{I}_0 \left(e^{\frac{q(\mathrm{V}+\mathrm{IR}_\mathrm{S})}{nk\mathrm{T}}} - 1 \right) \tag{4.1}$$

$$\mathrm{I}_{ph} = \mathrm{I}_{ph}(\mathrm{T}-1) + \mathrm{K}_0(\mathrm{T}-\mathrm{T}_1) \tag{4.2}$$

$$\mathrm{I}_{ph}(\mathrm{T1}) = \mathrm{I}_{\mathrm{SC}}(\mathrm{T}_1)\frac{\mathrm{S}}{\mathrm{S}_{nom}} \tag{4.3}$$

$$\mathrm{K}_0 = \frac{\mathrm{I}_{sc}(\mathrm{T}_2) - \mathrm{I}_{sc}(\mathrm{T}_1)}{\mathrm{T}_2 - \mathrm{T}_1} \tag{4.4}$$

$$\mathrm{I}_0 = \mathrm{I}_0(\mathrm{T}_1)\left(\frac{\mathrm{T}}{\mathrm{T}_1}\right)^{\frac{3}{n}} e^{\frac{qVg}{nk\left(\frac{1}{\mathrm{T}}-\frac{1}{\mathrm{T}_1}\right)}} \tag{4.5}$$

$$\mathrm{R}_\mathrm{S} = -\frac{d\mathrm{V}}{d\mathrm{I}_{\mathrm{V}_{\mathrm{OC}}}} - \frac{1}{\mathrm{X}_\mathrm{V}} \tag{4.6}$$

$$\mathrm{X}_\mathrm{V} = \mathrm{I}_0(\mathrm{T}_1)\frac{q}{nk\mathrm{T}_1} e^{\frac{q\mathrm{V}_{\mathrm{OC}}(\mathrm{T}_1)}{nk\mathrm{T}_1}} \tag{4.7}$$

The description of a MG source is required for applications such as control, stability, monitoring and protection. This modelling process can have two approaches: the first, finding the model for each component, which can cost difficulties, and methods for reduction can be useful to limit the complexity. The second derives the model for the overall system using stochastic or predictive algorithms.
It is important to mention that there is not an unique representation for a system and it is preferable to have the least order possible. A system can be represented by a transfer function or a state-space model (Sen and Kumar, 2018).

The research (Popov et al., 2010) presents a DER DC source connected to a LV distribution network by an power inverter, the model includes a Distributed Generation (RLC) load and the distribution network dynamics is not taking into account. The model is described by Eqs. 4.8-4.10.

Table 4.2: Parameters and variables for MG modelling.

Nomenclature	Description
V_{DC}	DC nominal voltage
r_1	Resistance filter
L_f o l	Inductance filter
C	Capacitance filter
ω_0	Nominal frequency
RLC	Flexible load
I_{fd}	Filter current in d frame
I_{fq}	Filter current in q frame
I_L	Output current
V_C	Capacitor/output voltage
T_S	Sample time
δ	Duty cycle from controller

$$A = \begin{bmatrix} -\frac{r_1}{L_t} & \omega_0 & 0 & -\frac{1}{L_t} \\ \omega_0 & -\frac{r_1}{L} & -2\omega_0 & \frac{R_l C\omega_0}{L} - \frac{\omega_0}{R} \\ 0 & \omega_0 & -\frac{R_l}{L} & \frac{1}{L} - \omega_0^2 C \\ \frac{1}{C} & 0 & -\frac{1}{C} & -\frac{1}{RC} \end{bmatrix} \tag{4.8}$$

$$B^T = \begin{bmatrix} \frac{1}{L_f} & 0 & 0 & 0 \end{bmatrix}; C = \begin{bmatrix} 0 & 0 & 0 & 1 \end{bmatrix}; D = [0] \tag{4.9}$$

$$X^T = \begin{bmatrix} I_{fd} & I_{fq} & I_L & V_c \end{bmatrix} \tag{4.10}$$

The selected model provides a simple approach to design the controller that is represented by model of Figure 4.3, where it is reduced from the 4^{th} to 3^{rd} order. Moreover, it presents the required dynamics to describes the system complexity. The input of the system is the duty cycle δ from the controller and the output is the voltage on the capacitor V_C. The Pulse Width Modulation (PWM) block represents the dynamics from the power electronics of the inverter represented by Eq. 4.13. Eq. 4.11 represents resistive and inductance filter, while Eq. 4.12 represents the capacitance of the filter. The feedback loop of $1/Z_L$ in series with Z_C gives the plant description by Eqs. 4.14 and 4.14 that show the output and input relationship.
Eq. 4.16 is used to determine the second order state-space model of Eqs. 4.17, 4.18, which represents the LV behaviour. On the other hand, Eq. 4.13 is considered in series to take into account the inverter components. The final description corresponds to

the 3^{rd} order model of Eq. 4.19. Its state-space representation has the form of 4.24, using equation 4.20-4.21 for facilitating representation.

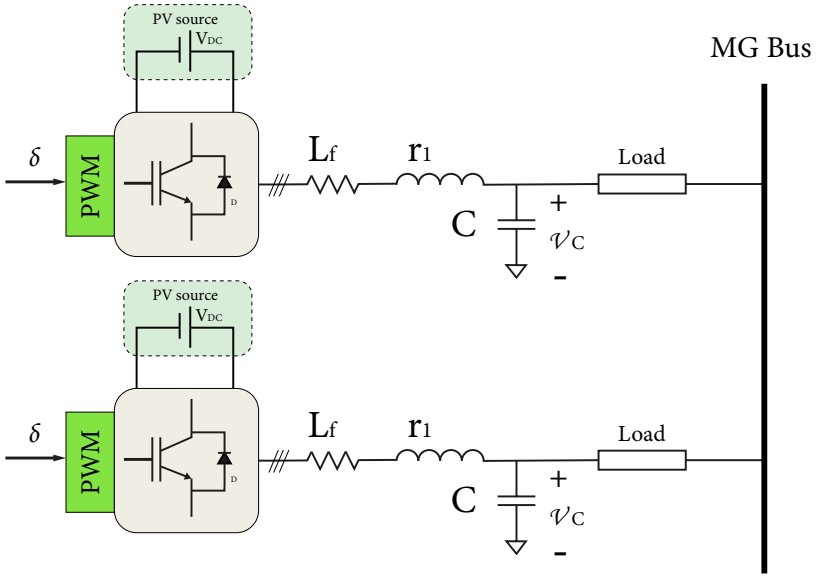

Figure 4.3: Electric representation of the MG for plant modelling.

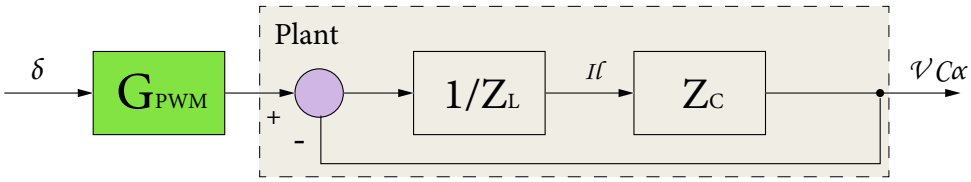

Figure 4.4: Block diagram of the plant model.

$$Z_L(s) = sL_f + r_1 \tag{4.11}$$

$$Z_C(s) = \frac{1}{sC} \tag{4.12}$$

$$G_{PWM}(s) = \frac{\frac{V_{dc}}{2}}{1 + 1.5T_s s} \tag{4.13}$$

$$G_P = \frac{\frac{Z_C}{Z_L}}{1 + \frac{Z_C}{Z_L}} = \frac{Z_C}{Z_L + Z_C} \tag{4.14}$$

$$G_P = \frac{1}{Clx^2 + Crx + 1} = \frac{V_{c\alpha}}{\delta} \tag{4.15}$$

$$C l \ddot{\mathrm{V}}_{\mathrm{C}} + C r \dot{\mathrm{V}}_{\mathrm{C}} + \mathrm{V}_{\mathrm{C}} = \delta \tag{4.16}$$

$$\begin{bmatrix} \dot{x_1} \\ \dot{x_2} \end{bmatrix} = \begin{bmatrix} 0 & 1 \\ -\frac{1}{Cl} & -\frac{r}{l} \end{bmatrix} \begin{bmatrix} x_1 \\ x_2 \end{bmatrix} + \begin{bmatrix} 0 \\ \frac{1}{Cl} \end{bmatrix} \delta \tag{4.17}$$

$$y = \begin{bmatrix} 1 & 0 \end{bmatrix} \begin{bmatrix} x_1 \\ x_2 \end{bmatrix} \tag{4.18}$$

$$\mathrm{G_P} * \mathrm{G_{PWM}} = \frac{\frac{\mathrm{V}_{dc}}{2}}{as^3 + bs^2 + cs + 1} \tag{4.19}$$

$$a = 1.5LCT \tag{4.20}$$

$$b = C(1.5Tr + \mathrm{L}) \tag{4.21}$$

$$c = 1.5T + Cr \tag{4.22}$$

$$a \dddot{\mathrm{V}}_{\mathrm{C}} + b \ddot{\mathrm{V}}_{\mathrm{C}} + c \dot{\mathrm{V}}_{\mathrm{C}} + \mathrm{V}_{\mathrm{C}} = \delta_{in} \tag{4.23}$$

$$\begin{bmatrix} \dot{x_1} \\ \dot{x_2} \\ \dot{x_3} \end{bmatrix} = \begin{bmatrix} 0 & 1 & 0 \\ 0 & 0 & 1 \\ -\frac{1}{a} & -\frac{c}{a} & -\frac{b}{a} \end{bmatrix} \begin{bmatrix} x_1 \\ x_2 \\ x_3 \end{bmatrix} + \begin{bmatrix} 0 \\ 0 \\ \frac{\mathrm{V}_{dc}}{2a} \end{bmatrix} \delta_{in} \tag{4.24}$$

$$\mathrm{X}^{\mathrm{T}} = \begin{bmatrix} \mathrm{V_C} & \mathrm{I_C} & \ddot{\mathrm{V}}_{\mathrm{C}} \end{bmatrix} \tag{4.25}$$

4.3 Primary Control

The design process for the hierarchical control is addressed in this sections, which is implemented for multiple control objectives and it is required for their coordination. Furthermore, the MG must operate in an optimal way in different time-scales, which allows the multiple layer control. In the literature it is difficult to define the best structure for hierarchical control. However, there are mainly two-layer and three-layer control. In this research it is applied the latter approach to control the MG (Shuai et al., 2018).

The hierarchical strategy starts with primary control, that is the lower level, which implements the voltage and current control loops. In Figure 4.5 it is shown a schematic diagram of primary control and electrical elements in the system, starting from the power stage, which implements the Power Electronics (PE). Next, the filter reduces the oscillation in the output voltage from VSI (Majumder et al., 2010).

The measurements are acquired from the voltage and current sensors, which are in each phase of filter and load, and they are implemented through voltage and current transformers. It is also included a conditioning and protection signal, to avoid high

voltage. Those measurements feed the controller that enables the operation of the VSI. Therefore, the isolation and driving circuit follow, which are associated to the connection between the source, in this case PV, and the power stage.
The primary level can be designed by means different strategies, for instance, impedance control. The reference values for this control are calculated by means of the secondary control system (Wang et al., 2018a,b).

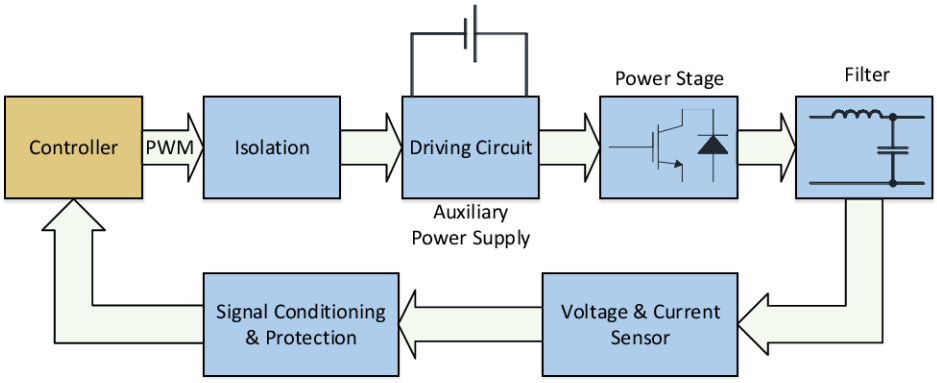

Figure 4.5: Primary Controller in SPSS.

The control approach is in cascade structure, using an inner and outer loop, of current and voltage, respectively. There are several advantages, for instance, shortening the THD in the voltage filter capacitor, preserving the inductor filter current within the operational limits, rejecting disturbances, and allowing change the operational mode, maintaining the control scheme (Unamuno and Barrena, 2015b).
There are several strategies for inner current and voltage-control loops. The research defines the inner loop as the primary control due to its importance in achieving maximum output power. In grid-connected, the MPPT specifies a certain current and voltage. Nevertheless, in stand-alone solutions, the produce power depends on the load (Hosseinzadeh and Salmasi, 2015).
In Figure 4.6 it is shown the control scheme for primary control. The α and β sequence used stationary reference frame by means of the Clarke transformation, which are expressed by Eq. 4.26. This transformation changes the 3-phase frame to the $\alpha\beta$ and zero input, in order to simplify the calculation due to it stationary behaviour (Antoniadou-Plytaria et al., 2017).
The applied method represents the voltage feedback, which regulates the voltage comparing the output voltage with the reference value (Palizban and Kauhaniemi, 2015). The same for the inner current loop, which compares the output inductor current with the reference voltage received from the voltage loop.
In Figure 4.6 it is shown the primary control, including the blocks that represent the defined plant. Before the G_{PWM} block, there is the current controller G_I, using the PID controller, implemented to follow the reference current. The feedback loop includes the relation $1/Z_C$, which transforms the output voltage into current to subtract it

to the reference current, Il_{ref}. Before it, there is the voltage controller G_V, applying Proportional Resonant (PR) scheme, to follow the reference voltage received from the secondary control and subtract the feedback output voltage (Ziouani et al., 2018; Teodorescu et al., 2006).

$$\begin{bmatrix} \alpha \\ \beta \\ 0 \end{bmatrix} = \frac{2}{3} \begin{bmatrix} 1 & -\frac{1}{2} & -\frac{1}{2} \\ 0 & \frac{\sqrt{3}}{2} & -\frac{\sqrt{3}}{2} \\ \frac{1}{2} & \frac{1}{2} & \frac{1}{2} \end{bmatrix} \begin{bmatrix} a \\ b \\ c \end{bmatrix} \tag{4.26}$$

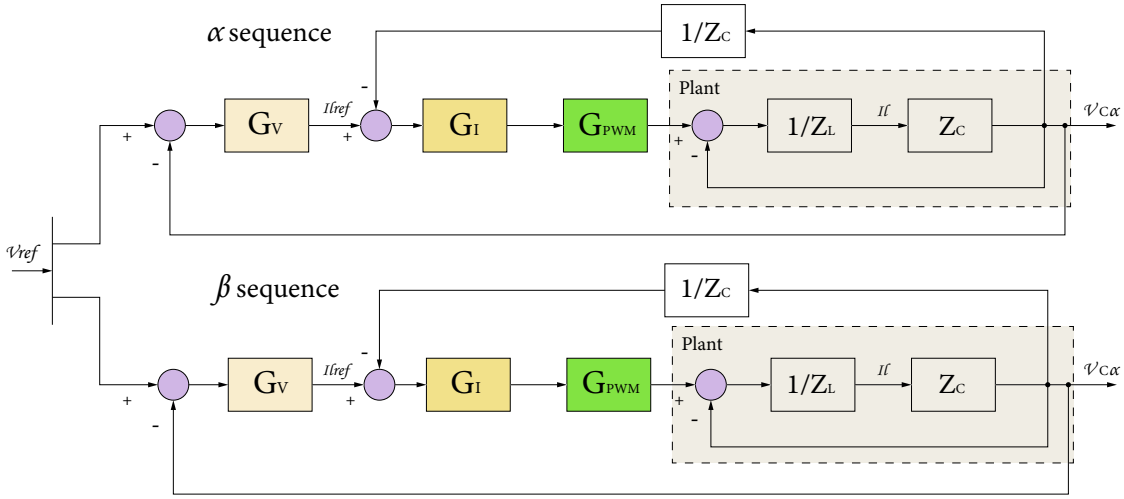

Figure 4.6: Block diagram of primary control the voltage and current structure.

The current loop objective is to inject a higher gain into the reference signal frequency, thus reducing the disturbance effects in the system, as shown by Eq. 4.27. On the other hand, the outer voltage control loop removes the voltage harmonics, whether there are nonlinear loads in the system, equation 4.28. The current and voltage loop are crucial in the system final performance (González-Castaño et al., 2020).
The voltage outer loop is responsible for controlling the capacitor filter voltage, comparing it with the reference signal received from the secondary loop. On the other hand, the output from voltage outer loop is the reference current for the inner current loop. The inner loop dynamics should be faster than the outer loop ones to maintain the stability in the system (Wang et al., 2019; Visioli, 2004).
The current controller is implemented by means PID controller of Eq. 4.27, which includes a a first-order low-pass filter, to reduce the noise in the control variables. The PID controller is probably the most common structure applied in industry. PID tuning is calculated with Ziegler-Nichols (ZN) or Force Oscillation Method (FOM)[1], using the

[1]Lorenzini, C., Bazanella, A. S., Pereira, L. F. A., Gonçalves da Silva, G. R. (2019). The generalized forced oscillation method for tuning PID controllers. ISA Transactions, 87, 68–87. https://doi.org/https://doi.org/10.1016/j.isatra.2018.11.014

Algorithm 2 and *3* (Lorenzini et al., 2019; Levine and Koltun, 2012).

$$G_i(s) = K_{pi}\left(1 + \frac{1}{T_{ii}s} + \frac{T_{di}s}{\frac{T_{di}}{N}s + 1}\right) \tag{4.27}$$

$$G_v(s) = k_{pv} + \frac{k_{rv}s}{s^2 + \omega_c s + \omega_0^2} \tag{4.28}$$

All the systems can be solely controlled by an integral action, the constraint is that the system must have minimum phase. But, the controller can cause poor transient response. A proposed solution is adding a proportional element to achieve a closed-loop stability and robustness (Pereira and Bazanella, 2015).
The first can be used for any ZN tuning process, where is important to define the transfer function for the controlled plant. After that, a PR is connected in series. Here, two method can be used, if the gain margin is determined through mathematical tools, and it can be used directly. While, the other possibility is applying the increase of the proportional gain towards the plant oscillation method in closed loop (Pinzón and Pavón, 2019).
The frequency where the gain margin is located is the W_{cg}, and it is part of the tuning process. If the gain margin cannot be computed, different methodologies can be implemented, for example PR.
Algorithm 3 calculates the PID coefficients using the result from *Algorithm 2*. In step 2, depending on the selected controller is determined the poles controller, 2 or 3, depending if is a Proportional Integral (PI) or PID is desired. Also, the PI or PID variables can be expressed as time constant to be implemented in some industrial devices. Finally, the controller denominator is an integrator s.

Table 4.3: Parameters and variables for primary control.

Nomenclature	Description
K_p	Proportional gain for controller
K_i	Integral term for controller
K_d	Derivative term for controller
K_{cr}	Critical gain for oscillation
P_{cr}	Oscillation period in resonance
ω_{cg}	Oscillation frequency in resonance
T_{ii}	Integral time term for current loop
T_{di}	Derivative time term for current loop
GM	Gain Margin
N	Gain for the derivative filter
DEN_{PI}	Denominator for PI controller
DEN_{PID}	Denominator for PID controller
G_C	Transfer function for controller
G_v	Voltage controller transfer function
K_{pv}	Proportional gain for controller
K_{rv}	Resonant term for controller
ω_c	Resonant frequency
ω_0	Fundamental frequency

Algorithm 2 Tuning procedure for open loop system using ZN.

procedure ZN TUNING(K_{cr}, P_{cr})
  Step: 1 Variables definition
  $K_p, K_i, K_d, K_{cr}, P_{cr}$
  Step: 2 Plant Definition
  Determining the complete transfer function
  $G_1 \leftarrow \frac{\frac{Z_C}{Z_L}}{1+\frac{Z_C}{Z_L}}$
  $G_P \leftarrow G_{PWM} * G_1$
  Step: 3 Eliminating components controller
  Guaranteeing proportional controller
  $K_i \leftarrow 0$
  $K_d \leftarrow 0$
  Step: 4 Proportional controller
  K proportional constant
  $G \leftarrow K * G_P$
  Step: 5 Determine gain margin
  if GM is determined = $True$ **then**
    $K_{cr} = GM$
  else
    while $K = O : constant : K_{cr}$ **do**
      if Closed loop GP is oscillating **then**
        $K_{cr} = K$
    if $GM = \infty$ **then**
      Applied PR controller
  Step: 6 Oscillation period
  W_{cg} where GM is measured
  $P_{cr} \leftarrow \frac{2\pi}{W_{cg}}$ ▷ Ending

Algorithm 3 PID initial coefficient using ZN tuning.

procedure PID INITIAL(G_c)
  Step: 1 Variables definition
  $K_p, K_i, K_d, T_i, T_d, K_{cr}, P_{cr}$
  Step: 2 PID denominator
  if $case = 1$ **then**
    PI controller
    $Den_{PI} = \frac{K_{cr}}{2.2}\left[1 \quad \frac{1.2}{P_{cr}}\right]$
  if $case = 2$ **then**
    PID controller
    $Den_{PID} = \frac{2*K_{cr}}{1.7*P_{cr}}\left[\frac{P_{cr}}{8} \quad 1 \quad \frac{2}{P_{cr}}\right]$
  Step: 3 Defining independent constants
  $K_p \leftarrow Den_{PI}(1)$
  $T_i \leftarrow Den_{PI}(2)$
  if $Den_{PD}(2) \neq 0$ **then**
    $T_d \leftarrow Den_{PI}(3)$
  $K_i \leftarrow \frac{K_p}{T_i}$
  $K_d \leftarrow K_p T_d$
  Step: 4 Proportional controller
  K proportional constant
  $G \leftarrow K * G_P$
  Step: 5 Defining controller
  if $case = 1$ **then**
    PD controller
    $G_c \leftarrow \frac{Den_{PI}}{s}$
  if $case = 2$ **then**
    PID controller
    $G_c \leftarrow \frac{Den_{PID}}{s}$
▷ Ending

A PR controller is implemented to control the voltage loop, which is used as this loop has infinite gain margin and it is not possible to find a PID controller with ZN. The PR controllers are applied to get a better voltage regulation with less harmonics and eliminates the steady state errors on the control system, and they can be expressed by means of Eq. 4.28 (Wang et al., 2017).
The PR has a resonant frequency, which matches the reference signal, and PR can track a sinusoidal reference signal. The pure integral control is a particular type of PR controller. Comparing with PID classical controllers, where the signal are RMS, the computation cost is increased. The PID modifies the phase and amplitude of the signal components, thus causing delay in the control loop. This solution can affect the overall performance (Teodorescu et al., 2006; Pereira and Bazanella, 2015).

4.4 Secondary and Tertiary Control

The secondary control level has the objective of adjusting references for voltage amplitude and frequency, which are injected into the primary control loops. Moreover, the secondary level control reduces the circulating current. The control strategies for DG units are mainly classified in grid forming and grid following.
The strategy based on the presence of communication implements the grid forming, for example, centralised or distributed control. Furthermore, the grid forming implements different frame, i.e, synchronous reference, stationary reference or natural frame; PI and PR controllers are the more classical approaches exploited for its implementation (Palizban and Kauhaniemi, 2015).
A grid forming approach without communication is droop control. It is usefully when remote DER are in the same MG. The advantages of this methodology includes the reduction of the complexity to cut down the cost of communication medium, effortless implementation and expansion, plug and play modules. However, there are disadvantages like difficulties for power trade-off and voltage deviation, which are solved in the third level control (Vandoorn et al., 2013).
The secondary control regulates the energy flow in the entire system, which is used for sharing the load demand through the generation and storage elements, as shown in Figure 4.7. The secondary loop output is a new reference voltage. Therefore, the secondary control ensures the energy balance and accomplishing the quality requirements, and operational limits of each devices (Naji Alhasnawi et al., 2020).
The Active Power-frequency (P-f) and *Reactive Power-Voltage (Q-V)* relationship based droop control schemes were tested on the inverters.

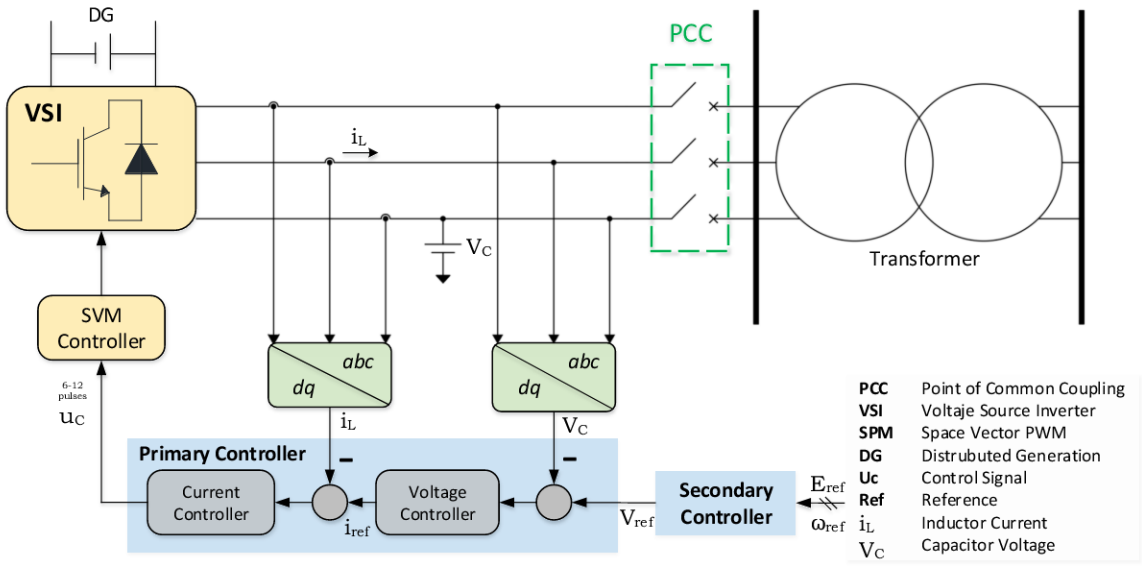

Figure 4.7: Secondary Controller in SPSS.

In a SG, there are several VSI connected in parallel, which produces net interchange. The secondary control provides the reference frequency and voltage to the inner loop . In addition, the secondary loop provides power sharing implementation by P-f and Q-V droop control of Figure 4.8. The compensation is represented by m and n or the deviations of $\delta Q/\delta V$ and $\delta P/\delta\omega$, which maintain the synchronisation in the system within the limits of voltage and stability.
The relations that represents the droop control are represented by Eqs. 4.29 and 4.30. ω and E represents the frequency and voltage, respectively, while ω^* and E^* are the references of these magnitude, respectively. $G_P(s)$ and $G_Q(s)$ are the control transfer functions: it is not possible to implement them by pure integral control, specially in islanded mode, due to the total injected power that will not match the total power (Marín et al., 2019).

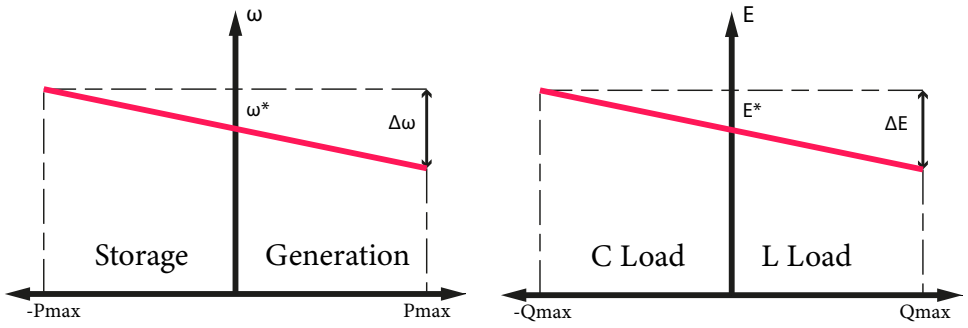

Figure 4.8: Droop control controlling active and reactive power.

Table 4.4: Parameters and variables for secondary and tertiary control.

Nomenclature	Description
G_P	Transfer function for active power controller
G_Q	Transfer function for reactive power controller
G_F	Filter transfer function
δ_E	Voltage variation
δ_ω	Frequency variation
K_e	Proportional gain for controller
V_{pcc}	Point of common coupling voltage
n, n_d	Drop coefficients for P power control
m, m_d	Drop coefficients for Q power control
k_{pE}	Proportional gain for voltage deviation
k_{iE}	Integral gain for voltage deviation
$k_{p\omega}$	Proportional gain for frequency deviation
$k_{i\omega}$	Integral gain for frequency deviation
G_{VR}	Voltage restoration controller
G_{FR}	Frequency restoration controller
G_{LPF}	Filter transfer function
G_d	Primary order transfer function

$$\omega = \omega^* - G_P(s)(P - P^*) \tag{4.29}$$

$$E = E^* - G_Q(s)(Q - Q^*) \tag{4.30}$$

$$\dot{E} = \left[K_e(E^* + \delta E - V_{pcc}) - n(P - P^*) - G_F * n_d(P - P^*)\right] \tag{4.31}$$

$$\omega = \left[\omega^* + \delta\omega + m(Q - Q^*) + G_F * m_d(Q - Q^*)\right] \tag{4.32}$$

$G_P(s)$ and $G_Q(s)$ can be implemented by different control techniques: in this research implements the universal droop control introduced by (Zhong and Zeng, 2016), according to Eqs. 4.31 and 4.32, whilst the implementation in the figure 4.9. E is the RMS voltage and ω is the frequency; both magnitudes are measured in the Point of Common Coupling (PCC), E^* and ω^* are the desired or nominal values, whilst the desired ones for the active and reactive power are P^* and Q^*, depending if the MG is connected to the grid. The desired active and reactive power values in islanded mode are normally zero.
The droop coefficients are n and m, while the droop coefficients due to the active and

reactive power are n_d and m_d, as shown by Eqs. 4.33 and 4.34. The constant K_e is a proportional controller used to regulate the PCC voltage within at a specific range. G_f is the filter implemented to reduce the noise in the signal, described by Eq. 4.35.

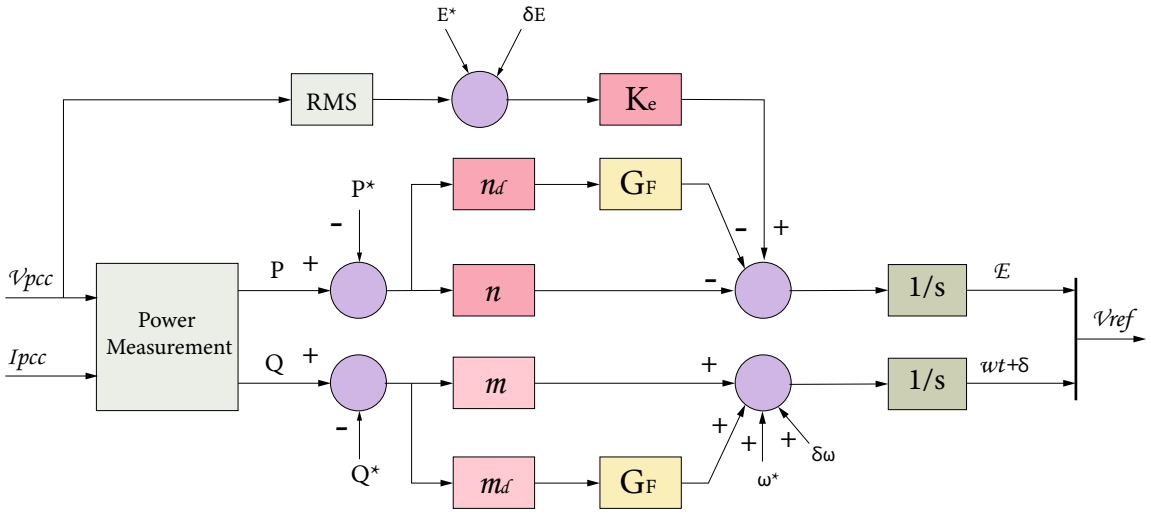

Figure 4.9: Block diagram for the secondary control.

$$n = \frac{\Delta\omega}{P_{max}} \tag{4.33}$$

$$m = \frac{\Delta V}{2 * Q_{max}} \tag{4.34}$$

$$G_F = \frac{100s}{100 + s} \tag{4.35}$$

The tertiary control focuses on the energy management, organising the energy dispatch according to the economic and efficiency point of view (Zheng et al., 2018). The outputs for the tertiary level are the deviation values of frequency and amplitude (Colak et al., 2015) that are used to compensate the deviations produce due to secondary control with respect to their nominal values.
Figure 4.11 shown the voltage and frequency restoration, which uses the V_{pcc} voltage. First, the RMS voltage is computed, which is the measured value for the MG and it is compared with the nominal voltage. Note that G_{VR} of Figure 4.11 controls the loop via Eq. 4.36.
The G_{VR} and G_{FR} in Figure 4.11 represent the PI controllers for the voltage and frequency restoration, described by Eqs. 4.36 and 4.37, respectively. On the other hand, the frequency restoration uses the Frequency Lock Loop (FLL), whose output is the MG frequency, and it is compared with the nominal frequency. The G_{FR} control is described by Eq. 4.37. Finally, the outputs δE and $\delta\omega$ are sent to the secondary loops in each DER.

$$\delta E = k_{pE}(E_{ref} - E_{pcc}) + k_{iE}\int (E_{ref} - E_{pcc})dt \tag{4.36}$$

$$\delta \omega = k_{p\omega}(\omega_{ref} - \omega_{pcc}) + k_{i\omega}\int (\omega_{ref} - \omega_{pcc})dt \tag{4.37}$$

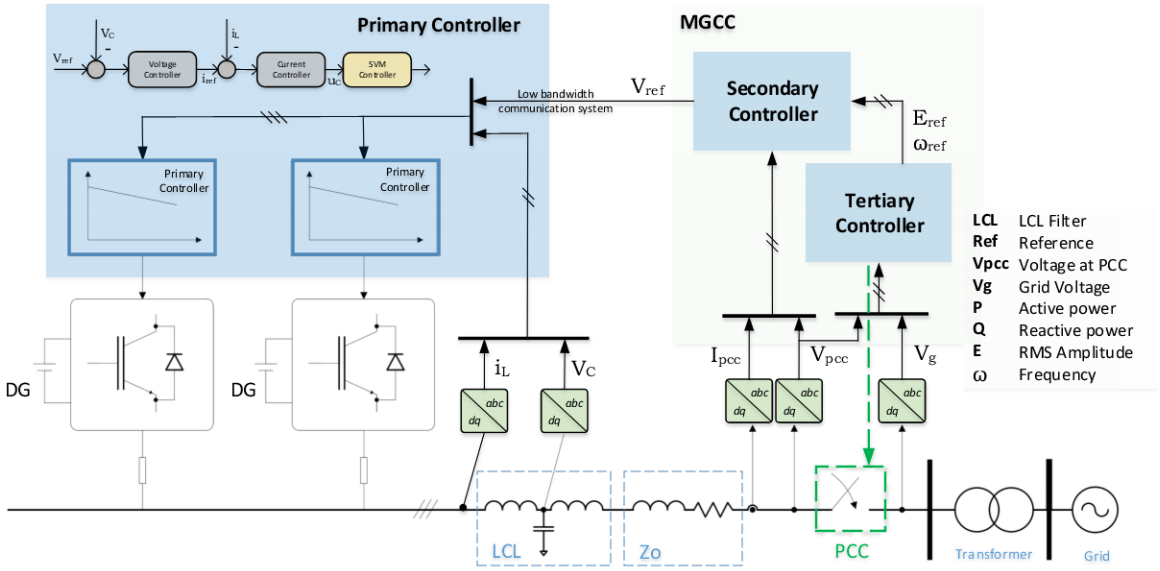

Figure 4.10: Tertiary controller in SPSS.

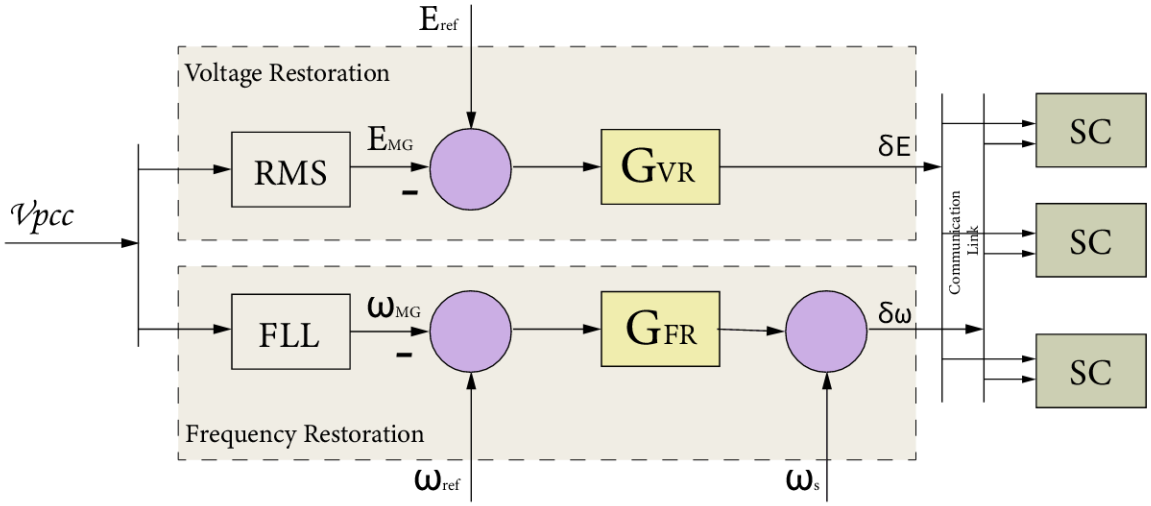

Figure 4.11: Block diagram of tertiary controller in SPSS.

$$G_{VR} = k_{pv} + \frac{k_{iv}}{s} \tag{4.38}$$

$$G_{FR} = k_{p\omega} + \frac{k_{i\omega}}{s} \tag{4.39}$$

The secondary controller receives the variations for δE and δω, shown in Figure 4.12. The implemented approach is based on the uniform changes in the equilibrium point and the dynamic differences between each hierarchical control. Therefore, each external loop should be slower compared with the its inner loop. The change in the dynamics allows to design the controllers independently.

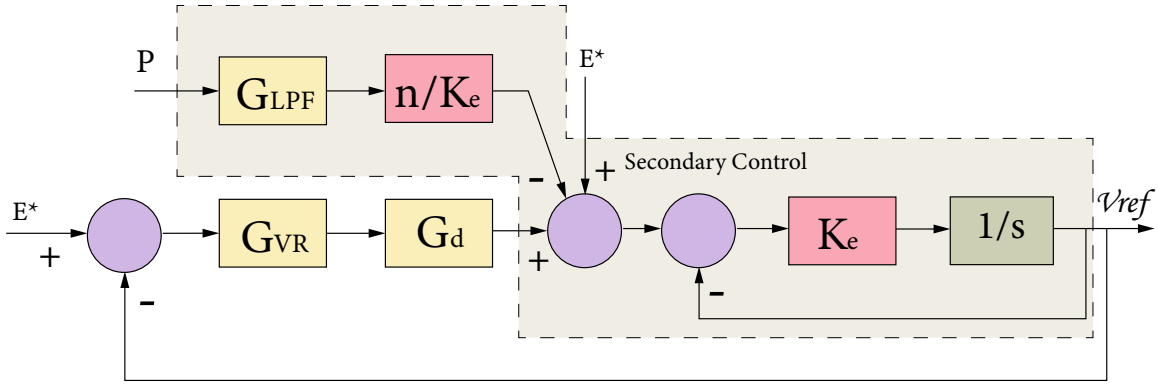

Figure 4.12: Block diagram for secondary and tertiary controller.

4.5 Optimal Control Strategies

This optimisation process is focused on the minimisation of the energy, which is achieved through the incorporation of certain elements in the control structure that allows the system to implement an on-line optimisation, as shown in Figure 4.13 (Ziouani et al., 2018).

The results of the present research to find the model and the optimal control of the substation may be extended to other areas of electrical engineering and other fields of applied control. For example, the optimal control considering energy consumption can be applied to the control centralised generators, where sometimes the determination of certain electrical parameters is most important than their efficiency.

Moreover, there are specific optimisation applications of control techniques in order to find the optimal solution of the regulation problem, which can be focused on search the best energy management in the controlled system.

There are several sub problems within the main fields of the research, for instance the droop control, which represents the main problem to reach the stability in any DER. On the other hand, the optimal operation, which aims to determine the best option to operate the SG; moreover, the optimal control, implemented in SPSS to satisfy all its the technical performances.

Finally, but it not less important, the cost related with the operation is one of the key points in the newest engineering technologies.

As far as it is known, there are no current implementations of optimal control applied in SPSS. Therefor, this research will show the implementation of the proposed solutions, which represents the impact in further investigations.
It is shown that the SPSS represents the principal section in a SG control, thus it should be designed in order to take into account energy efficiency parameters. Moreover, it is supposed that an optimisation approach can be applied to an on-line controller in the system (Padula and Visioli, 2011).
ZN is considered one of the best methods for tuning PID controllers, which uses the step plant response, also it has become a standard in industrial applications.
The cost function can be implemented via performance indices such as Integral Square Error (ISE) in Eq. 4.41, Integral Absolute Error (IAE) in Eq. 4.42, Integral Time Absolute Error (ITAE) in Eq. 4.43 and Integral Time Square Error (ITSE) in Eq. 4.44 (ÖZDEMİR and ÖZTÜRK, 2017; Veronesi and Visioli, 2010).

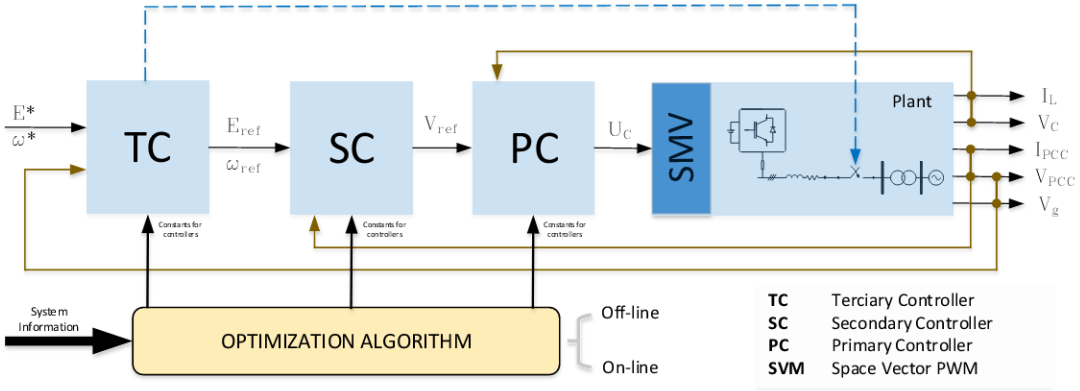

Figure 4.13: Optimization algorithm for SPSS controllers.

$$e(t) = \left[\left(v_{refa} - \frac{v_{Ca}(\theta)}{Z_C}\right) + \left(v_{refb} - \frac{v_{Cb}(\theta)}{Z_C}\right) + \left(v_{refc} - \frac{v_{Cc}(\theta)}{Z_C}\right)\right] \tag{4.40}$$

$$[\text{ISE}]\ \text{J} = \int_0^\infty [e(t)]^2\, dt \tag{4.41}$$

$$[\text{IAE}]\ \text{J} = \int_0^\infty |e(t)|\, dt \tag{4.42}$$

$$[\text{ITAE}]\ \text{J} = \int_0^\infty t\,|e(t)|\, dt \tag{4.43}$$

$$[\text{ITSE}]\ \text{J} = \int_0^\infty t\,[e(t)]^2\, dt \tag{4.44}$$

$$Minimize\ \text{J} = \int_0^\infty [e(t)]^2\, dt \tag{4.45}$$

$$Subject\ to\ 0 < \theta_{1,i} \leq \theta_{imax},\ i = 1,2,3 \tag{4.46}$$

$$Subject\ to\ 0 < \theta_{2,j} \leq \theta_{imax},\ j = 1,2,3 \tag{4.47}$$

$$\theta_1 = \left[K_{pi}\, T_{ii}\, T_{di}\right]^T \tag{4.48}$$

$$\theta_2 = \left[K_{pv}\, K_{rv}\, \omega_C\right]^T \tag{4.49}$$

The performance parameter used to determine whether a control accomplish an objective mainly represented by settling time and maximum overshoot. The t_s, in Eq. 4.50 represents the smallest time where the tracking error is sufficiently small. The normalised tracking error is in equation 4.51, while ϵ is the tolerance that is normally 2% or 5%. In the considered simulation, the reference is a sinusoidal signal, t_s is fixed to 4.55.
M_0 is the maximum overshoot expressed by Eq. 4.53, r is the reference signal. M is the maximum amplitude reached by the output signal when the system is in the transient response, and when the input is an unit step reference. On the other hand, if the reference input is a sinusoidal signal, Eq. 4.54 has an amplitude a_r and a frequency ω_r, t_s and M_0 refer to Eq. 4.55 and 4.56 (Pereira and Bazanella, 2015).

$$t_s = min_{t1} : |e_n(t)| < \epsilon \tag{4.50}$$

$$e_n(t) = e(t)/r \tag{4.51}$$

$$M = max_t \left|y(t)\right| \tag{4.52}$$

$$M_0 = max\left(\frac{M - |r|}{|r|}\right) \tag{4.53}$$

$$r(t) = 0\ \forall\, t < 0, r(t) = a_r sin(\omega_r t)\ \forall\, t > 0 \tag{4.54}$$

$$n_s = \frac{t_s \omega_r}{2\pi} \tag{4.55}$$

$$M_0 = max\left(\frac{M - a_r}{a_r}\right) \tag{4.56}$$

The *Algorithm 4* explains the calculation for the OCP, and the meaning for the variables are in the Table 4.5. The step 1 is the parameter initialisation, defining the tolerance for the procedure. Next, the step 2 is the objective function minimisation; starting from calculating the general error in the line 11. Next, depending of the value of idx is calculated the error; if idx is 1, the calculation is ISE. Finally, in the line 24 is

decided the best calculation method.

Table 4.5: Algorithm parameters for determining the optimal controllers values.

Nomenclature	Description
t	Range of time for evaluating function
dt	Interval time for evaluating function
idx	Index selection for cost function evaluation
θ	Objective function variables vector
F$val(\theta)$	Value at solution for objective function
$Tolfun$	Algorithm toleration termination for F$val(\theta)$
Flag	Flag algorithm for showing the tolerance accomplish
$v_{refa,b,c}$	Reference sinusoidal signals in a,b,c phases
e	error between the reference and output signal
J	Cost function under different performance index

Algorithm 4 Algorithm for determining the optimal parameters for controllers.

procedure OPTIMAL CONTROLLER
  Step: 1 Initial parameters
  $dt \leftarrow t(n) - t(n-1)$
  $t \leftarrow 0 : dt : t(end) * 2$
  $\mathrm{T}olx \leftarrow 1e^{-9}$
  $\mathrm{T}olfun \leftarrow 1e^{-9}$
  $\mathrm{F}lag \leftarrow 0$
  Step: 2 Objective function Minimisation
  while $flag = 0$ **do**

    $e = \sum_{t=0}^{\infty} \left[\left(v_{refabc} - \frac{v_{Cabc}(\theta)}{\mathrm{Z_C}} \right)^2 \right]$
    if $idx == 1$ **then**
      ISE
      $\mathrm{J} \leftarrow \sum e^2 dt$
    if $idx == 2$ **then**
      IAE
      $\mathrm{J} \leftarrow \sum |e| \, dt$
    if $idx == 3$ **then**
      ITAE
      $\mathrm{J} \leftarrow \sum t |e| \, dt$
    if $idx == 4$ **then**
      ITSE
      $\mathrm{J} \leftarrow \sum t \left| e^2 \right| dt$
    if $\mathrm{J} < \mathrm{F}val$ **then**
      Flag=1
    $\mathrm{R}eturn\,\theta$
  EndWhile ▷ Ending

Chapter 5

Simulations, Experiments and Results

This chapter shows the simulations related to the optimal control system, in which the proposed solutions for the optimal control of a smart power substation have been implemented. Firstly, the focus is placed on plant identification for a PV panel. Then, their performances are compared to those of other control methodologies, commonly adopted in the related literature.
After this analysis, the complete system is evaluated. Similarly to the analysis carried out for the single inverter, the optimal control systems for substation are tested, validated and evaluated with respect to other commonly adopted solutions.

5.1 Model Verification

The implemented PV panel parameters are shown in Table 5.1. The system DC bus is 1000 [V], which is a nominal value for DC link generation. The values for shunt and series resistance are represented by R_{sh} and R_s, respectively. There is a DC filter for reducing oscillations, with resistance and inductance, represented by R_{fcd} and L_{fcd}. The power parameters are expressed for each module, for example, the power is 213 [W], the V_{OC} and I_{SC} are 36.3 [V] and 7.84 [A], respectively. While the desired voltage and current are 29 [V] and 7.35 [A], which is the desired Point of Maximum Power (MPP). Then, those values are multiplied by the number of modules in parallel and series, resulting a total current of 345 [A] and a total voltage of 812 [V].
In the model, there are constants for adjusting the PV curve, for example, the parameter, T_r is the reference temperature and K_0 is the temperature coefficient. Additionally, 60 is the number of cells per module, determining the among of power delivered for the entire panel.
Figure 5.1 shows the final I-V curve for the entire array, for example, 15[žC] of temperature, the total V_{MPP} is 812 [V] and the total I_{MPP} is 370 [A]. Those parameters result from the multiplication of V_{MPP} by the modules in series, and I_{MPP} by the modules in parallel. The coordinate (V_{MPP}, I_{MPP}) is the point, corresponding to the maximum power from the panel; normally this point is the desired for extracting the maximum power from the PV module.

Both PV curves demonstrate the temperature dependency of this type of generation system. Comparing their behavior, both curves intersect with X and Y axis in the same point, V_{OC} and I_{SC}, respectively. However, the MPP reduces towards the origins; if the temperature is higher the power delivered to load reduces, for instance with a temperature 10ºC less than the nominal case of 25ºC, the possible power increases.
The power delivered to a load from PV module is represented by a linear relationship $y = \frac{1}{R}x$, starting in the centre of the coordinate axis. The line slope 1/R, then the power delivered to load depends on its resistance value. Then, the objective is to find the optimal value for the resistance R_{opt}, changed virtually by the controller, where the PV module generates the maximum power amount.
I-V curve can be divided by R_{opt} line. Above the line, the resistance is small, and PV acts like a constant current source and the current delivered to the load is close to I_{SC}. On the other hand, below the line, PV acts like a constant voltage source, and the load is fed by a voltage close to V_{OC}.
Figure 5.2 shows the relation between the voltage and the output power. The MPP changes as the temperature varies, the maximum possible power in 15[žC] is higher than 25[žC] of temperature. Moreover, the voltage of the MPP varies with the temperature, the possible voltage would be higher with smaller temperature. The initial slope is similar, starting from the beginning of the coordinate axis.
There are control strategies for extracting the maximum amount of power from the PV, and these methods are called MPPT, which are applied specially to DC MG with a DC-DC converter or when the connected load is purely resistive. The MPP is optimally reached by means $1/R_{opt}$; then the control method implements the variable virtual resistance to change the load and modifying the point of power.

Table 5.1: System parameters for PV source.

Parameter	Symbol	Value	Units
Nominal voltage	V∗	800	Vdc
Shunt resistance	R_{sh}	313	Ω
Series resistance	R_s	0.39	Ω
DC filter resistance	R_{fcd}	1	$m\Omega$
DC filter inductance	L_{fdc}	1000	υH
Maximum power per module	P_{max}	213	W
Open circuit voltage	(Voc)	36.3	V
Short-circuit current	(Isc)	7.84	A
MPP voltage	V_{MPP}	29	V
MPP current	I_{MPP}	7.35	A
Reference temperature	T_r	25	T
Temperature coefficient of Isc	K_0	0.06	
Modules in parallel		47	u
Total MPP current	I_{MPP}	345	A
Modules in series		28	u
Total MPP voltage	V_{MPP}	812	V
Cells per module		60	u

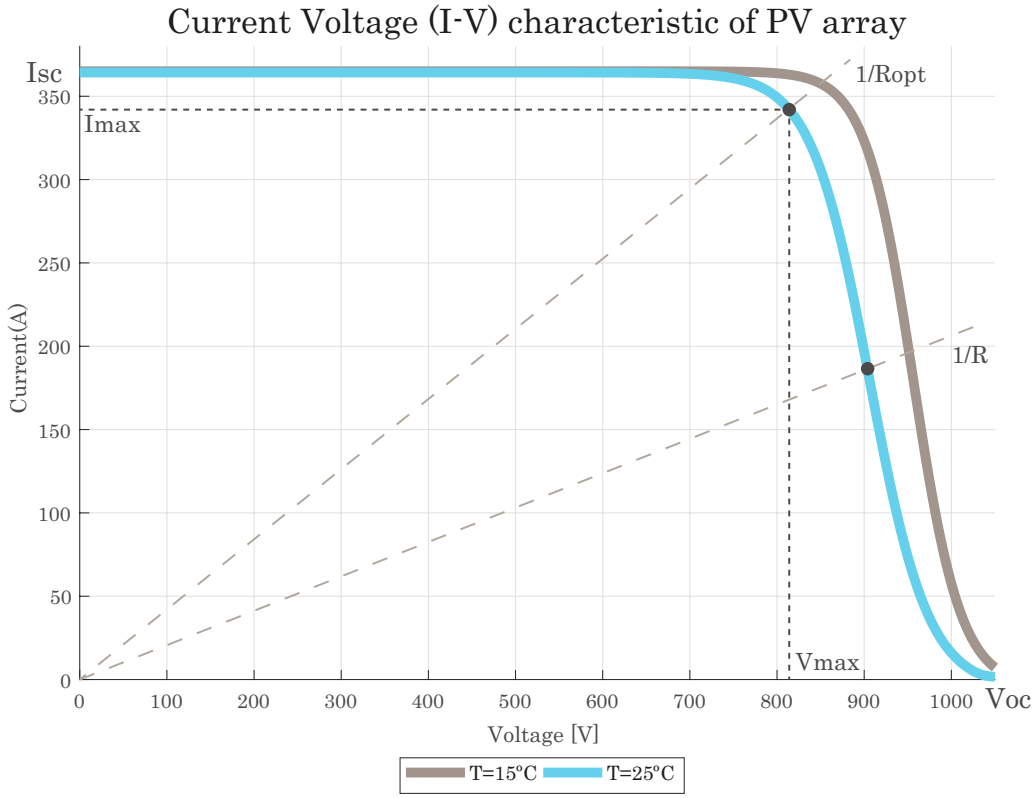

Figure 5.1: I-V curve for PV source.

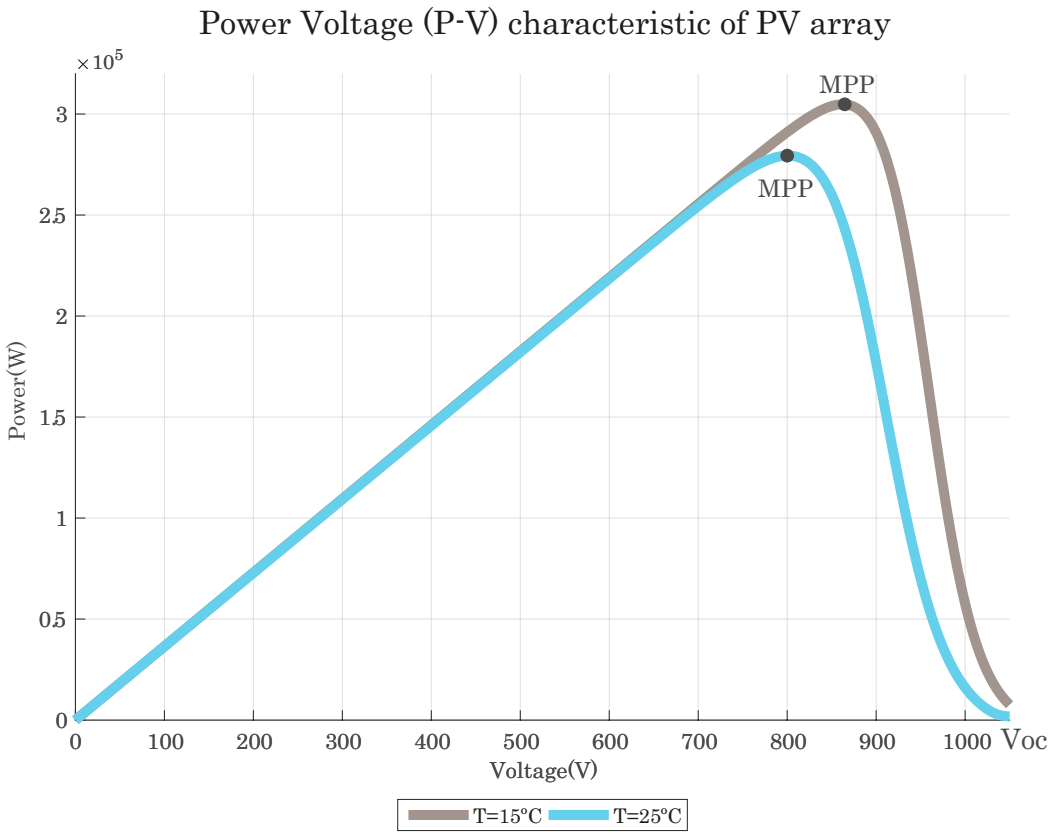

Figure 5.2: P-V curve for PV source.

The parameters selected for the inverter are shown in Table 5.2. 2.5[$msec$] is the sample time, hence the computational effort is important, which has to be considered in the analysis. The nominal frequency is 2π60, which is an standard in this region. The desired AC RMS voltage E$*$ is 450 [Vrms], which is an standard for AC MG. The filter parameters, r_1,L$_f$ and C$_f$ are considered for eliminating the undesired frequencies and amplifying the fundamental sinusoidal signal with 0.38[Ω], 3.83[mH] and 92[μC], respectively.

Table 5.2: Electrical AC system parameters.

Parameter	**Symbol**	**Value**	**Units**
Sample time	T$_S$	2.5 $*$ 10^{-6}	sec
Nominal frequency	ω*	2π60	rad/sec
AC nominal RMS voltage	V_{rms}	450	Vrms
Nominal peak voltage	E*	600	Vp
Filter resistance	r_1	0.38	Ω
Filter inductance	L$_f$	3.83	mH
Filter capacitance	C$_f$	92	μC

The resulting state space identification is a Simple-Input-Simple-Ouput (SISO) system and it is represented by the equations 5.1-5.3, where the system input is the duty cycle feeded to the inverter and the output is the capacitor voltage.
Eq. 5.1 shows the states, which are capacitor voltage, inductor current, and the rate of capacitor voltage reported as V_C, I_C and $\ddot{V}_C$, in Eq. 5.3. The matrix A represents the relation between the first derivative of the state with the second state and the second derivative of the state with the third state, while the third derivative of the state represents the dynamics of the three state in one relation. The matrix A coefficients are quite high due to the difference of magnitudes between the input and the output. The C matrix shows the relation among the system input and the states, the while the system input is δ_{in}, which is the duty cycle received from the controller. The duty cycle affects directly the third state equation.
The output is V_C, as shown by Eq. 5.2, however it is possible to monitor the voltage in the capacitor and the output current measured in the filter capacitor, if required.
The results of the identification of the state-space model are shown in Figure 5.3. It is shown two curves; the first is the $3^r d$ order system represented in state space, while the second is the PV + inverter system. The duty cycle used as input is the unity step, which is applied in both systems. Comparing the model with the real system, it can be noted that the overshoot is 91.1% compared to 80%, respectively.
The system in state space has a damped behaviour while the real system has more complex dynamics. However, the system response and its overall dynamic is well represented by the state-space model. Therefore, the state state model is useful to design a simple controller, but it is not suitable for advanced methodologies, for example, an adaptative control approach.

$$\begin{bmatrix} \dot{x_1} \\ \dot{x_2} \\ \dot{x_3} \end{bmatrix} = \begin{bmatrix} 0 & 1 & 0 \\ 0 & 0 & 1 \\ -7.58 * 10^{11} & -2.95 * 10^{7} & -2.67 * 10^{5} \end{bmatrix} \begin{bmatrix} x_1 \\ x_2 \\ x_3 \end{bmatrix} + \begin{bmatrix} 0 \\ 0 \\ 3.79 * 10^{14} \end{bmatrix} \delta_{in} \tag{5.1}$$

$$y = \begin{bmatrix} 1 & 0 & 0 \end{bmatrix} \begin{bmatrix} x_1 \\ x_2 \\ x_3 \end{bmatrix} \tag{5.2}$$

$$\mathrm{X^T} = \begin{bmatrix} \mathrm{V_C} & \mathrm{I_C} & \dot{\mathrm{V}}_\mathrm{C} \end{bmatrix} \tag{5.3}$$

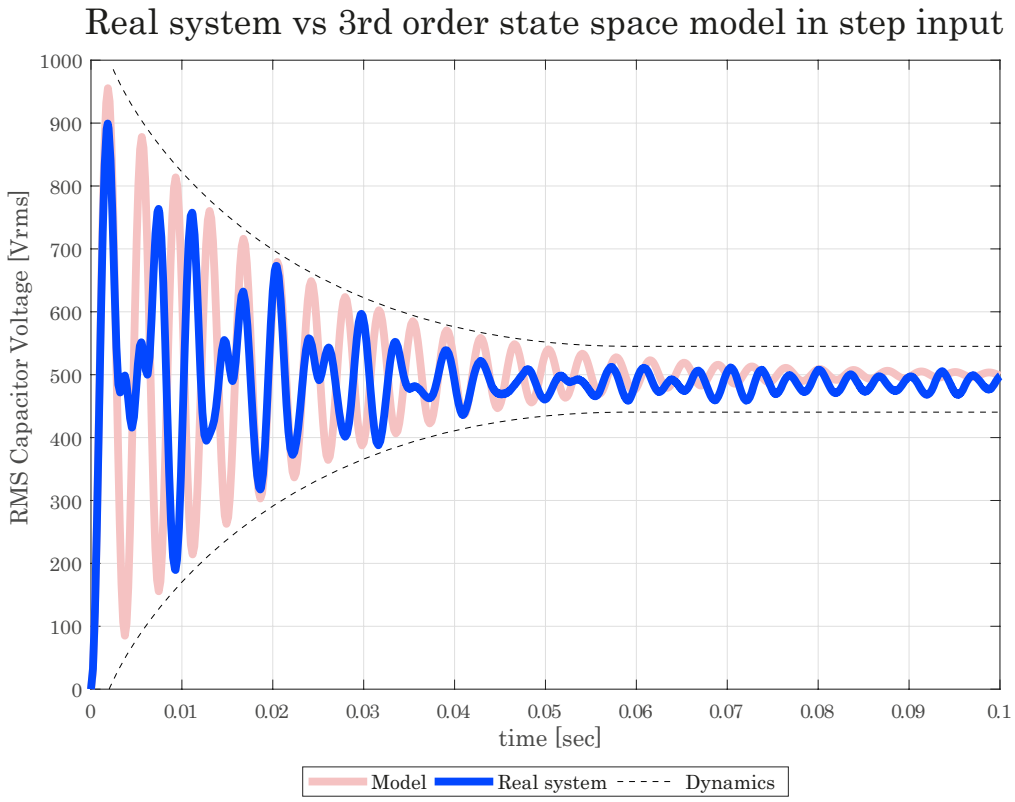

Figure 5.3: Model verification, real system vs 3rd order state space model.

Figure 5.4 displays the identification result using different approaches to determine which is the best methodology to identity the PV and inverter system. There are four different graphics: the first is the real system output, the second is the identification via polynomial structure, specifically an ARX771.
While, the third is a second order discrete transfer function, with one zero; in total, there are three free coefficients to be determined. Finally, a NN using the $Levenberg-Marquardt$ training, its structure is three layers, including the input, hidden and output layer.
The Pseudorandom Binary Sequence (PRBS) is the input used for determining the output information. It contributes with several frequency components, in order to simulate the system behaviour under a real control devices. It may represent the duty cycle, which is the sequence used for controlling the power switches in the inverter.
These methodologies can generate models with different features. The polynomial and transfer function identified models have problems for reproducing constant and peak values; however, the overall fitness level is good, and these methods can be used to accurately represent the system.
Table 5.3 depicts the Mean Squared Error (MSE) comparison among the strategies. The discrete transfer function gives the worst results, but it can be improved using different structures, perhaps increasing the pole number. The polynomial identification leads

to very good results, with with a MSE value small enough.
Finally, the NN has an outstanding performance and it is the best identified model with an MSE very close to zero. It can accurately track all the dynamics of the output, including the maximum and minimum output values. The NN can reach this superior result because it is an heuristic method, particularly efficient with nonlinear systems. The test scenario for the NN identification includes uncertainty in the input and output signals. The variance of each noise process affecting the input and the output for each noise is 0.25 and 1, respectively.

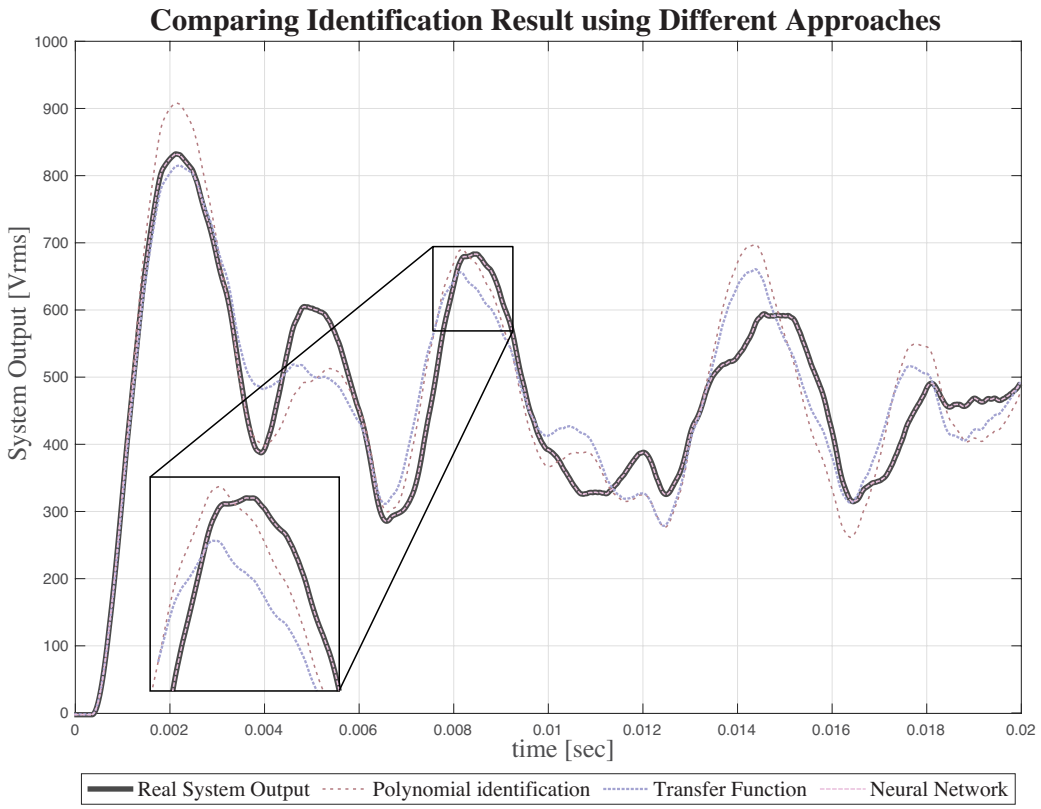

Figure 5.4: Comparison of different identification strategies.

Table 5.3: Identification result using different methodologies.

Methodology	**MSE**
Polynomial ARX751	$4.91 * 10^{-8}$
Discrete Transfer Function	4445
Neural Network	$\rightarrow 0$

5.2 Control System Simulations

The primary control is implemented in the system with the parameters of Table 5.4. The first and second parameter, GM and P_{cr}, are the gain margin and oscillation period, which have been calculated as initial values for the optimisation algorithm. While the following parameters K_{pi}, K_{ii}, K_{pv}, K_{rv} and ω_c are the constants for the primary controller.
It is composed by the voltage and current controller, implemented by a PR and a PID controller, respectively. The resulting parameters have been calculated by means the proposed optimisation algorithm.
Figure 5.5 shows two signals, which represent the comparison the system output and its reference voltage. The reference is calculated by the secondary controller, while it is the input of primary loop control. The reference voltage has a amplitude of *600 [Vp]* and a frequency of *60 [Hz]*, nominal values for MG.
The primary controller effectively tracks the reference signal, as shown by the graph. There is not delay between the signals, but there is a small reduction in the maximum voltage. It is present a steady-state error in the system, which can be neglected because it is less than 5%.
Moreover, the RMS output of the inverter is shown in Figure 5.7. The rise time to reach the nominal value is around $0.15[sec]$. The system is over-damped and there is no overshoot, but it is seen 5% of oscillations around the desired voltage. The oscillations maintain a constant pattern, the response is fast and has acceptable performance considering the included elements and multiple system interactions.
In Figure 5.6 it is shown the comparison between the output system voltage, resulting from the proposed methodology, and the performance of a classical PID. It is important to mention, that the second controller can control the output voltage, but it cannot maintain the limit in current or interchange power between converters. It is seen that the SPSS is more stable and there is not an overshoot, due to there is an over-damped response. The performance in general terms is better the SPSS, without consider the advantages in other control level.

Table 5.4: Parameters for primary control.

Parameter	Symbol	Value
Gain margin	GM	2.15
Oscillation period	P_{cr}	0.116 m
Integral time term	K_{pi}	0.22
Derivative time term	K_{ii}	201.6
Proportional gain	K_{pv}	0.1
Resonant term	K_{rv}	209.9
Resonant frequency	ω_c	0.001
Filter gain	N	100

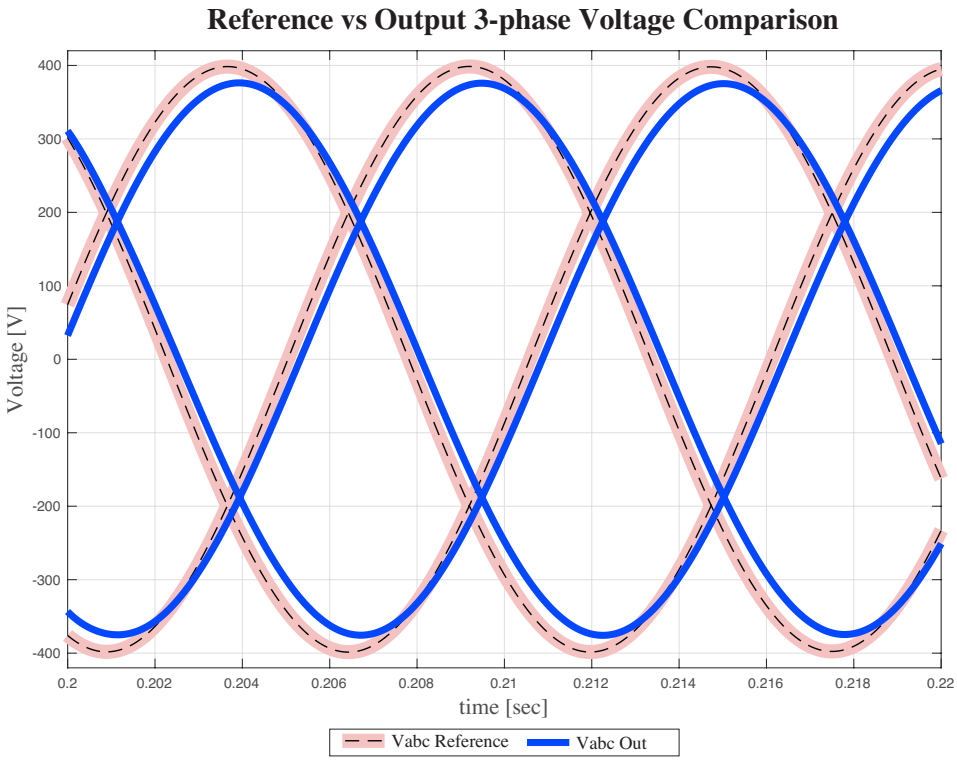

Figure 5.5: Voltage output inverter.

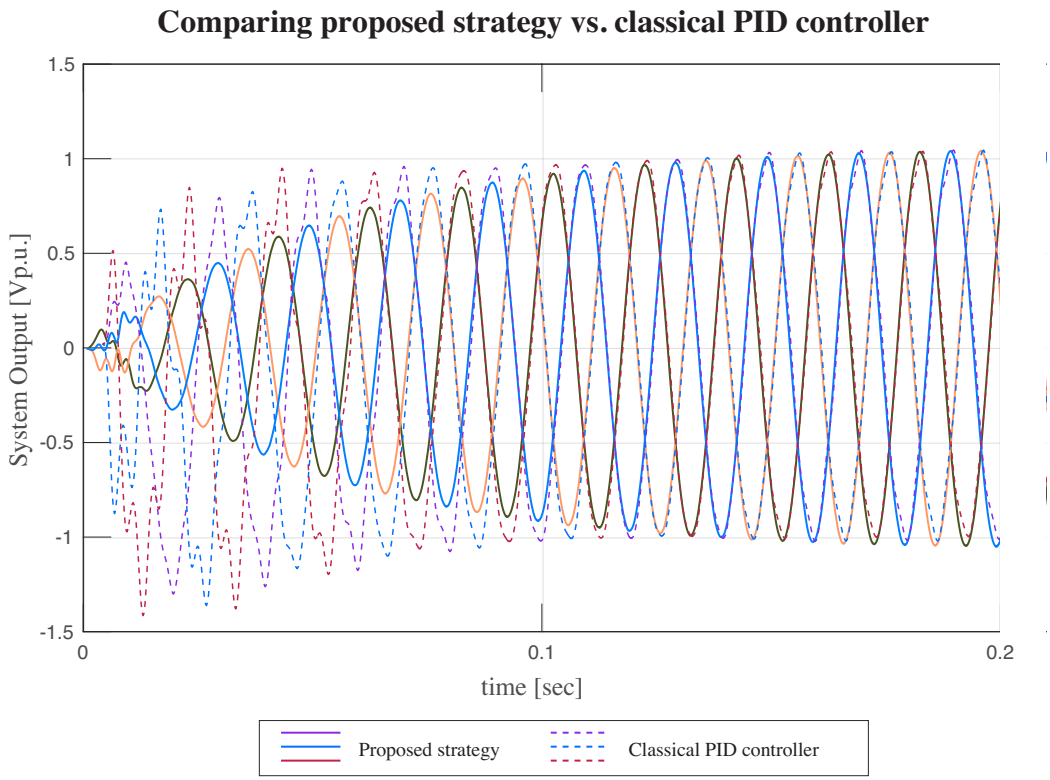

Figure 5.6: Comparing 3-phase output voltage of the proposed strategy vs. classical PID controller, in per-unit values.

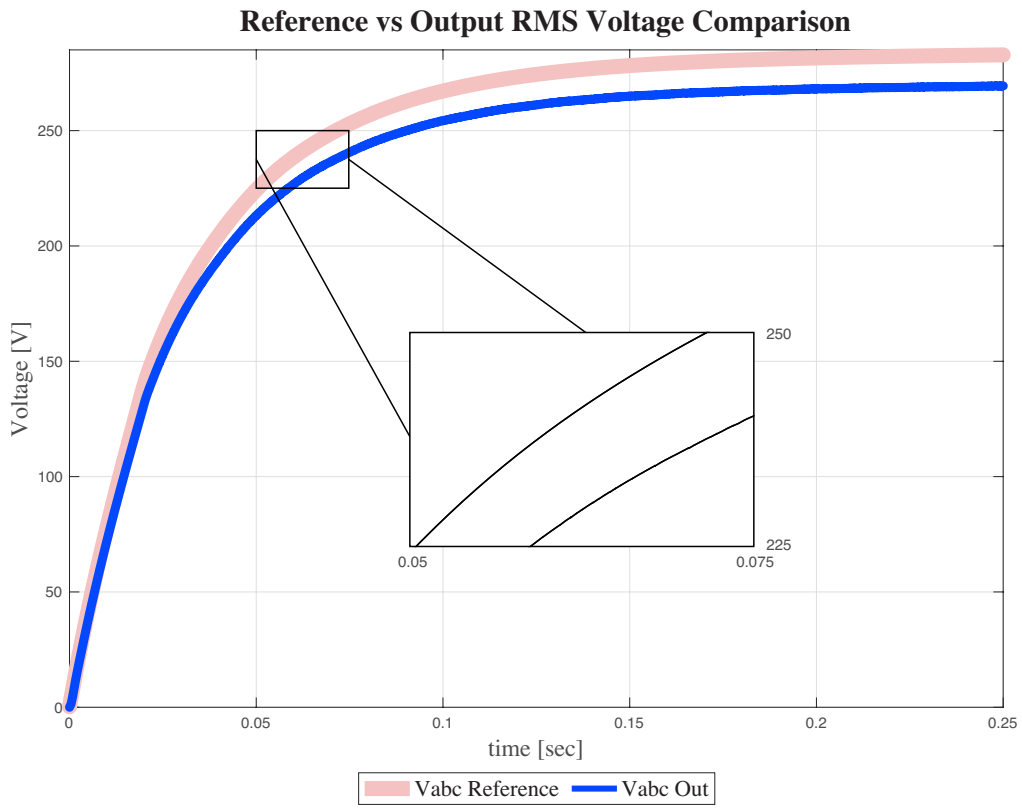

Figure 5.7: Voltage output inverter RMS.

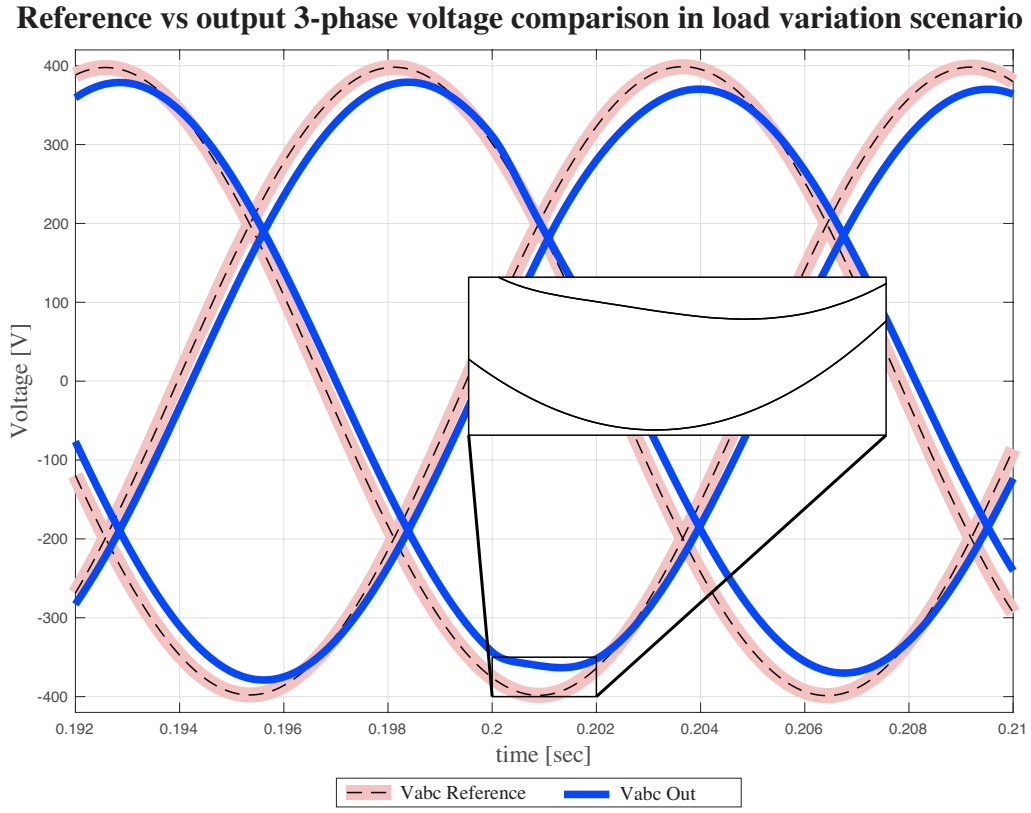

Figure 5.8: Voltage output in load variation scenario.

The results for the optimisation algorithm implemented in the primary loop are shown in Figures 5.9 and 5.10.
Figure 5.9 reports 5 system responses, each one corresponding to a PID controller calculated by ISE, IAE, ITSE, ITAE and ZN approaches. The objective of each strategy is to find the controller coefficients, which produce the minimum steady state error in the system.
Each of the ISE, IAE, ITSE, ITAE and ZN approaches consider the step input. It is seen that all responses more or less have the same behaviour. They reach the step input in step in $4.5x10^{-4}[sec]$. The system has an over-damped response, and thus there is not overshoot. In the magnified square, the highest differences among the four methodologies and the ZN approach are highlighted. The ZN method provides the initial values for the considered optimisation procedures.
The values of the optimisation indices are reported in Table 5.5, where the methods are sorted with respect to the achieved minimum value. For the current control loop with the ITSE is the best the optimal strategy to find the smallest error in steady state.

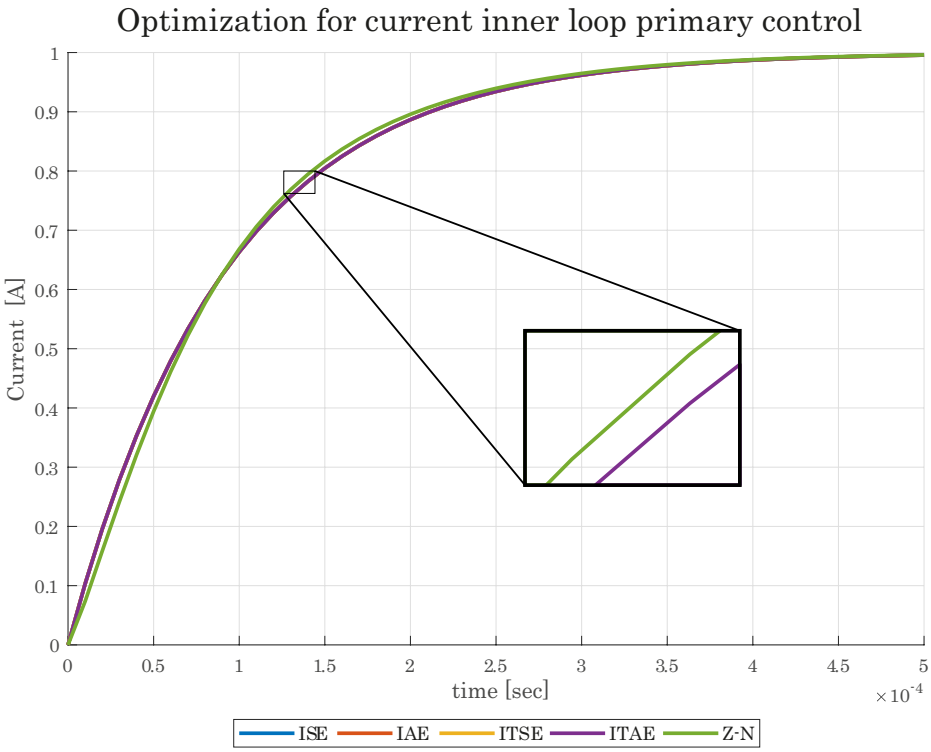

Figure 5.9: Comparing of the optimisation techniques for the current inner loop of the primary control.

Table 5.5: Minimisation results for the current loop.

Methodology	**Value**
ITSE	$1.15 * 10^{-11}$
ITAE	$5.84 * 10^{-11}$
ISE	$1.81 * 10^{-6}$
IAE	$6.09 * 10^{-6}$

Figure 5.10 displays the voltage closed-loop response feeded by a 60[Hz] sinusoidal input, which is controlled by the PR approach. The ZN was not exploited, as the current does not correspond to any magnitude margin. Therefore, there are not a resonant constant to derive the initial values for the algorithm. However, the methodology implements random values as a initial guess in the controller optimal calculation, and the algorithm should find the same values as optimal parameters.
The methods ISE, IAE, ITSE and ITAE have been compared with respect to a sinusoidal reference. Note that there is an important difference between the reference and ITSE. Table 5.6 shows the evaluation of the objective functions, and the ITSE has led to the

least effectiveness.
ISE and ITAE are the closes to the reference, with a small difference in the reference peak, but the objective function evaluation has led to quite good results. Finally, IAE is the best approach as the results in the experiments, and there is not a significant difference reference and the controller under IAE optimisation.
The values for determined from the function minimisation are summarised in Table 5.6. The methods are sorted starting from the least value. Therefore, the best method for voltage loop control is IAE optimisation.
Figure 5.11 shows the comparison between the current and the voltage bode diagrams. The magnitude and phase, in voltage loop present abrupt changes around the desired frequency under desired frequency, 60[Hz]. While, the current loop magnitude and phase is more smooth, and it has not amplification or gap frequency.
About the phase margin, it can be computed for the current and voltage loops, in 0[rad/sec] and 60[rad/sec], respectively. While, magnitude margin can be evaluated only for the voltage loop. This problem affects the algorithm and the initial values for the optimisation algorithm are based on random values.

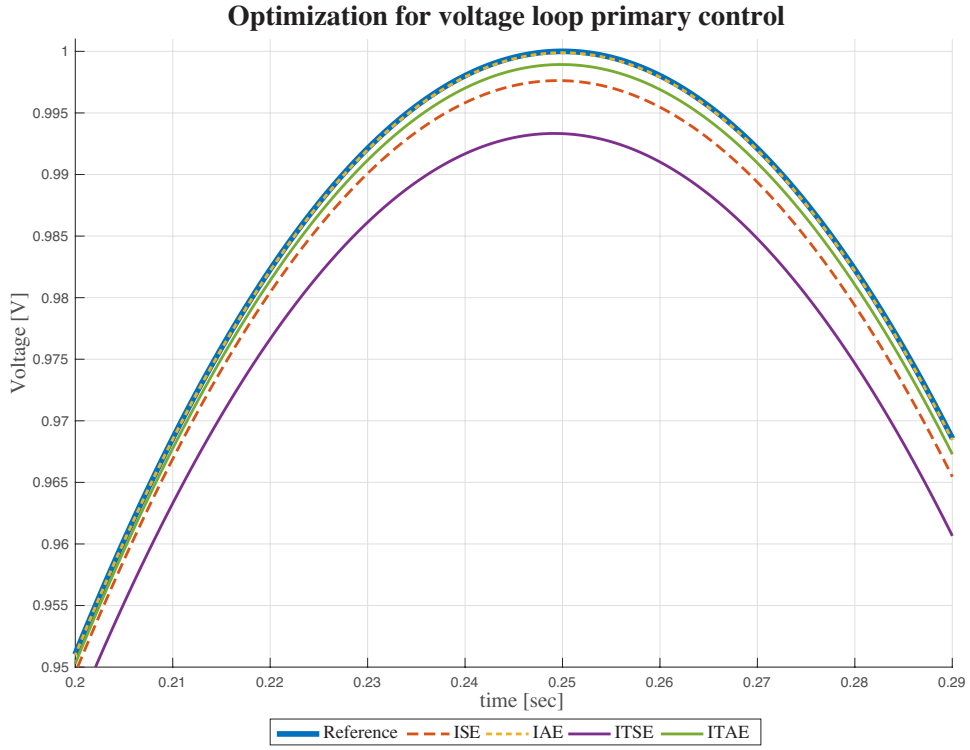

Figure 5.10: Comparison of the optimisation techniques for voltage inner loop primary control.

Table 5.6: Minimisation results for the voltage loop.

Methodology	Value
IAE	$5.84 * 10^{-5}$
ITAE	$9.32 * 10^{-5}$
ISE	$2.50 * 10^{-4}$
ITSE	$7.31 * 10^{-4}$

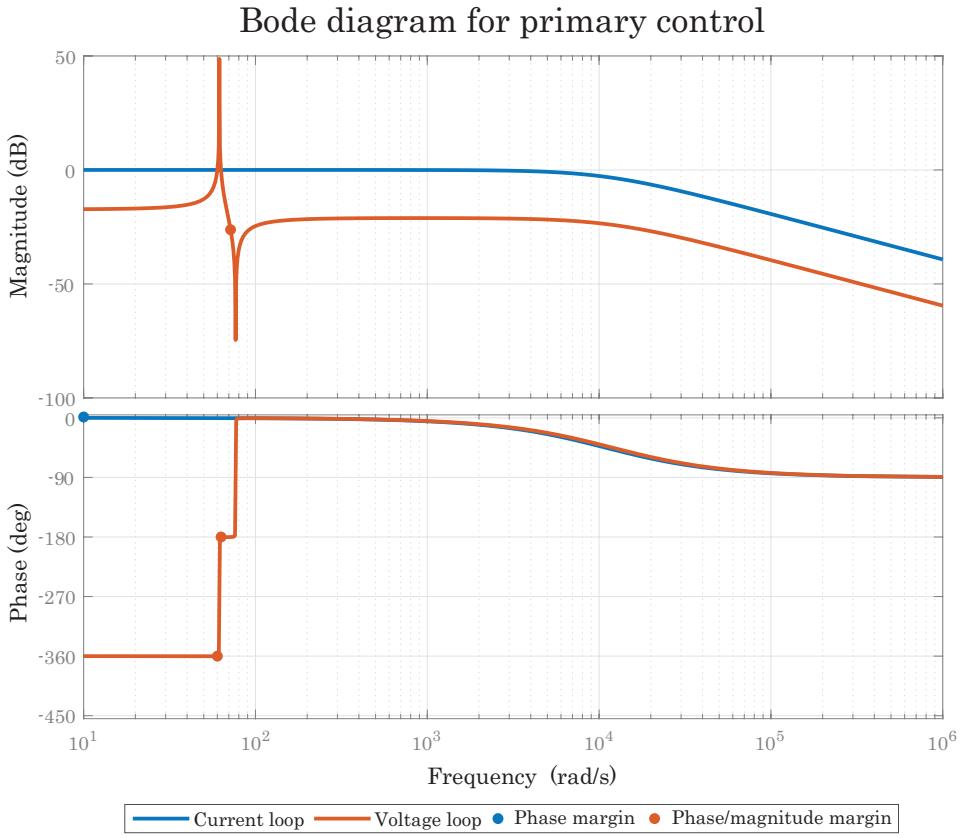

Figure 5.11: Bode diagram comparing the current and voltage primary control.

The secondary control level has the objective of adjusting the voltage and frequency reference values for the primary level. Also The secondary one reduces the circulating current, which is generated by the non-lineal elements.
The secondary level controls the energy flow in the entire MG, using the evaluation between the generation and consumption.
In this section, the interconnection and the relations existing among the VSI have been considered. The values for the secondary control level are summarised in Table 5.7.
The methodology for calculating the parameter was summarised in the previous chap-

ter, where the mathematical relations were also recalled and referenced. There are two controller, one for the active power P control and the other for the reactive power Q control. The both the feed-forward schemes include a PI controller. The parameters of the PI regulator for Active Power (P) power control are $k_{p\mathrm{E}}$ and $k_{i\mathrm{E}}$, while for the Q power control are $k_{p\omega}$ and $k_{i\omega}$.
Also the parameters for droop control are divided in P and Q control, and the constants n and n_d for P, while m and m_d for Q controller. Finally, K_e is the controller proportional constant used to compensate the voltage variation and its effect in the final result.
The active and reactive power values generated by a generator, for the stand-alone, are shown in Figure 5.12. At the beginning, the signals are the same, but they change transient behaviour. Moreover, after $0.01[s]$, each model follows a response as a second-order system. Both signals reach a maximum point around 0.25 seconds and after that, they follow the individual reference, 375[W] and 220[VAr], respectively. In the stand-alone case, the source response to the load power, while the load is not perfectly linear, and includes capacity and inductance elements in order to supply an imaginary part of power.

Table 5.7: Parameters for secondary and tertiary control.

Parameter	**Symbol**	**Value**
Proportional gain for controller	K_e	7
Drop coefficient for P power control	n	0.21
Drop coefficient for P power control	n_d	0.003
Drop coefficient for Q power control	m	160µ
Drop coefficient for Q power control	m_d	2µ
P gain for voltage deviation	$k_{p\mathrm{E}}$	1.82
I gain for voltage deviation	$k_{i\mathrm{E}}$	4.29
P gain for frequency deviation	$k_{p\omega}$	2.23
I gain for frequency deviation	$k_{i\omega}$	7.68

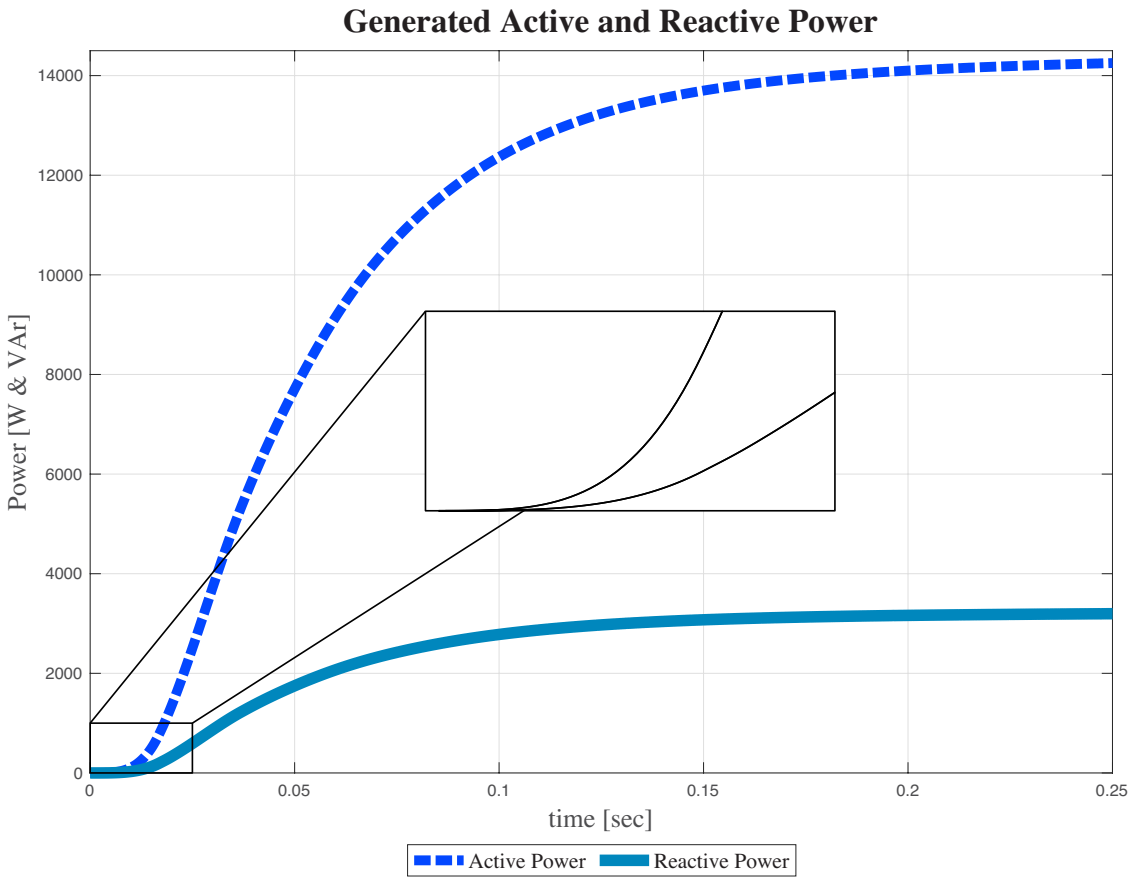

Figure 5.12: Inverter active and reactive power delivered to the stand-alone load.

Chapter 6

Conclusions and Future Works

The thesis firstly proposes a strategy for controlling an electrical substation of a smart grid with photo-voltaic generation, adopting an optimal approach for network layout and control. It relies on heuristic approach and hierarchical control, and involving a design based on optimisation for reducing the network length and steady state error. The plant under study involves a complex non-linear behaviour, and its know that classical controller might not control this system. Clearly, power electronics has multiples non-linear components and the photo-voltaic generation is unpredictable and changeable.
The author based the proposed method on scientific documents and information extract from the established state-of-the art. For this reason, the based papers are the most cited and relevant investigations in the fields of electrical power system, power electronics, renewable generation, smart grid, heuristics methodologies, and intelligent control system.
Optimal routing method relies on heuristic algorithms, including Prim, Haversine, K-medoids and Minimal Steiner Tree application. This method determined the underground electrical networks routing problem in geo-referenced areas. The model is a multi-layered algorithm. Where, the first part algorithm deals with the transformer allocation and the medium voltage network routing. Then, the second part designs the low voltage grid and transformer sizing. Finally, the third part optimally allocates the photo-voltaic rooftop panels with a specific criterion. A simulation software determined the designed method feasibility and performance.
The proposed routing optimal algorithm can route a grid in a geo-referenced area, dealing with the terrain attributes, such as roads or junctions, building scenarios without squared streets. In fact, the modelled network achieves distance and customer transformer number constraint.
Optimising network algorithm minimised the implementation cost and the length network, while maximised the power quality and the network reliability. Thus, the farthest node becomes a greatest 2% of dropping voltage. The optimal implementation based on heuristic methodologies reduces the medium and low voltage grid dimension, keeping a specific number for electricity customer in each individual sub-network.
Smart power substations is the name for the planned control scheme, which controls

the entire system hierarchically. Hence, the hierarchical control appears from the primary controller, which controls the current and the voltage outputs. The secondary control regulates the references for voltage amplitude and frequency, which based on the expected active and reactive power. Finally, the tertiary control deals with energy management and dispatching, which implements a communication coordination among the individual controllers.

The cost functions determined the optimal coefficients values for each individual controller to reduce the steady state error. For this purpose, the investigation tested several performance indices to notice which reach the less error, like as integral square error indices methods. The control strategy had excellent results compared with similar facilities. In fact, the parameter variation and some faults implementation verified the system robustness.

The system steady state is over-damped, and it has not over-shoot. However, it has a 5% of oscillations around the desired voltage level, which keep a constant pattern. The response time is fast, considering the non-linear elements behaviour and the multiple system interactions. Hence, the establishing time is less than 0.4 seconds where, despite the increase in load, the system output satisfies the system's requirements in terms of power and voltage.

Further it can carry out similar researches, aimed at optimising the optimal power interchange, in particular with other generation, as wind or hydroelectricity generation. As well as, it can explore different bio-inspired controllers, as fuzzy or neural network, to improve the nonlinear adaptability. Also, the power electronics would develop by exploring different solutions for the new electronic arrangement. They should fulfil a noteworthy validation by testing the proposed power substations in different benchmark systems, first the energy reduction, and the most power point efficiency.

The overall achieved result induces future considerations about introducing distributed generation, smart grid and photo-voltaic installations. The adopted control strategy is often too conservative, as they involve the classical individual controller, as proportional-integral derivative and proportional resonant. Future research will concentrate on a broader analysis including economical and social fields involved in smart grid.

In conclusion, smart grid is a fast-growing technology, and this growth implies an enormous demand for better modelling and control. Non-linear behaviour and uncertainties represent for control a challenging task to overcome. These considerations drive the lack of advanced modelling and further development of optimal control strategies, with the primary aim of maximising the energy efficiency. This renewable energy source could match the global electricity demands, specially in rural areas, if it will overcome the technological barriers. The industrial application of sustainable control is still in its prototyping phase, and it means many opportunities to improve.

Chapter 7

Glossary

AC Alternating Current.

AMI Advanced Metering Infrastructure.

ANFIS Adaptive Neuro-Fuzzy Inference System.

BESS Battery Energy Storage System.

CHP Combined Heat and Power.

CPC Centralized Substation Protection and Control.

CSI Current Source Inverter.

DC Direct Current.

DER Distributed Energy Resources.

DG Distributed Generation.

EDS Electrical Distribution System.

ESS Energy Storage System.

EV Electric Vehicles.

FC Fuel Cell.

FLL Frequency Lock Loop.

FOM Force Oscillation Method.

FPGA Field Programmable Gate Array.

GCM Grid-Connected Mode.

HCS Hierarchical Control System.

HG Hydraulic Power Generation.

I-V Current-Voltage.

IAE Integral Absolute Error.

IED Intelligent Electric Device.

Isc Current in Short Circuit.

ISE Integral Square Error.

ITAE Integral Time Absolute Error.

ITSE Integral Time Square Error.

LV Lower Voltage.

MG Micro Grid.

MILP Mixed Integer Linear Programming.

MPP Point of Maximum Power.

MPPT Point of Maximum Power Tracking.

MSE Mean Squared Error.

MST Minimal Spanning Tree.

MV Medium Voltage.

NN Neural Network.

OCP Optimal Control Problem.

P Active Power.

P-f Active Power-frequency.

P-V Power-Voltage.

PCC Point of Common Coupling.

PE Power Electronics.

PEC Power Energy Converter.

PI Proportional Integral.

PID Proportional Integral Derivative.

PMU Phase Measurement Unit.

PR Proportional Resonant.

PRBS Pseudorandom Binary Sequence.

PV Photovoltaic Generation.

PWM Pulse Width Modulation.

Q-V Reactive Power-Voltage.

RES Renewable Energy Resources.

RLC Resistor Inductor and Capacitor.

RMS Root Mean Square.

SCADA Supervision and Control Data Acquisition.

SG Smart Grid.

SISO Simple-Input-Simple-Ouput.

SoTA State of the Art.

SPSS Smart Power Substation.

SVR Static Var Compesator.

THD Total Harmonics Distortion.

Voc Voltage in Open Circuit.

VR-FCL Variable Resistance for Fault Current Limiter.

VSI Voltage Source Inverter.

WECS Wind Energy Conversion Systems.

ZN Ziegler-Nichols.

Bibliography

Aghaei, J., Muttaqi, K. M., Azizivahed, A., and Gitizadeh, M. (2014). Distribution expansion planning considering reliability and security of energy using modified PSO (Particle Swarm Optimization) algorithm. *Energy*, 65:398–411.

Ahmed, M. N., Hojabri, M., Humada, A. M., Daniyal, H. B., and Fahad Frayyeh, H. (2015). An Overview on Microgrid Control Strategies. *International Journal of Engineering and Advanced Technology (IJEAT)*.

Andersson, J. A., Gillis, J., Horn, G., Rawlings, J. B., and Diehl, M. (2019). CasADi: a software framework for nonlinear optimization and optimal control. *Mathematical Programming Computation*.

Antoniadou-Plytaria, K. E., Kouveliotis-Lysikatos, I. N., Georgilakis, P. S., and Hatziargyriou, N. D. (2017). Distributed and Decentralized Voltage Control of Smart Distribution Networks. *IEEE Transactions on Smart Grid*, 8(6):2999–3008.

Bahrani, B., Saeedifard, M., Karimi, A., and Rufer, A. (2013). A multivariable design methodology for voltage control of a single-DG-unit microgrid. *IEEE Transactions on Industrial Informatics*.

Bao Nguyen, D., Scherpen, J. M., and Bliek, F. (2017). Distributed Optimal Control of Smart Electricity Grids with Congestion Management. *IEEE Transactions on Automation Science and Engineering*.

Bhowmik, C., Bhowmik, S., Ray, A., and Pandey, K. M. (2017). Optimal green energy planning for sustainable development: A review.

Brahma, S. (2016). Advancements in Centralized Protection and Control Within a Substation. *IEEE Transactions on Power Delivery*, 31(4):1945–1952.

Chethan Raj, D. and Gaonkar, D. N. (2016). Frequency and voltage droop control of parallel inverters in microgrid. *2016 2nd International Conference on Control, Instrumentation, Energy and Communication, CIEC 2016*, 2(3):407–411.

Cintuglu, M. H., de Azevedo, R., Ma, T., and Mohammed, O. A. (2015). Real-time experimental analysis for protection and control of smart substations. In *2015 IEEE PES Innovative Smart Grid Technologies Latin America (ISGT LATAM)*, pages 485–490.

Colak, I., Kabalci, E., Fulli, G., and Lazarou, S. (2015). A survey on the contributions of power electronics to smart grid systems.

Dineva, A., Mosavi, A., Ardabili, S. F., Vajda, I., Shamshirband, S., Rabczuk, T., and Chau, K. (2019). Review of Soft Computing Models in Design and Control of Rotating Electrical Machines. *Energies*, 12(6):1049.

Dissanayake, A. M. and Ekneligoda, N. C. (2018). Transient Optimization of Parallel Connected Inverters in Islanded AC Microgrids. *IEEE Transactions on Smart Grid*, 10(5):4951–4961.

Dkhili, N., Eynard, J., Thil, S., and Grieu, S. (2020). A survey of modelling and smart management tools for power grids with prolific distributed generation. *Sustainable Energy, Grids and Networks*, 21:100284.

Dong, P., Xu, L., Lin, Y., and Liu, M. (2018). Multi-Objective Coordinated Control of Reactive Compensation Devices Among Multiple Substations. *IEEE Transactions on Power Systems*.

Duque, F. G., de Oliveira, L. W., de Oliveira, E. J., and Augusto, A. A. (2017). State estimator for electrical distribution systems based on an optimization model. *Electric Power Systems Research*, 152:122–129.

Eghtedarpour, N. and Farjah, E. (2014). Power Control and Management in a Hybrid AC/DC Microgrid. *IEEE Transactions on Smart Grid*, 5(3):1494–1505.

Ehsan, A. and Yang, Q. (2019). State-of-the-art techniques for modelling of uncertainties in active distribution network planning: A review.

Eppstein, D. (1994). Finding the k shortest paths. In *Proceedings 35th Annual Symposium on Foundations of Computer Science*, pages 154–165.

Fatih, K., AcikgozHakan, YildizCeyhun, GaniAhmet, and SekkeliMustafa (2017). Power Quality Improvement Using Hybrid Passive Filter Configuration for Wind Energy Systems. *Journal of Electrical Engineering and Technology*, 12(1):207–216.

Feng, C., Wang, Y., Chen, Q., Ding, Y., Strbac, G., and Kang, C. (2021). Smart grid encounters edge computing: opportunities and applications. *Advances in Applied Energy*, 1:100006.

Gajić, Z., Lim, M., Škatarić, D., Su, W., and Kecman, V. (2008). *Optimal control: Weakly coupled systems and applications*. CRC Press.

Gangl, P., Langer, U., Laurain, A., Meftahi, H., and Sturm, K. (2015). Shape optimization of an electric motor subject to nonlinear magnetostatics. *SIAM Journal on Scientific Computing*.

Ghadi, M. J., Rajabi, A., Ghavidel, S., Azizivahed, A., Li, L., and Zhang, J. (2019). From active distribution systems to decentralized microgrids: A review on regulations and planning approaches based on operational factors. *Applied Energy*, 253:113543.

Giustina, D. D., Dede, A., Invernizzi, G., Valle, D. P., Franzoni, F., Pegoiani, A., and Cremaschini, L. (2015). Smart Grid Automation Based on IEC 61850: An Experimental Characterization. *IEEE Transactions on Instrumentation and Measurement*, 64(8):2055–2063.

González-Castaño, C., Restrepo, C., Giral, R., Vidal-Idiarte, E., and Calvente, J. (2020). ADC Quantization Effects in Two-Loop Digital Current Controlled DC-DC Power Converters: Analysis and Design Guidelines.

Guerrero, J. M., Vasquez, J. C., Matas, J., de Vicuna, L. G., and Castilla, M. (2011). Hierarchical Control of Droop-Controlled AC and DC Microgrids—A General Approach Toward Standardization. *IEEE Transactions on Industrial Electronics*, 58(1):158–172.

Hajiakbari Fini, M. and Hamedani Golshan, M. E. (2018). Determining optimal virtual inertia and frequency control parameters to preserve the frequency stability in islanded microgrids with high penetration of renewables. *Electric Power Systems Research*.

Hajimiragha, A. and Zadeh, M. R. (2011). Practical aspects of storage modeling in the framework of Microgrid real-time optimal control. In *IET Conference Publications*.

Heymann, B., Bonnans, J. F., Martinon, P., Silva, F. J., Lanas, F., and Jiménez-Estévez, G. (2018). Continuous optimal control approaches to microgrid energy management. *Energy Systems*.

Hirsch, A., Parag, Y., and Guerrero, J. (2018). Microgrids: A review of technologies, key drivers, and outstanding issues. *Renewable and Sustainable Energy Reviews*, 90(September 2017):402–411.

Hossain, E., Kabalci, E., Bayindir, R., and Perez, R. (2014). Microgrid testbeds around the world: State of art. *Energy Conversion and Management*, 86:132–153.

Hossain, M. K. and Ali, M. H. (2015). Transient Stability Augmentation of PV/DFIG/SG-Based Hybrid Power System by Nonlinear Control-Based Variable Resistive FCL. *IEEE Transactions on Sustainable Energy*, 6(4):1638–1649.

Hosseinzadeh, M. and Salmasi, F. R. (2015). Power management of an isolated hybrid AC/DC micro-grid with fuzzy control of battery banks. *IET Renewable Power Generation*, 9(5):484–493.

Huang, Q., Jing, S., Li, J., Cai, D., Wu, J., and Zhen, W. (2017). Smart Substation: State of the Art and Future Development. *IEEE Transactions on Power Delivery*, 32(2):1098–1105.

Humayun, M., Safdarian, A., Ali, M., Degefa, M. Z., and Lehtonen, M. (2016). Optimal capacity planning of substation transformers by demand response combined with network automation. *Electric Power Systems Research*, 134:176–185.

IEEE (1970). IEEE Standard Definitions of Terms for Automatic Generation Control on Electric Power Systems. *IEEE Transactions on Power Apparatus and Systems*, PAS-89(6):1356–1364.

Imase, M. and Waxman, B. M. (1991). Dynamic Steiner Tree Problem. *SIAM Journal on Discrete Mathematics*, 4(3):369–384.

Inga, E., Carrion, D., Aguila, A., Garcia, E., Hincapie, R., and González, J. W. (2016). Minimal Deployment and Routing Geographic of PMUs on Electrical Power System based on MST Algorithm. *IEEE Latin America Transactions*.

Iqbal, M., Azam, M., Naeem, M., Khwaja, A. S., and Anpalagan, A. (2014). Optimization classification, algorithms and tools for renewable energy: A review. *Renewable and Sustainable Energy Reviews*, 39:640–654.

Irfan, M., Iqbal, J., Iqbal, A., Iqbal, Z., Riaz, R. A., and Mehmood, A. (2017). Opportunities and challenges in control of smart grids – Pakistani perspective. *Renewable and Sustainable Energy Reviews*, 71:652–674.

Isermann, R. and Balle, P. (1997). Trends in the application of model-based fault detection and diagnosis of technical processes. *Control engineering practice*, 5(5):709–719.

Jadeja, R., Ved, A., Trivedi, T., and Khanduja, G. (2020). Control of Power Electronic Converters in AC Microgrid. In *Power Systems*. Springer.

Jain, A. K., Murty, M. N., and Flynn, P. J. (1999). Data clustering: a review. *ACM computing surveys (CSUR)*, 31(3):264–323.

Khalid, A., Aslam, S., Aurangzeb, K., Haider, S., Ashraf, M., and Javaid, N. (2018). An Efficient Energy Management Approach Using Fog-as-a-Service for Sharing Economy in a Smart Grid. *Energies*, 11(12):3500.

Khodr, H., Salloum, G., Saraiva, J., and Matos, M. (2009). Design of grounding systems in substations using a mixed-integer linear programming formulation. *Electric Power Systems Research*, 79(1):126–133.

Kleftakis, V. A. and Hatziargyriou, N. D. (2019). Optimal control of reversible substations and wayside storage devices for voltage stabilization and energy savings in metro railway networks. *IEEE Transactions on Transportation Electrification*.

Lee, D. and Wang, L. (2008). Small-Signal Stability Analysis of an Autonomous Hybrid Renewable Energy Power Generation/Energy Storage System Part I: Time-Domain Simulations. *IEEE Transactions on Energy Conversion*, 23(1):311–320.

Leek, V. (2016). *An Optimal Control Toolbox for MATLAB Based on CasADi*. PhD thesis, Linkoping University, Vehicular Systems, Department of Electrical Engineering, Linköping University.

Levine, S. and Koltun, V. (2012). Continuous Inverse Optimal Control with Locally Optimal Examples. In *International Conference on Machine Learning (ICML)*.

Li, H., Mao, W., Zhang, A., and Li, C. (2016). An improved distribution network reconfiguration method based on minimum spanning tree algorithm and heuristic rules. *International Journal of Electrical Power & Energy Systems*, 82:466–473.

Li, H. and Wang, L. (2011). Research on Technologies in Smart Substation. *Energy Procedia*, 12:113–119.

Li, Z., Zheng, T., Wang, Y., and Yang, C. (2020). A Hierarchical Coordinative Control Strategy for Solid State Transformer Based DC Microgrids.

Lidula, N. W. A. and Rajapakse, A. D. (2011). Microgrids research: A review of experimental microgrids and test systems. *Renewable and Sustainable Energy Reviews*, 15(1):186–202.

Liu, Y., Han, Y., Lin, C., Yang, P., and Wang, C. (2019). Design and Implementation of Droop Control Strategy for DC Microgrid Based on Multiple DC/DC Converters. In *2019 IEEE Innovative Smart Grid Technologies - Asia (ISGT Asia)*, pages 3896–3901.

Lorenzini, C., Bazanella, A. S., Pereira, L. F. A., and Gonçalves da Silva, G. R. (2019). The generalized forced oscillation method for tuning PID controllers. *ISA Transactions*, 87:68–87.

Majeed Butt, O., Zulqarnain, M., and Majeed Butt, T. (2021). Recent advancement in smart grid technology: Future prospects in the electrical power network. *Ain Shams Engineering Journal*, 12(1):687–695.

Majumder, R., Chaudhuri, B., Ghosh, A., Majumder, R., Ledwich, G., and Zare, F. (2010). Improvement of Stability and Load Sharing in an Autonomous Microgrid Using Supplementary Droop Control Loop. *IEEE Transactions on Power Systems*, 25(2):796–808.

Marín, L. G., Sumner, M., Muñoz-Carpintero, D., Köbrich, D., Pholboon, S., Sáez, D., and Núñez, A. (2019). Hierarchical Energy Management System for Microgrid Operation Based on Robust Model Predictive Control.

Marzal, S., Salas, R., González-Medina, R., Garcerá, G., and Figueres, E. (2018). Current challenges and future trends in the field of communication architectures for microgrids. *Renewable and Sustainable Energy Reviews*, 82:3610–3622.

McDonald, J. D., Wojszczyk, B., Flynn, B., and Voloh, I. (2013). Distribution Systems, Substations, and Integration of Distributed Generation. In *Electrical Transmission Systems and Smart Grids*, pages 7–68. Springer New York, New York.

Mhankale, S. E. and Thorat, A. R. (2018). Droop Control Strategies of DC Microgrid: A Review. *Proceedings of the 2018 International Conference on Current Trends towards Converging Technologies, ICCTCT 2018*, pages 372–376.

Mirakhorli, A. and Dong, B. (2018). Model predictive control for building loads connected with a residential distribution grid. *Applied Energy*.

Miret, J., De Vicuña, J. L. G., Guzmán, R., Camacho, A., and Ghahderijani, M. M. (2017). A flexible experimental laboratory for distributed generation networks based on power inverters. *Energies*.

Mostafaie, T., Modarres Khiyabani, F., and Navimipour, N. J. (2020). A systematic study on meta-heuristic approaches for solving the graph coloring problem. *Computers & Operations Research*, 120:104850.

Naji Alhasnawi, B., Jasim, B. H., Anvari-Moghaddam, A., and Blaabjerg, F. (2020). A New Robust Control Strategy for Parallel Operated Inverters in Green Energy Applications.

Nutkani, I. U., Loh, P. C., Wang, P., Jet, T. K., and Blaabjerg, F. (2015). Intertied ac–ac microgrids with autonomous power import and export. *International Journal of Electrical Power & Energy Systems*, 65:385–393.

Olivares, D. E., Mehrizi-Sani, A., Etemadi, A. H., Cañizares, C. A., Iravani, R., Kazerani, M., Hajimiragha, A. H., Gomis-Bellmunt, O., Saeedifard, M., Palma-Behnke, R., Jiménez-Estévez, G. A., and Hatziargyriou, N. D. (2014). Trends in microgrid control. *IEEE Transactions on Smart Grid*.

Ortiz, L., Orizondo, R., Águila, A., González, J. W., López, G. J., and Isaac, I. (2019). Hybrid AC/DC microgrid test system simulation: grid-connected mode. *Heliyon*, 5(12):e02862.

ÖZDEMİR, M. T. and ÖZTÜRK, D. (2017). Comparative Performance Analysis of Optimal PID Parameters Tuning Based on the Optics Inspired Optimization Methods for Automatic Generation Control.

Padula, F. and Visioli, A. (2011). Tuning rules for optimal PID and fractional-order PID controllers. *Journal of Process Control*, 21(1):69–81.

Palizban, O. and Kauhaniemi, K. (2015). Hierarchical control structure in microgrids with distributed generation: Island and grid-connected mode.

Pauwels, E., Henrion, D., and Lasserre, J. B. (2014). Inverse optimal control with polynomial optimization. In *Proceedings of the IEEE Conference on Decision and Control*.

Pavón, W., Inga, E., and Simani, S. (2019). Optimal Routing an Ungrounded Electrical Distribution System Based on Heuristic Method with Micro Grids Integration. *Sustainability*, 11(6):1607.

Pavón, W., Inga, E., and Simani, S. (2020). Optimal Distribution Network Planning applying Heuristic Algorithms Considering allocation of PV Rooftop Generation. In *2020 IEEE ANDESCON*, pages 1–6.

Pereira, L. F. A. and Bazanella, A. S. (2015). Tuning Rules for Proportional Resonant Controllers. *IEEE Transactions on Control Systems Technology*, 23(5):2010–2017.

Piliougine, M., Guejia-Burbano, R. A., Petrone, G., Sánchez-Pacheco, F. J., Mora-López, L., and Sidrach-de Cardona, M. (2021). Parameters extraction of single diode model for degraded photovoltaic modules. *Renewable Energy*.

Pinzón, S. and Pavón, W. (2019). Diseño de Sistemas de Control Basados en el Análisis del Dominio en Frecuencia. *Revista Técnica "Energía"*, 15(2):76–82.

Planas, E., Andreu, J., Gárate, J. I., Martínez De Alegría, I., and Ibarra, E. (2015). AC and DC technology in microgrids: A review. *Renewable and Sustainable Energy Reviews*, 43:726–749.

Planas, E., Gil-de Muro, A., Andreu, J., Kortabarria, I., and Martínez de Alegría, I. (2013). General aspects, hierarchical controls and droop methods in microgrids: A review. *Renewable and Sustainable Energy Reviews*, 17:147–159.

Popov, M., Karimi, H., Nikkhajoei, H., and Terzija, V. (2010). Modeling, control and islanding detection of microgrids with passive loads. In *Proceedings of EPE-PEMC 2010 - 14th International Power Electronics and Motion Control Conference*.

Prim, R. C. (1957). Shortest connection networks and some generalizations. *The Bell System Technical Journal*, 36(6):1389–1401.

Rahmani-Andebili, M. (2017). Stochastic, adaptive, and dynamic control of energy storage systems integrated with renewable energy sources for power loss minimization. *Renewable Energy*.

Rocabert, J., Luna, A., Blaabjerg, F., and Rodríguez, P. (2012). Control of power converters in AC microgrids. *IEEE Transactions on Power Electronics*.

Sen, S. and Kumar, V. (2018). Microgrid modelling: A comprehensive survey. *Annual Reviews in Control*, 46:216–250.

Shuai, Z., Fang, J., Ning, F., and Shen, Z. J. (2018). Hierarchical structure and bus voltage control of DC microgrid. *Renewable and Sustainable Energy Reviews*, 82(2):3670–3682.

Simani, S., Alvisi, S., and Venturini, M. (2018). Self–Tuning Control Techniques for Wind Turbine and Hydroelectric Plant Systems. *Scientific Research*.

Simani, S., Castaldi, P., and Tilli, A. (2011). Data—Driven Approach for Wind Turbine Actuator and Sensor Fault Detection and Isolation. *IFAC Proceedings Volumes*, 44(1):8301–8306.

Sun, C.-C., Hahn, A., and Liu, C.-C. (2018). Cyber security of a power grid: State-of-the-art. *International Journal of Electrical Power & Energy Systems*, 99:45–56.

Tareen, W. U., Mekhilef, S., Seyedmahmoudian, M., and Horan, B. (2017). Active power filter (APF) for mitigation of power quality issues in grid integration of wind and photovoltaic energy conversion system. *Renewable and Sustainable Energy Reviews*, 70:635–655.

Teodorescu, R., Blaabjerg, F., Liserre, M., and Loh, P. C. (2006). Proportional-resonant controllers and filters for grid-connected voltage-source converters. *IEE Proceedings - Electric Power Applications*, 153(5):750–762.

Theo, W. L., Lim, J. S., Ho, W. S., Hashim, H., and Lee, C. T. (2017). Review of distributed generation (DG) system planning and optimisation techniques: Comparison of numerical and mathematical modelling methods.

Tulabing, R., Yin, R., DeForest, N., Li, Y., Wang, K., Yong, T., and Stadler, M. (2016). Modeling study on flexible load's demand response potentials for providing ancillary services at the substation level. *Electric Power Systems Research*, 140:240–252.

Twaha, S. and Ramli, M. A. M. (2018). A review of optimization approaches for hybrid distributed energy generation systems: Off-grid and grid-connected systems. *Sustainable Cities and Society*, 41:320–331.

Unamuno, E. and Barrena, J. A. (2015a). Hybrid ac/dc microgrids - Part I: Review and classification of topologies. *Renewable and Sustainable Energy Reviews*, 52(December):1251–1259.

Unamuno, E. and Barrena, J. A. (2015b). Hybrid ac/dc microgrids—Part II: Review and classification of control strategies. *Renewable and Sustainable Energy Reviews*, 52:1123–1134.

Ustun, T. S., Ozansoy, C., and Zayegh, A. (2011). Recent developments in microgrids and example cases around the world—A review. *Renewable and Sustainable Energy Reviews*, 15(8):4030–4041.

Vallejos, W. D. P. (2017). Standalone photovoltaic system, using a single stage boost DC/AC power inverter controlled by a double loop control. In *2017 IEEE PES Innovative Smart Grid Technologies Conference - Latin America (ISGT Latin America)*, pages 1–6.

Valverde Gil, R. and Gachet Páez, D. (2007). Identificación de sistemas dinámicos utilizando redes neuronales RBF. *Revista Iberoamericana de Automática e Informática Industrial RIAI*, 4(2):32–42.

Vandoorn, T. L., De Kooning, J. D., Meersman, B., and Vandevelde, L. (2013). Review of primary control strategies for islanded microgrids with power-electronic interfaces.

Vargas, S. and Pavón, W. (2020). Optimal sizing and allocation of photovoltaic generation in a georeferenced micro grid using column generation. *Revista Técnica Energía*, 17:71–79.

Veronesi, M. and Visioli, A. (2010). Performance assessment and retuning of PID controllers for integral processes. *Journal of Process Control*, 20(3):261–269.

Visioli, A. (2004). A new design for a PID plus feedforward controller. *Journal of Process Control*, 14(4):457–463.

Wang, C., Minjian, C., and Martínez, L. R. (2018a). Design of load optimal control algorithm for smart grid based on demand response in different scenarios.

Wang, G., Wang, X., Wang, F., and Han, Z. (2020). Research on Hierarchical Control Strategy of AC/DC Hybrid Microgrid Based on Power Coordination Control.

Wang, J., Jin, C., and Wang, P. (2018b). A Uniform Control Strategy for the Interlinking Converter in Hierarchical Controlled Hybrid AC/DC Microgrids. *IEEE Transactions on Industrial Electronics*, 65(8):6188–6197.

Wang, Q., Zuo, W., Cheng, M., Deng, F., and Buja, G. (2019). Hierarchical control with fast primary control for multiple single-phase electric springs. *Energies*, 12(18).

Wang, X., Lv, H., Sun, Q., Mi, Y., and Gao, P. (2017). A Proportional Resonant Control Strategy for Efficiency Improvement in Extended Range Electric Vehicles.

Wei, Q., Liu, D., Lewis, F. L., Liu, Y., and Zhang, J. (2017). Mixed Iterative Adaptive Dynamic Programming for Optimal Battery Energy Control in Smart Residential Microgrids. *IEEE Transactions on Industrial Electronics*.

Wu, N. and Wang, H. (2018). Deep learning adaptive dynamic programming for real time energy management and control strategy of micro-grid. *Journal of Cleaner Production*.

Zhang, B., Wu, Y., Jin, Z., and Wang, Y. (2017). A Real-Time Digital Solver for Smart Substation Based on Orders. *Energies*, 10(11):1795.

Zhang, Z., Cui, P., and Zhu, W. (2020). Deep Learning on Graphs: A Survey. *IEEE Transactions on Knowledge and Data Engineering*.

Zheng, P., Wang, H., Sang, Z., Zhong, R. Y., Liu, Y., Liu, C., Mubarok, K., Yu, S., and Xu, X. (2018). Smart manufacturing systems for Industry 4.0: Conceptual framework, scenarios, and future perspectives. *Frontiers of Mechanical Engineering*, 13(2):137–150.

Zhong, Q. C. and Zeng, Y. (2016). Universal Droop Control of Inverters with Different Types of Output Impedance. *IEEE Access*, 4:702–712.

Ziouani, I., Boukhetala, D., Darcherif, A. M., Amghar, B., and El Abbassi, I. (2018). Hierarchical control for flexible microgrid based on three-phase voltage source inverters operated in parallel.

Zubo, R. H., Mokryani, G., Rajamani, H. S., Aghaei, J., Niknam, T., and Pillai, P. (2017). Operation and planning of distribution networks with integration of renewable distributed generators considering uncertainties: A review.